University of Natural Resources
and Life Sciences, Vienna

MASTER THESIS

Potential of bio-based friction modifiers for safe use in food-grade lubrication

Rosa Maria Eder, BSc.

01440703

Aspired academic degree: Dipl.-Ing.

Master studies: Safety in the Food Chain (UH 066 451)

durchgeführt bei:
AC2T research GmbH
Viktor-Kaplan-Straße 2/C
2700 Wiener Neustadt
Österreich
Dr. Marcella Frauscher (AC2T research GmbH)

Betreuer:
Priv.-Doz. Dr. Matthias Schreiner
Department für Lebensmittelwissenschaften und -technologie
Arbeitsgruppe Lebensmittelchemie und -authentizität
Universität der Bodenkultur Wien

Wiener Neustadt, Mai 2021

Acknowledgments

The research results presented in this thesis were generated at AC2T research GmbH (Wiener Neustadt) and funded by the Austrian COMET program (Project: COMET K2 InTribology, No. 872176; Project Management Agency: AC2T research GmbH, Austrian Competence Center for Tribology).

Especially I would like to thank my professor at BOKU Priv.-Doz. Dr. Matthias Schreiner, my supervisor Dr. Marcella Frauscher at AC2T research GmbH, Dr. Guido Boidi and finally my department head Ing. Rainer Franz at AC2T research GmbH for the excellent and always supportive supervision.

Finally, I would also like to thank all scientific and non-scientific staff at AC2T research GmbH for their constant support and excellent cooperation.

Abstract

Energy often originates from fossil sources, consequently the need to use it and its resources efficiently is even more essential than for renewable raw materials. Film-forming friction modifier (FM) additives are used in lubricating oils of industrial devices and automotives. The main function of a FM is to optimize friction in tribological contacts. Ecologically harmless lubricants and lubricant components, including FM, have been available on the market for centuries.

This thesis aims at the evaluation of sustainable and innocuous lubricant additives (FM) used for different industrial applications, reaching from the automotive industry to devices used for e.g., food production such as an extruder. For this purpose, bio-based FM, consisting of natural raw materials, were compared to bio-based conventionally used FM in lubricants in terms of tribological performance. A toxicological assessment based on literature, proposed information on FM and their influence on living organisms.

A set of step-by-step instructions leading to an internal standard operating procedure (SOP) was performed to obtain reliable data using the rheometer MCR302. The method was designed under variation of normal force [N], temperature [°C] and sliding speed [m/s]. Repeatability and reproducibility tests enclose the method development of the rheometer MCR302. Resulting from the tests performed in this thesis, the used method for the rheometer MCR302 using a ball (100Cr6) on three plates (1.4301 steel) was determined to be accurate.

Comparing the conventional FM in polyalphaolefin (PAO8) to the bio-based FM in PAO8 at 80 °C and in distilled water at 30 °C, revealed that bio-based FM, namely rapeseed oil and salmon oil, can perform at least as good as the best performing conventional FM, namely tallow amine.

The performed comparison can be seen as a starting point, indicating the advantages and disadvantages of both biobased and conventionally used friction modifiers and thereby presents a step in the right direction towards developing innovative sustainable technological solutions in lubricant research.

Zusammenfassung

Energie wird heutzutage immer noch oft aus der Petrochemie gewonnen, daher ist es der Umwelt zuliebe unerlässlich diese und ihre Ressourcen effizient zu nutzen. Konventionell erhältliche filmbildende Reibungsmodifikatoren (FM), die in Schmierölen von Industriegeräten und auch in Automobilen verwendet werden, sind Schmierstoffadditive und werden oft aus ökologisch bedenklichen Stoffen hergestellt. Die Hauptfunktion dieser FM ist es, die Reibung der tribologischen Kontakte zu reduzieren. Ökologisch unbedenkliche Schmierstoffe und Schmierstoffkomponenten, darunter auch FM, sind seit Jahrhunderten auf dem Markt erhältlich.

Ziel dieser Arbeit ist der chemische und tribologische Vergleich biobasierter, aus natürlichen Rohstoffen bestehenden, FM mit konventionell verwendeten FM petrochemischen Ursprungs in Schmierstoffen, die für verschiedene industrielle Anwendungen eingesetzt werden, unter anderem die Automobilindustrie bis hin zu Geräten der Lebensmittelproduktion (z.B. Extruder). Zu diesem Zweck wurde eine literaturbasierte toxikologische Bewertung durchgeführt, welche über die konventionell verwendeten FM und ihren Einfluss auf lebende Organismen informiert.

Eine Schritt-für-Schritt-Anweisung, die zu einer internen Standardarbeitsanweisung (SOP) führten, wurde durchgeführt, um mit Hilfe des Rheometers MCR302 zuverlässige Daten zu erhalten. Die Methode wurde unter Variation der Normalkraft [N], der Temperatur [°C] und der Gleitgeschwindigkeit [m/s] entwickelt. Wiederholbarkeits- und Reproduzierbarkeitstests umschließen die tribologische Methodenentwicklung für das Rheometers MCR302.

Als Ergebnis konnte die verwendete Methode für das Rheometer MCR302 unter Verwendung einer Kugel (100Cr6) auf drei Platten (1.4301 Stahl) und 5 N konstanter Normalkraft als genau bestimmt werden, da das Messergebnis mit dem „wahren“ Wert übereinstimmte. Bei dem Vergleich von konventionellen FM in PAO8 mit den biobasierten FM in PAO8 bei 80 °C und in destilliertem Wasser bei 30 °C, wurde festgestellt, dass biobasierte FM, im speziellen Rapsöl und Lachsöl, mindestens so gut abschneiden wie der beste ausgewählte konventionelle FM, nämlich Talgamin.

Der durchgeführte tribologische Vergleich, welcher die Vor- und Nachteile sowohl von biobasierten als auch von konventionell verwendeten FM aufzeigt, kann als Ausgangspunkt für die Entwicklung von ölbasierten zu wasserbasierten Schmierstoffen und allgemein zu innovativen und nachhaltigen Schmierstofflösungen verwendet werden.

Eidesstattliche Erklärung

Ich erkläre eidesstattlich, dass ich die Arbeit selbständig angefertigt, keine anderen als die angegebenen Hilfsmittel benutzt und alle aus ungedruckten Quellen, gedruckter Literatur oder aus dem Internet im Wortlaut oder im wesentlichen Inhalt übernommenen Formulierungen und Konzepte gemäß den Richtlinien wissenschaftlicher Arbeiten zitiert, durch Fußnoten gekennzeichnet bzw. mit genauer Quellenangabe kenntlich gemacht habe.

List of contents

1. Introduction

Considering a more sustainable future, 2021 marks the beginning of the action plan set by the European Green Deal being the map towards a sustainable EU economy, according to REGULATION (EU) No 2018/1999 OF THE EUROPEAN PARLIAMENT AND OF THE COUNCIL. This further includes REGULATION (EEC) No 880/1992 OF THE COUNCIL OF THE EUROPEAN COMMUNITIES, being the European Ecolabel for Lubricants. This Ecolabel helps to achieve essential climate goals until 2030, including CO_2 reduction (to at least 55 % below the levels of 1990) incorporating both emissions and removal, diminution of the impact on the aquatic environment and soil during the use of lubricants and limited use of hazardous substances. Essentially, lubricants with the European Ecolabel guarantee high technical performance.
By 2050, the long-term strategy of the EU is to be climate neutral, having an economy with net-zero greenhouse gas emissions, being in-line with the European Green Deal and the Paris Agreement (COP21, entry into force 4th of November 2016), pursuing efforts to limit global warming below 1.5 °C (global average temperature). (European Union, 2021)

Based on the addressed goals of the Green Deal, this thesis aims at the evaluation of sustainable and innocuous lubricant additives (friction modifiers, FM). These FM can be used for different industrial applications, reaching from the automotive industry to devices used for e.g., food production such as an extruder. In terms of tribological performance, bio-based FM, consisting of natural raw materials, were compared to bio-based conventionally used FM. Literature research resulted in a toxicological assessment, proposing information on FM and their influence on living organisms.

The bio-based FM assessed in this thesis should be considered for the European Ecolabel to further achieve an energy proportion of 32.5 % from renewable source, being one of the main goals of the European Green Deal until 2030. (European Union, 2021)

Concluding, the research performed in this thesis and follow-up projects could significantly contribute to achieving the climate goals set in the European Green Deal.

2. Fundamentals

2.1. Tribology

The experimental part of this thesis is mainly enclosed by tribological tests, which are performed on the rheometer MCR302 (Anton Paar GmbH, Graz, Austria). Therefore, this first chapter of introduction includes a short section tribology and lubrication.
Generally, tribology is the science of friction, wear, and lubrication. Friction is the resistance against movement, wear indicates the loss of material and lubrication expresses the use of a lubricant. (Grote, Bender, & Göhlich, 2018)
The goal of tribology is to optimize friction and wear, this optimization means in many applications a minimization. However, friction and wear are to a limited extent advantageous, as for examples in brakes, wheels on rails and car tires on roads. (Grote & Antonsson, 2009)

2.1.1. Friction tests

There are two types of friction, on the one hand static and on the other hand dynamic (kinetic) friction. As the names indicates, static friction occurs between two bodies not in movement, whereas dynamic friction takes place between two bodies in movement. There are different types of relative movement, such as sliding, rolling, and drilling. When those relative movements occur, the frictional forces try to act against the direction of movement and thereby their aim is to inhibit the movement. (Sommer, Heinz, & Schöfer, 2010) In order to characterize the friction of a tribological system, the so-called Stribeck curve is used (see Figure 1). For the x-axis, the Hersey number $\frac{oil\ viscosity\ x\ speed}{pressure}$ is used.

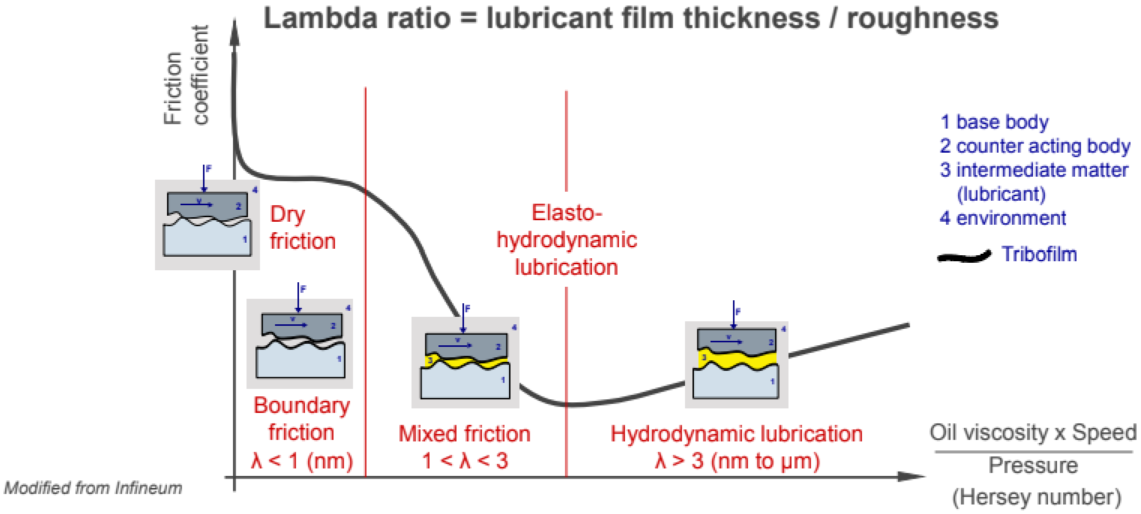

Figure 1: Schematic Stribeck curve including boundary, mixed, elasto- and hydrodynamic friction (Dörr, 2019)

In the Stribeck curve above three types of lubrication regimes are shown. Boundary friction means there is no or only few lubricant available which results in direct body on counter body contact, leading to an undesired event of high friction and wear. Mixed friction describes a situation, where there is a lubricant available, however it is not thick enough yet, which still results in enhanced friction and wear. As soon as the lubricant between the body and counter body is thick enough to separate almost all roughness spikes, hydrodynamic friction is reached, and the two bodies are completely separated by the lubricant. The friction increase in hydrodynamic friction is only due to the viscosity of the lubricant. (Antonsson & Grote, 2009) (Anton Paar, 2020)

The Hersey number and the resulting Stribeck curve indicate the important effect of viscosity and pressure, next to speed, on the coefficient of friction [µ]. By using friction modifiers in this thesis, the aim is to reach the minimum of the Stribeck curve, also called elastohydrodynamic lubrication (EHL). A concentrated load at a "point", leads to a very high pressure at the concerned contact region, which further leads to the "viscosity effect" meaning that the viscosity of the lubricant close to the contact region is increased. (Spikes H. , 2006)

The aspired goal of this thesis was to find a bio-based friction modifier in a water-based system, which behaves tribologically comparable to a conventional friction modifier in a petrochemical system. Therefore, a theoretical lubrication regime calculation was essential for the selection of the comparative petrochemical base oil, resulting in the calculation of alpha (α), which is further used for calculating the minimum film thickness (h_{min}), ultimately leading to the determination of the specific film thickness, the lambda (λ) values. With the help of the α-value, being the viscosity-pressure value, the λ-value can be determined, implicating the theoretically calculated lubrication regime. (Khonsari & Booser, 2008) For the selection of base oils, four conventionally used base oils with comparably low viscosity (PAO8, PAO4, SN450, SN150W) were chosen.
The lubrication regime is defined by the lambda ratio (λ), being the minimum film thickness (h_{min}) in relation to the composite surface roughness (R_{qA} and R_{qB}) according to the following formula: (Stachowiak & Batchelor, 2000)

$$\lambda = \frac{h_{min}}{\sqrt{\left(R_{qA}^2 + R_{qB}^2\right)}}$$

After performing in-house minimum film thickness and surface roughness tests, the α-value was still needed to calculate the λ-value. The following calculation steps were performed according to Khonsari and Booser (2008). The pressure viscosity value describes the viscosity that changes with different pressures. (Matthies & Renius, 2008) With increasing pressure, the viscosity also increases. Generally, the pressure-viscosity relation depends on the base oil and the used additives. Pressure induced viscosity changes are commonly more pronounced for paraffinic base oils than for naphthenic base oils. (Watter, 2017) The Stabinger Viscometer SVM 3000 (Anton Paar GmbH, Graz, Austria) measured the kinematic viscosity $[\frac{mm^2}{s}]$ (μ_0) was obtained for the tested base oils PAO8, PAO4, SN450 and SN150W, whereas PAO8 and PAO4 belong to group IV and SN450 and SN150W belong to group I, (see chapter 2.2). The lubrication regime calculation was used for the final selection of one of the four tested base oils.

By using the calculated kinematic viscosity values and by using literature values for the viscosity-pressure index Z for the respective lubricants, α-values of the addressed base oils were determined using the following formula (Khonsari & Booser, 2008):

$$\alpha_{EHL} = Z[5.1 * \ 10^{-9} * \ (ln\mu_0 + 9.67)]$$

For PAO8 at 80 °C a $\mu_0$value of 12.477 $\frac{mm^2}{s}$ and α value of 1.16E-08 $\frac{1}{Pa}$ was determined. In comparison at 80 °C a $\mu_0$value of 4.6403 $\frac{mm^2}{s}$ and α value of 9.86E-09 $\frac{1}{Pa}$ was calculated for PAO4. The overview including all μ_0- and α-values for all base oils in question at 80 °C and different temperatures of PAO8 can be found in Appendix 23 and Appendix 24. From this overview it can also be concluded that with increasing temperature, the viscosity value, as well as the α value, decreases, and the oil sample gets thinner.

To further calculate the λ-values, the minimum film thickness was calculated using the following formula (Hamrock & Dowson, 1977):

$$h_{min} = \left(3.63 \ G^{0.49} \ U^{0.68} \ W^{-0.073} \ (1 - e^{-0.68k})\right) * R_x$$

G being the dimensionless material parameter (including α_{EHL}), U being the dimensionless speed parameter, W being the dimensionless load parameter, R being the effective radius and k being the ellipticity parameter. The effective radius of the ball R is 6.35 mm, whereas the pin and plate are flat. Formulas for the individual parameters can be found in Hamrock and Dowson (1977).

2.1.2. Lubricant in the tribosystem

Figure 2 gives an overview of the tribological system including the lubricating medium shown in yellow.

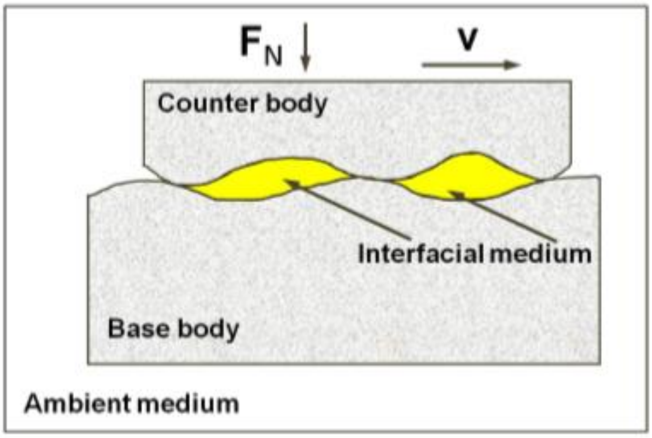

Figure 2: Basic structural elements (base body, counter body, intermediate/interfacial material, and surrounding/ambient medium) of a tribological system (Widder, 2014) (Czichos & Mang, 2014)

It is depicted that velocity (v) and normal force (F_N) are resulting output variables of the system. Focusing on the intermediate/interfacial medium, namely the lubricant, lubricants are machine elements, which must be adapted to the lubricated system and the aggregate. Lubricating oils only include base oils and additives, whereas lubricating greases also incorporate thickeners. Generally, the lubricant has several tasks to fulfil in the tribosystem:

- reduce friction and wear
- remove heat by cooling the system
- remove wear particles and dirt by transporting them among the system

(Rizvi, 2009) (Dörr, 2019)

2.2.Basic solutions

According to the European Commission, a base fluid is defined as “a lubricating fluid which flow, ageing, lubricity, and anti-wear properties, as well as its properties regarding contaminant suspension, have not been improved by the inclusion of additive(s). (European Commission, 2018)

Basic solutions can be further categorized in group I (mineral oils, solvent neutral), group II (mineral oils, hydrogenated), group III (hydrocrack oils), group IV (polyalphaolefin, PAO) and group V (all other categories, e.g., esters, animal/vegetable oils). These basic solutions provide essential properties to the lubricants such as stability, additive activity and solubility, rheological properties and amongst other toxicology. (Dörr, 2019) (Mang & Dresel, 2017)

2.3. Additives

According to the European Commission, an additive is further defined as “a substance or mixture, which primary functions are the improvement of one or several of the following aspects: flow, ageing, lubricity, anti-wear properties and contaminant suspension”. Additives can make up from 0.1 to up to 20 % of the formulation. (European Commission, 2018) Together with the choice of base oil, the choice of additive determines the quality of the lubricant and the application. (Dörr, 2019) (Mang & Dresel, 2017) Additives generally alter properties of lubricants by either conferring new or desired properties or by removing or attenuating undesired properties. (European Commission, 2018)

Additives can be further categorized by Table 1.

Table 1: Categorization of additives

Surface	**Performance**	**Base oil**	**Other**
Friction modifiers	Pourpoint-Depressants	Oxidation inhibitors	Dyes and fragrances
Extreme-Pressure-Agents (EP)	Viscosity Index inhibitors (VII)	Antifoam agents	Antistatic additive (LF)
Anti-Wear-Agents (AW)	Demulsifiers		Bactericides
Corrosion inhibitors	Adhesion additives		Emulsifiers
Rust inhibitors	Detergents		Solid lubricants
Metal deactivators	Dispersants		Antimist

The headings “surface”, “performance”, “base oil” and “other” refer to the principle of operation of the corresponding additives. For example, friction modifiers, being the additives used in this thesis, carry out their function, reduction of friction especially in boundary and mixed lubrication, by forming an adsorbed film at the surface of metals via their polar head group. (Spikes H. , 2015) This reduction of friction is achieved by working on the surface directly and further leads to the reduction of energy consumption and thus carbon dioxide emissions by the resulting low friction in machine components. (Spikes H. , 2015)

Figure 3 gives an overview of the development of lubricant additives over time with focus on the different types of FM.

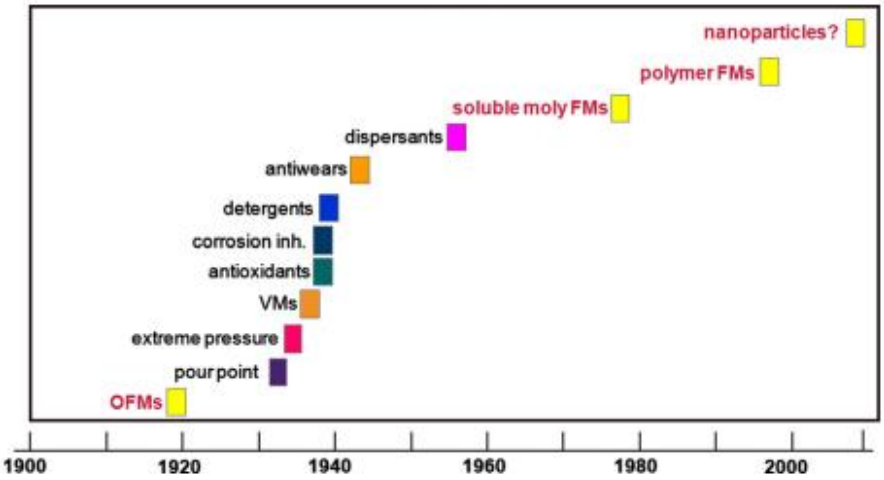

Figure 3: Lubricant additives – timeline for development (Spikes H. , 2015)

When categorizing friction modifiers, there are four main classes, marked in pink in Figure 3. The first class of friction modifiers, namely organic friction modifiers (OFM) based on amphiphilic surfactants, were already developed, and used in the early 1920s. The first OFM were free fatty acids obtained from fats and vegetable oils. The second class are organo-molybdenum compounds (“soluble moly FMs”), which were developed in the 1980s. They are oil-soluble and were initially developed to be antiwear additives. The third class are functionalized polymers (e.g., PMMA being poly methyl methacrylate), which are made to adsorb on polar tribological surfaces (e.g., water and glass) specifically, to increase the viscosity index and to further reduce friction in hydrodynamic conditions. Lastly, the fourth class are dispersed nanoparticles, having great potential to replace OFMs and zinc dithiophosphate (ZDDP), being one of the main antiwear compounds. (Spikes H. , 2015)

2.3.1. Friction modifiers

This chapter depicts the selected bio-based conventionally established, further termed conventional FM, and bio-based friction modifiers thematized in this thesis. For the conventional friction modifiers, all being from the first class (OFM), a toxicological assessment is included.

2.3.1.1. Conventional friction modifiers – toxicological assessment

To obtain a better overview of the toxicological assessment, the conventional friction modifiers were listed starting from the least to the most toxic.
Figure 4 illustrates the structural formula of the selected conventional friction modifiers.

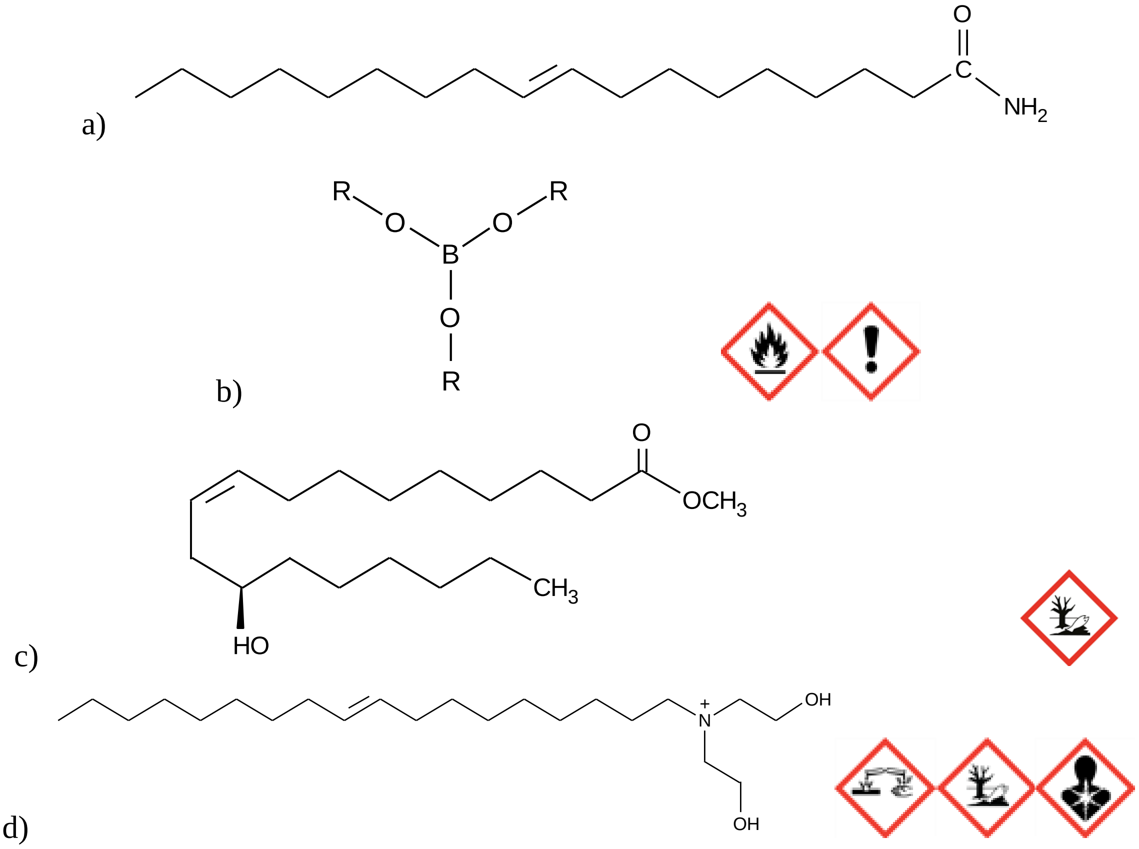

Figure 4: Structural formula of selected conventional FM: a) oleamide b) borate ester c) methyl ricinoleate d) tallow amine

According to the European Chemicals Agency (ECHA), oleamide may cause long lasting harmful effects to aquatic life, which may further lead to serious eye, respiratory or skin irritation. However, oleamide can only be classified, as aquatic chronic toxic 4, which does not yet require the hazard symbol, as depicted in Figure 4. (ECHA, 2020) Only aquatic acute toxic 1, aquatic chronic toxic 1 and 2 need the hazard symbol having a harmful effect on aquatic life. For this categorization long lasting effects, bioaccumulation and degradability are essential. The category aquatic chronic toxic 4 fulfills the function of a "safety net", as there is cause for concern for the substances. This includes, among others, poorly soluble substances that do not show acute toxicity in the range up to water solubility but are not rapidly degradable and have a bioaccumulation potential. (Umweltbundesamt, 2020) As biodegradability tests (OECD TG 301C or 301D) indicate a value below 60 %, persistence in the environment is suspected. Being a lipophilic compound, oleamide may easily accumulate in animal cells. (ECHA, 2020)

Borate ester is the second substance with low toxicity, according to the European Union approved harmonized classification and labelling (CLP00) and according to the REACH registrations in ECHA. Further borate ester is a flammable liquid and vapor, which is harmful in contact with skin. (ECHA, 2020)

Ricinoleic acid methyl esters are used to produce cosmetics and as plasticizers, lubricant/cutting oil additives and wetting agents. Especially, dermal contact during production seems to be problematic. As indicated by the hazard symbol, methyl ricinoleate falls under aquatic chronic toxic category 2. Comparing the estimated volatilization half-lives of a model river (10 months) to a lake (9 years) and a pond (175 years), huge differences can be seen. Moreover, a bioconcentration factor (BCF) - indicating the accumulation in living organisms - of 370 indicates possible bioaccumulation for methyl ricinoleate. (PubChem, 2020)

Indicated by the hazard symbols tallow amine seems to be the most hazardous substance of the selected conventional friction modifiers. Tallow amine might even be fatal if swallowed or by entering the airways (category 4 acute oral toxicity), might cause severe skin burns and eye damage and is very toxic (category 1 acute aquatic toxicity). (ECHA, 2020) Tallow amine is used as surfactant in the glyphosate-based broad-spectrum herbicide “Roundup”. This herbicide is used worldwide, also in genetically modified plants that were specifically designed to tolerate it. Thereby, this herbicide may possibly enter the food chain, causing harm for both animals and humans. Moreover, the presence of Roundup adjuvants, such as tallow amine, enhances both the bioavailability and bioaccumulation of glyphosate. (Richard, Moslemi, Sipahutar, Benachour , & Seralini, 2005)

2.3.1.2. Bio-based friction modifiers

The following figures give an overview of the structural formulas of the selected bio-based friction modifiers. This overview will be helpful for the interpretation of elemental analysis, namely the Inductively coupled plasma optical emission spectrometry (ICP-OES).
Figure 5 illustrates the structural formula of the selected bio-based friction modifiers.

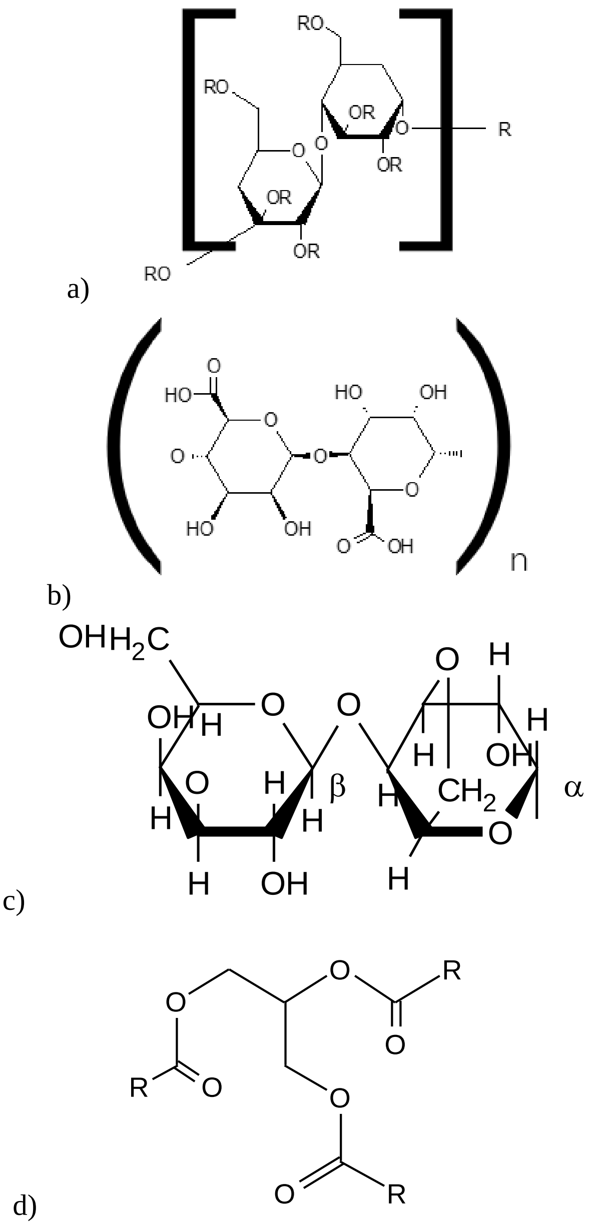

Figure 5: Structural formula of selected bio-based FM: hydroxypropyl methylcellulose (HPMC) b) alginic acid calcium salt from brown algae (alginate) c) agarose d) general formula of oils (including rapeseed oil and salmon oil)

The following paragraph gives an overview of the differences of the residuals (R) seen in Figure 5, when comparing rapeseed and salmon oil. Comparing the fatty acid profile of rapeseed oil to salmon oil, salmon oil seems to have a wider range of saturated (approximately 27 %) and unsaturated (approximately 73 %) fatty acids than plant oils in general. (El-Mashad, Zhang, & Avena-Bustillos, 2008) Salmon oil is mainly comprised of oleic acid (C18:1, 18.22 g/100g) and palmitic acid (C16:0, 14.83 g/100g), whereas in rapeseed oil oleic acid (C18:1, 62.5 %) clearly dominates. Going into more detail for rapeseed oil, linoleic acid (C18:2, 19.6 %) and linolenic acid (C18:3, 10.0 %) play an essential role. (Lewinska, Zebrowski, Duda, Gorka, & Wnuk, 2015) This underlines that unsaturated fatty acids are far more dominant in rapeseed oil than saturated fatty acids. To complete the fatty acid profile analysis, docosahexaenoic acid DHA (C22:6, 13.63 g/100g), linolenic acid (C18:3, 11.67 g/100g), eicosapentaenoic acid EPA (C20:5, 11.13 g/100g) and myristic acid (C14:0, 6.85 g/100g) are found in high concentrations in salmon oil. (El-Mashad, Zhang, & Avena-Bustillos, 2008) The structural formula of the addressed fatty acids (i.e., residuals) for salmon and rapeseed oil can be found in Appendix 1 and 2.

2.4.Literature tribological method development

As a basis for the tribological method development on the rheometer MCR302, prior literature research was essential to determine both the test parameters and set-up.

Table 2 gives an overview of the papers concerning tribological tests of friction modifiers using a ball-on-disc set-up and tests on the ball-on-three-plates set-up. Generally, most tribological measurements on friction modifiers were performed with a ball-on-disc set-up.

Table 2: Overview of ball-on-disc and ball-on-three-plates tribological tests

Parameters	**Kozdrach (2020)**	**He, et al. (2017)**	**Gallego, et al. (2015)**	**Spikes (2015)**	**Guegan, et al.-(2019)**
Normal force [N]	39.24 N	10-40 N	20 N	3 N	40 N
Sliding speed	300 rpm	0.02-0.1 m/s	2^{-5} – 1 m/s	1^{-7} – 1^{-3} m/s	0.005– 3 m/s
Temperature [°C]	20 °C	-	25-125 °C	100 °C	100°C
Type (set-up)	Ball-on-three-plates	Ball-on-three-plates	Ball-on-three-plates	Ball-on-disc	Ball-on-disc (MTM)
Material	Ball on plates both bearing steel LH 15	Ball on plates	Ball on plates	Ball against rotating, flat surface disc	Ball against flat surface of a rotating disc
Ball	12.7 mm diameter	AISI 52100 alloy steel ball	6.35 mm diameter steel 1.4401 grade 100	6 mm diameter AISI 512100	19 mm diameter steel
Plates/ Discs	15x5x2 mm	AISI 304 stainless steel plate	steel 1.4301	AISI 512100	steel
Usage	Immersion lubrication	Slow sliding speed	Very slow sliding speed	Very slow sliding speed	Slow sliding speed

As indicated Table 2 in high normal forces are used for the ball-on-three-plates tests. However, the minimum sliding speeds of the tests must also be considered, as the rheometer MCR302 with the tribological set-up can measure up to 1E-09 m/s.

2.4.1. Ball-on-disc

The following figures show results for either individual friction modifiers as pure component (see Figure 7) or 0.01 molar mass (M) [kg/mol] friction modifiers in hexadecane (see Figure 6). Notably, the tribological set-up for these experiments was similar (both ball on rotating disc), however different normal forces were used (see Figure 6 and Figure 7).

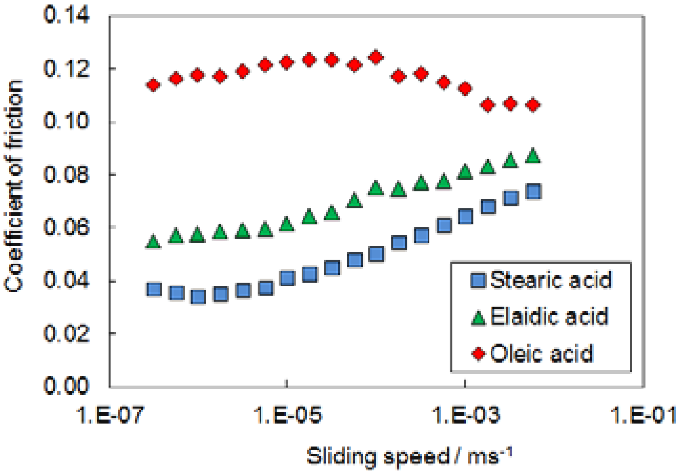

Figure 6: Friction versus sliding speed for 0.01 M fatty acid solutions in hexadecane at 100 °C, 3 N (Spikes, 2015)

According to Figure 6 stearic acid and elaidic acid perform similar depicting a very low coefficient of friction at low speeds and increasing approximately linearly with logarithmic (speed). Oleic acid on the other hand behaves completely different, as the coefficient of friction slightly decreases with increasing speed, is however nearly constant. Therefore, oleic acid was considered for further investigations in this master thesis.

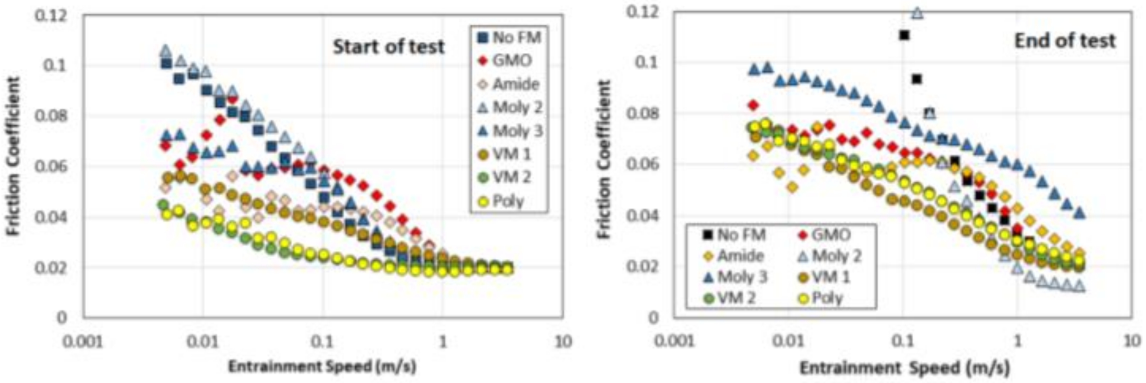

Figure 7: Friction tests for individual FM solutions in GTL4, 40 N (Guegan, Southby, & Spikes, 2019)

When comparing the course of the curves of glycerol monooleate (GMO) in Figure 7 and oleic acid in Figure 6, a similar trend can be seen. However, due to different normal forces, namely 3 N for the friction test including oleic acid and 40 N for the friction test including GMO, the coefficient of frictions [1] cannot be directly compared. This indicates that the normal force (load) does not significantly alter the coefficient of friction.

2.4.2. Ball-on-three-plates

Literature research indicated that the used tribological set-up in this thesis, ball-on-three-plates, has not yet been often used. However, the interest for this set-up remained, as the plates are made of stainless steel, which is mandatorily needed in the chemical, pharmaceutical and food industry, making it a target for this thesis. (Rähse, 2014)
Figure 8 and Figure 9 depict results from tribological tests using ball-on-three-plates set-ups leading to identical contact situations, using a rheometer from Anton Paar. However, different normal forces, temperatures and sliding speeds were applied (see Figure 8and Figure 9).

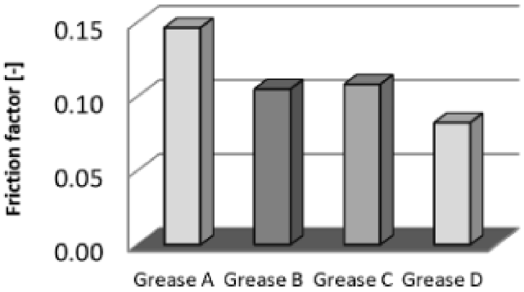

Figure 8: Average value of coefficient of friction for unmodified vegetable greases (A), vegetable lubricants modified 1% (B), 3 % (C) and 5 % (D) polytetrafluoroethylene (PTFE), 39.24 N, 20 °C, 300 rpm (Kozdrach R. , 2020)

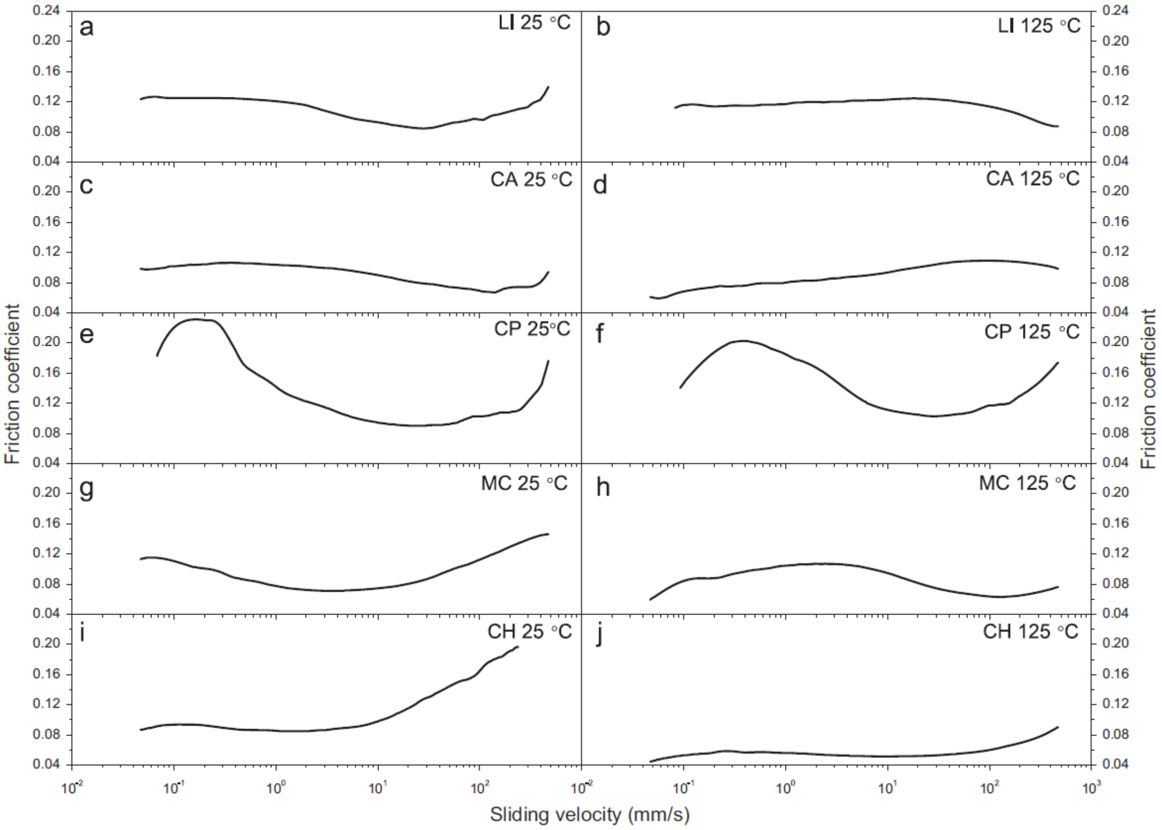

Figure 9: Coefficient of friction versus sliding velocity [mm/s] for biopolymer based (CP, MC, CH) and commercial lubricating greases (LI , CA), 20 N (Gallego, Arteaga, Valencia, Díaz, & Franco, 2015)

As stated before, generally more literature can be found on tribological tests using the ball-on-disc set-up. (Wang, Zhou, Duszczyk, & Katgerman) However, from Figure 8 and Figure 9 it can be seen, that the ball-on-three-plates set-up, which is also used in this thesis, has also already been used successfully in previous studies.

2.5.Lubricants used in food technology

Food grade lubricants used for food applications are not categorized by European standards, therefore an unofficial industrial standard was adopted by the U.S. Food and Drug Administration (FDA) and the U.S. Department of Agriculture (USDA). However, since 1st of September 1998, USDA approval for a product can no longer be obtained since this authority was shifted to the food manufacturer himself in accordance with the hazard analysis and critical control points (HACCP) concept. (T+S Tribologie und Schmierungstechnik, 2016) (Stempfel & Baumann, 2012)

Consequently, the lubricants are not FDA approved, however US H1 lubricants for example comply with FDA "Regulation 178.3570" or "21 Code of Federal Regulations (CFR) 178.3570". (European Lubricating Grease Institution, 2016) Thereby, hygiene, quality and product liability are essential topics to prevent recalls, as they are not only expensive, but also endanger the consumer and damage the image of the company. This suggests that laws, regulations, and national directives are the building blocks for food grade lubricants. (T+S Tribologie und Schmierungstechnik, 2016) (Stempfel & Baumann, 2012)

Requirements for food grade lubricants are essentially built up of technical aspects and hygienic aspects, which are covered by the HACCP concept, which is mandatory according to REGULATION (EC) No 852/2004 OF THE EUROPEAN PARLIAMENT AND OF THE COUNCIL. Moreover, the requirements for the produced goods, such as purity, taste, odor, color, and toxicity must not be forgotten. Substantially, the food grade lubricant must not have a negative effect on the food while fulfilling technical requirements, such as good tribological. (T+S Tribologie und Schmierungstechnik, 2016) (Stempfel & Baumann, 2012)

Generally, there are three main classes categorizing the topic of food grade lubricants. In industry, commonly class H2 lubricants referring to "lubricants with no food contact" are used. Classification starts with H1 "food grade lubricants": lubricants which may have incidental contact with food, however this food contact should be kept to a minimum to still fulfill the required application. If a substance is for example used as a corrosion inhibitor, it must be removed by washing or wiping before food processing. (T+S Tribologie und Schmierungstechnik, 2016) (Stempfel & Baumann, 2012) Therefore, from a safety point of view only H1 lubricants are recommended to be used in food processing, however the price of lubricants must also be considered. Additionally, the International Organization for Standardization ISO 21469 provides assurance of both process and product quality beyond the H1 registration by setting hygiene requirements for H1 incidental food contact lubricants. (European Lubricating Grease Institution, 2016)

Class H2 "lubricants with no food contact" may only be used in closed systems (e.g., hydraulic systems), where there is no possibility that the lubricants may encounter food products. H2 lubricants can be used as anti-adhesive agents or corrosion protection. (T+S Tribologie und Schmierungstechnik, 2016)

Class H3 "soluble oils" may be used as cleaning lubricants or corrosion protection for hooks, trolleys, or similar equipment. (T+S Tribologie und Schmierungstechnik, 2016) (Stempfel & Baumann, 2012)

In addition to the classification of H1, H2 and H3 lubricants, new approvals for better distinction were introduced by the National Science Foundation (NSF). These include HX-1 "raw materials for the formulation of H1 lubricants", HX-2 "raw materials for the formulation of H2 lubricants" and HX-3 "raw materials for the formulation of H3 lubricants". Such raw materials are for example heat transfer lubricants, which may not necessarily be described as lubricants.

Exemplary machines from the food industry, where H1 lubricants are essential, are for example a twin-screw extruder and two roll press. Both aim to compact fine material by using high pressures. (Vauck & Müller, 1999) Extrusion is a modern high temperature short time (HTST) cooking process using different temperature settings (60 to 300 °C) and high pressures (10 to 300 bar) leading to a small an opening, where the pressure drastically drops, resulting to different products, mainly snacks such as snips. (Adekola, 2016) (Techpilot, 2021)

Intertwining these different classes of lubricants with the addressed bio-based friction modifiers, in question for this thesis, some alternative friction modifiers are already successfully used. Continuing with the topic of extrusion, inulin, being a soluble fiber with neutral taste promoting the good function of the intestine, was further investigated. The resulting high moisture of extruded products leads to a decrease in viscosity, due to the changes in the molecular structure of amylopectin, which further results in a low, a high apparent density and ultimately a low friction between dough and screw. Moreover, an increasing extrusion temperature and an increasing screw speed both lead to the opposite, namely a decreased apparent density, eventually depicting increasing friction between dough and screw. (Tsokolar-Tsikopoulos, Katsavou, & Krokida, 2015) Inulin was further considered as a texture modifier, as a fat replacer, in dairy products, where also oral friction was observed. In the paper 1wt %, 3wt % and 5wt % inulin was assessed. (Meyer, Bayarri, Tarrega, & Costell, 2011)

Next to inulin, fatty acid amide concentrations in 1wt %, 3wt % and 5wt %, including lauryl amide, myristyl amide, palmityl amide, stearyl amide, oleyl amide and erucic amide, were tested for their physicochemical and tribological properties. All compounds were determined to be good friction, antiwear and extreme pressure additives. Erucic amide has the lowest coefficient of friction and lauryl amide has the highest coefficient of friction for 150N and 500N base stock. The highest coefficient of friction is approximately 0.1, whereas the lowest coefficient of friction is approximately 0.02. (Khalkar, Bhowmick, & Pratap, 2013)

2.6.Risk management

Human influence is often underestimated in analytical validations, where all technical and instrumental parameters (accuracy, precision, reproducibility, repeatability, intermediate precision, specificity, detection limit, quantification limit and linearity) are considered. The instrumental parameters, namely accuracy, trueness, and precision, are further explained in chapter 2.6.3 and the subchapters. Consequently, human error can be assessed by using risk analysis. (Oldehof, et al., 2011)

These methods are further categorized in two generic groups namely inductive and deductive methods. Inductive methods include, among others, failure mode and effects analysis (FMEA) and deductive methods contain inter alia fault tree analysis (FTA). (Misra, 2008)

2.6.1. Cause-and-effect-diagram

Before conducting an FTA or FMEA analysis, brainstorming the problematic steps in the analysis are essential. After brainstorming, another crucial intermediate step includes an Ishikawa diagram also referred to as cause-and-effect-diagram. This diagram can either be used for an inductive or deductive system analysis and is a useful tool to identify the influencing parameters. When developing a completely new method, the entire test procedure can be evaluated, however also only single working steps can be discussed. (Meyer V. , 2007)

Figure 10 gives an exemplary application of the cause-and-effect-diagram in the oil industry in Iran:

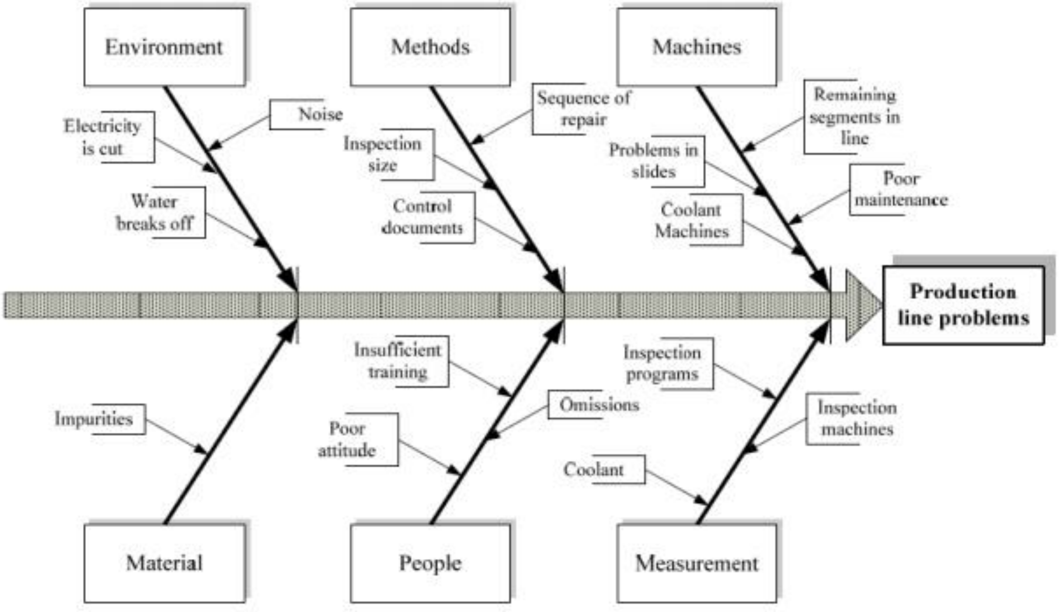

Figure 10: Exemplary cause-and-effect-diagram used in the oil industry in Iran (Hekmatpanah, 2011)

Among the 4 Ms (methods, machines, material, measurement) the cause-and-effect-diagram shown above also additionally includes environment and people.

2.6.2. FTA analysis

A fault tree analysis (FTA) is defined by depicting ways in which a system might fail by defining an undesirable event. As FTA analysis is a top-down deductive failure analysis, the causes for the undesirable event are listed on the bottom and by adding up those causes, the top event is obtained. (Misra, 2008) FTA analysis also enables a quantitatively evaluation based on the probability estimation of the occurrence of each risk factor. (Hyun, Min, Choi, Park, & Lee, 2015)

Figure 11 illustrates the general structure of an FTA analysis, which is commonly used for causal analysis in risk and reliability studies. (Rausand & Hoyland, 2004)

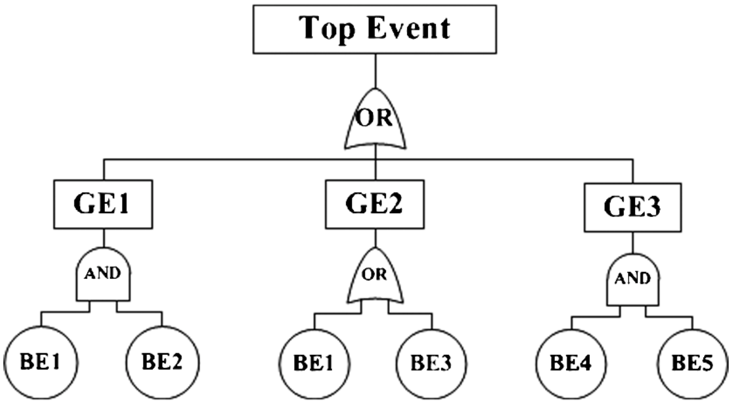

Figure 11: General structure of an FTA analysis (Abdollahzadeh & Rastgoo, 2015)

According to Rausand and Hoyland (2004), the first step is to define the top event clear and unambiguously. This is done by answering the questions “What?”, “Where?” and “When?”. As a second step, events causing this top event are defined. As it can be seen in Figure 11, there are both “and” and “or” gates that can be used. (Rausand & Hoyland, 2004)

2.6.3. Accuracy

Accuracy is a generic term for precision and correctness, as it is the total error measurement of the analysis. Thereby, a result is accurate, if it is free of random and systematic errors. To specify, if a result is accurate, the systematic error (trueness) and random error (precision including repeatability and reproducibility) are considered. By determining the accuracy, essential steps towards method validation are taken. (Wellmitz & Glutschke, 2005)

2.6.3.1. Trueness

Due to a systematic error, a deviation of the measured value from the “true” value occurs. (Wellmitz & Glutschke, 2005)

2.6.3.2. Precision

Using random error, the precision can be described by using the standard deviation or a confidence interval. (Wellmitz & Glutschke, 2005)

Precision determination includes both repeatability and reproducibility.

Repeatability can be measured by performing the same procedure on the same test object in the same laboratory by the same operator with the same equipment at different days.

Reproducibility can be obtained by measuring the same method on the same test object in the same laboratories by different operators with the same equipment.

(Wellmitz & Glutschke, 2005)

2.6.4. SWOT analysis

According to Sarsby (2016), SWOT (strength, weaknesses, opportunities, and threats) analysis is a popular strategy development framework and four-box strategy analysis. (Sarsby, 2016)

Figure 12 illustrates the SWOT analysis diagram.

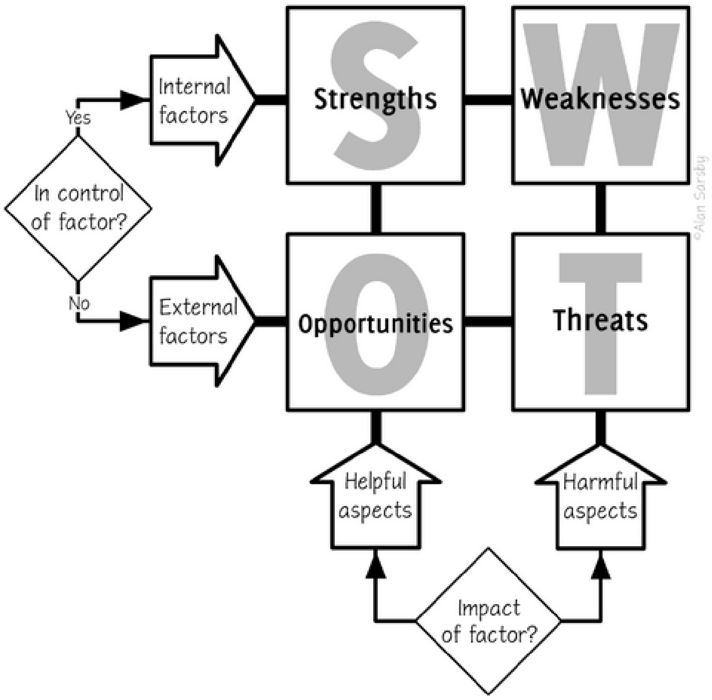

Figure 12: SWOT analysis diagram (Sarsby, 2016)

As it can be seen in Figure 12, a SWOT analysis is largely influenced by on the one hand internal and external factors and on the other hand by helpful and harmful aspects. Generally, the realization of a SWOT analysis should start by brainstorming about the external factors, being threats and opportunities. Further filling-in of the diagram should be done by using both matching, which connects the external to the internal factors, and converting, that changes a harmful to a helpful factor. (Sarsby, 2016)

3. Material and Methods

3.1. Materials

Table 3 depicts an overview of the used laboratory equipment.

Table 3: Laboratory equipment overview

Product description	Manufacturer	Type
ICP Spectrometer	Thermo scientific	iCAP7000 series
Rheometer MCR302	Anton Paar GmbH, Graz, Austria	Modular Compact Rheometer
FTIR – ATR	Bruker Optics GmbH Germany	Tensor 27
Stabinger Viscometer	Anton Paar GmbH, Graz, Austria	SVM 3000

Table 4 depicts an overview of the used base oils and additives used as friction modifiers.

Table 4: Conventional and bio-based friction modifiers overview

Product description	Manufacturer	Category
Polyalphaolefin (PAO) 8	OMV AG, Austria	Base oil
Borate ester	Infineum International Limited, United Kingdom	Additive
Oleamide	Infineum International Limited, United Kingdom	Additive
Methyl ricinoleate	Vertellus Specialties, United Kingdom	Additive
Tallow amine	Infineum International Limited, United Kingdom	Additive
ICP-grade water	VWR International, USA	Base oil
Glycerin	Sigma-Aldrich, USA	Base oil
Polyethylene glycol	Sigma-Aldrich, USA	Base oil
Hydroxypropyl methylcellulose	Alfa Aesar, Thermo Fisher Scientific, USA	Additive
Alginic acid calcium salt from brown algae	Sigma-Aldrich, USA	Additive
Agar	Sigma-Aldrich, USA	Additive
Salmon oil	Multifit Tiernahrungs GmbH, Germany	Additive
Rapeseed oil	Kronenöl, Austria	Additive

3.2. Methods

3.2.1. Infrared spectroscopy: Attenuated total reflection (ATR)

According to Hershel (1800), spectroscopy is a part of physics studying the intensity distribution of the electromagnetic radiation following to the wavelength and frequency. (Günzler & Böck, 1975)

The used infrared spectroscopy, attenuated total reflection (ATR), enables a rapid determination of components while using only small sample quantities. It is mainly used for an overview of the lubricant components, additives, and contaminants, but is also used for the purpose of interpreting spectra for contaminations and alteration procedures, such as sulfation, nitration, oxidation, and additive depletion. (Besser C. , 2015)

The measurements were conducted via a Bruker Tensor 27 FT-IR spectrometer (Bruker Optics GmbH, Ettlingen, Germany). The samples were applied onto an ATR crystal (in this specific case diamond) and were pressed with a constant and reproducible force onto the samples. The measurement was performed between the wavelengths 600 cm^{-1} and 4000 cm^{-1}, and an averaged spectrum of 30 repetitions was evaluated. The intensity of the monochromatic infrared radiation was detected after multiple reflections from the sample surface, which resulted in a transmittance measurement (in %). The interaction of the infrared radiation and the sample resulted in the excitation of molecular vibrations and the subsequent absorption of some infrared radiation. The wavenumber of the absorbed radiation is characteristic for the molecular vibration and corresponds to the Lambert-Beer law. The infrared spectrum was exported by LIMS (laboratory information management system) into the database, where it was adapted (e.g., baseline correction) and evaluated using the “OPUS” software (Version 5.0, Bruker Optics GmbH, Ettlingen, Germany). After the measurement, the device was cleaned with isopropanol and consequently the next sample was applied.

3.2.2. Elemental analysis - Inductively coupled plasma optical emission spectrometry (ICP-OES)

Inductively coupled plasma optical emission spectrometry (ICP-OES) is used for elemental analysis of the eligible friction modifiers (FM) and the aim is to determine the elemental content of a sample.

First, organic samples underwent a microwave assisted digestion. Performed via an Anton Paar Mulitwave Pro (Anton Paar GmbH, Graz, Austria). In doing so, 100 mg of sample, 3 mL of deionized water, 3 mL of nitric acid (supra quality) and 3 mL of hydrogen peroxide (supra quality) were inserted in a special Teflon vessel (liner). As a blank, 6 mL deionized water, 6 mL of nitric acid (supra quality) and 6 mL of hydrogen peroxide (supra quality) were added. The closed Teflon liners were inserted in a rotor. Intactness of the Teflon liners must be checked beforehand. Subsequently, the digestion of the samples began, where they were tempered at an elevated pressure for approx. 2 h. During this process, oxidative reactions took place, which converted the organic sample matrix into carbon dioxide, as well as most present inorganic elements were oxidized. The liners had to be closed and especially opened with care, due to the pressure inside the liner, which was caused by the carbon dioxide and nitric oxides that were formed during the oxidative digestion reaction. The liners were cleaned with isopropanol and deionized water. After microwave treatment of the samples, the prepared samples were diluted (filled up to 30 mL with deionized water), which resulted in a total dilution factor of 1:300. The dilution factor was determined gravimetrically by weighting the original sample and the total digested solution.

The ICP-OES measurements were performed on an iCAP 7400 duo spectrometer (Thermo Fisher Scientific, Waltham, Massachusetts, USA). The digested samples were introduced as aerosols into a plasma at a temperature of 6000 to 10000 °C, where the samples were further atomized and excited. The excited atoms emit radiation in the UV and VIS range upon reaching their respective ground state, where the wavelength of the radiation is characteristic for the respective elements. The emitted radiation of the samples was split by an optic into monochromatic parts (resolution < 0,1 nm) and detected by a CCD detector.

Quantitative determination was achieved by an external calibration, where the intensity of the samples was compared to a calibration matrix, which consists of multielement solutions and a blank solution corresponding to the digestion matrix. Additionally, two quality control (QC) measurements were performed, at the beginning and the end of the measurement sequence. The QC measurements consist of certified reference materials (CRM), namely a 100 ppm multielement standard in mineral oil (similarly prepared by microwave-assisted digestion) and a 1000 ppm multielement standard in water. The calibration of a single wavelength was considered valid if both the 100 ppm and 1000 ppm CRMs were within ± 10% of the nominal value.

All reported elements were measured at 3 independent wavelengths, to mitigate the possibility of spectral interferences falsifying the quantification. Furthermore, three repetitions of every sample were performed. The reported concentrations were averaged from the three measurements on all wavelengths (on total nine values), whereas the validation-criteria was a standard deviation under 10 % of the mean value. In case the measured emission was above the most concentrated calibration standard, the digested samples were further diluted (1:100) and re-measured by the ICP-OES.

Generally, the ICP-OES can detect all chemical elements, except halogens, inert gases, hydrogen, oxygen, and carbon. Additionally, it must be stated that the ICP-OES only provides information about the concentration of an element, however it does not assess the chemical binding state.

(Thermo Scientific , 2015) (Besser, et al., 2019) (Dörr, Agocs, Besser, Ristic , & Frauscher, 2019)

3.3. Tribological analysis

After calculating and testing the minimum and maximum capacities of the rheometer by, among others prolonging the measurement duration, the following settings were chosen:

Table 5: Normal force settings for Stribeck curve and Stribeck curve settings

	300 points 1 s per point
$F_{N.Tribo}$	5 N
T	80 °C

	81 points (30 minutes)
$F_{N.Tribo}$	5 N
v_S	1E-08 to 0,1 m/s

The absolute maximum sliding speed of the rheometer MCR 302 is 1.41 m/s. However, as soon as the sliding speed exceeded 0.1 m/s, the plates were destroyed (see Appendix 7, Appendix 38 and Appendix 39), resulting in immense wear production. Therefore, 0.1 m/s was chosen to be the maximum sliding speed of the performed tests. As a minimum sliding speed 1E-08 m/s, being the absolute minimum, was defined. Additionally, one empty run without sample is recommended before testing samples, indicated by reproducibility studies. Sample amounts between 0.7 and 1 mL were used. The total normal force (10.61 N) was calculated using the following formula depicted in Figure 13.

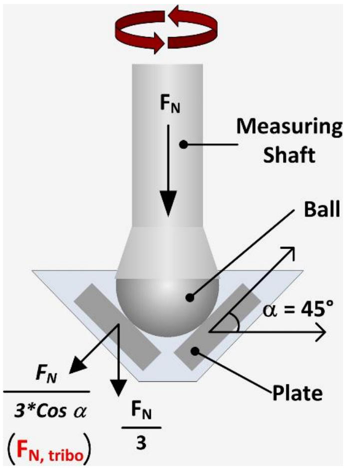

Figure 13: Formula for F_N calculation (Anton Paar, 2020)

Figure 14 depicts an exemplary measurement of PAO8 at 80 °C.

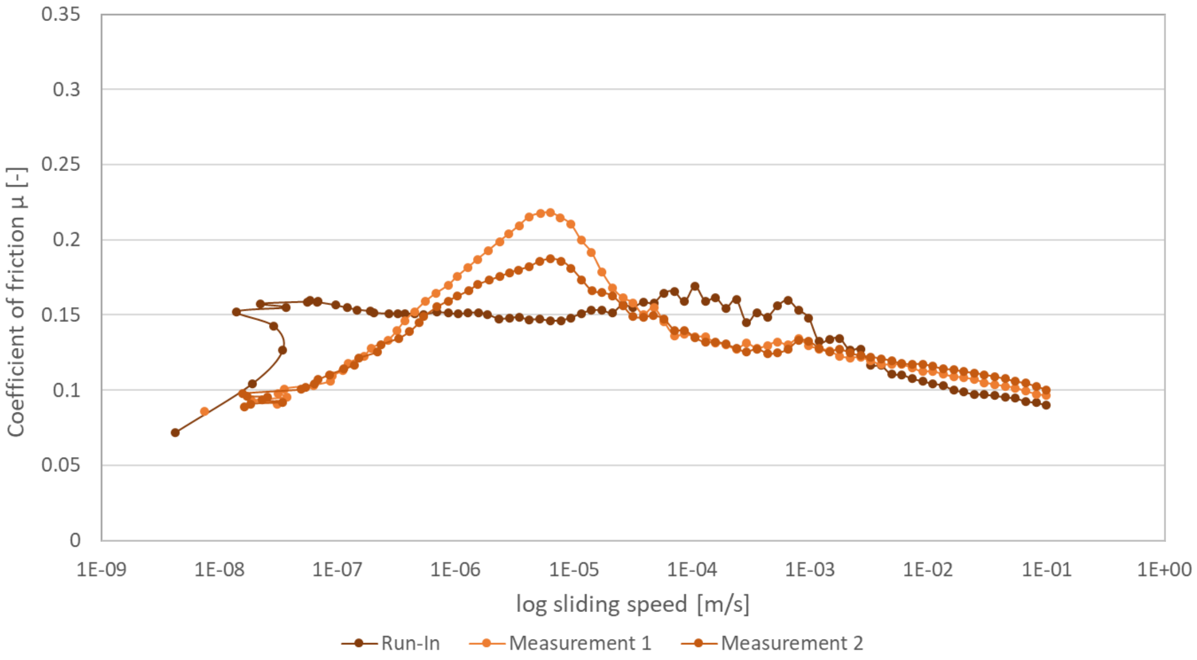

Figure 14: PAO8 80 °C run-in, 1st measurement and 2nd measurement with a maximum coefficient of friction of 0.35 µ

The Stribeck curve settings are repeated 3 times on the same point of the plates and ball, whereas the first of those represent the run-in, where plates and ball adjust to the sample. The run-in is not considered for the data evaluation and mean values of the 1st and 2nd measurement represent the final Stribeck curve for the individual samples.

After every sample, the set-up must be disassembled, all parts are placed in a measuring beaker filled with isopropanol and are placed in the ultrasonic bath for at least 10 minutes. Additionally, when using new parts (balls or plates), these also must be cleaned with isopropanol before using them for the first time.

4. Results and Discussion

4.1. Chemical analysis

4.1.1. Infrared spectroscopy – Attenuated total reflection (ATR)

When the light and the respective compound interact, light quantum absorption is caused resulting in the attenuation of light intensity. Every molecule species has a unique energy demand, making the infrared spectroscopy specific for every substance. Figure 15 illustrates an exemplary ATR-Spectrum interpretation for the bio-based friction modifier, salmon oil. (Coates, 2000)

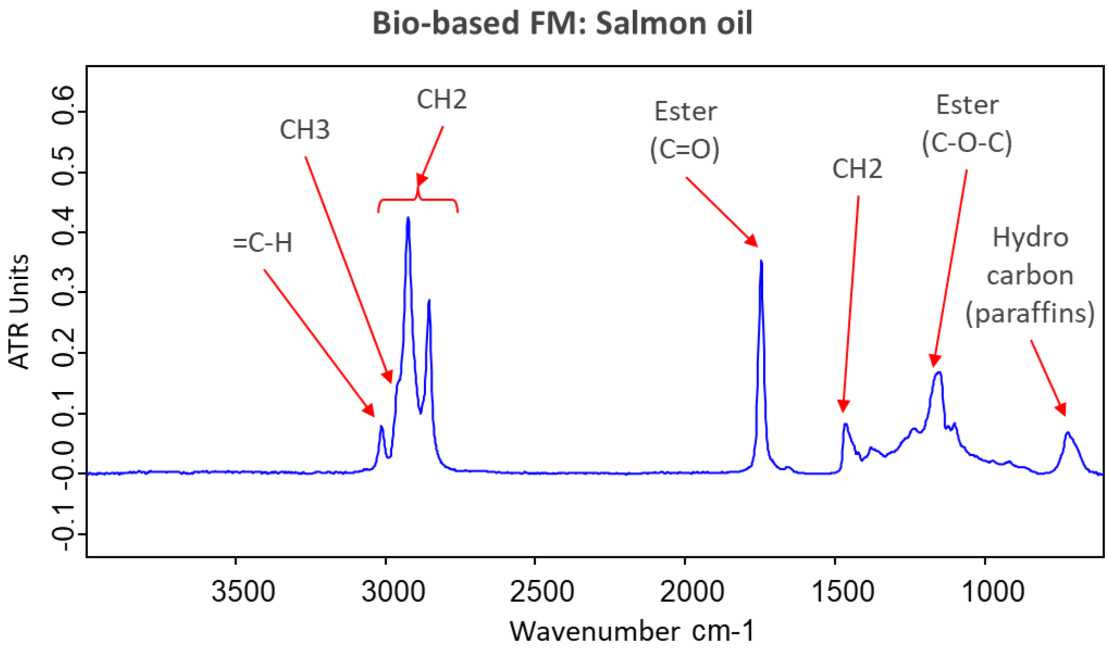

Figure 15: Exemplary ATR-Spectrum Salmon oil

Results of the ATR analysis can be found in Appendix 4. Generally, it can be stated that both the conventional and the bio-based FM depict the expected bands.

4.1.2. Elemental analysis – Inductively coupled plasma optical emission spectrometry (ICP-OES)

The results for the ICP-OES analysis can be found in Appendix 5. Results marked in yellow indicate high amounts of elements. Alginic acid salt depicts high amounts of calcium (Ca), magnesium (Mg), sodium (Na) and sulfur (S). For alginic acid salts, the high amount of calcium and sodium is due to the reaction with those metals to form alginates, the high amount of magnesium is because of the natural weathering of mineral-bearing rocks, whereas the amount of sulfur can be traced back to an approximately 33 % residue of sulfates. (Sigma Aldrich, 2020) Similarly, agar depicts high amounts of calcium (Ca), magnesium (Mg) and sodium (Na). For agar, an addition of 2 to 4.5 % ash leads to the high amount of calcium, whereas also the addition of salts in agar enlightens about the high amounts of both calcium, magnesium, and sodium. (Sigma Aldrich, 2020) As expected, the boric (B) amount of borate ester is out of the detection range. The elements copper (Co), lithium (Li), molybdenum (Mo), lead (Pb), tin (Sn), antimony (Sb), vanadium (V), tungsten (W) and zinc (Zn) are marked in green, as for all samples the values are below the minimum. These stated elements are essential for the detection of additives used in fully formulated oil, such as zinc dithiophosphate (ZDDP). Summarizing the ICP-OES results, these are not surprising, since most of the analyzed samples in question consist of carbon, hydrogen, and oxygen, except for borate ester and alginic acid calcium salt.

4.2. Tribological analysis

4.2.1. Method development

4.2.1.1. Selection of tribological contact and material

Anton Paar GmbH on the one hand offers a ball-on-three-pins set-up and on the other hand a ball-on-three-plates set-up for tribological analysis. Table 6 gives an overview of the materials for both set-ups:

Table 6: Comparison of tribological materials (ball-on-three-plates v.s. ball-on-three-pins) (Saarstahl, 2020) (HSM Hochleistungswerkstoffe Stahl & Metall, 2020)

	Ball & pins (100Cr6)	**Plates (stainless steel)**
Carbon [%]	0.90-1.05	≤ 0.07
Silicon [%]	0.15-0.35	≤ 1.00
Manganese [%]	0.25-0.45	≤ 2.00
Chrome [%]	1.35-1.65	17.5-19.5
Nickel [%]	≤ 0.30	8.0-10.5
Phosphor [%]	≤ 0.030	≤ 0.045
Sulphur [%]	≤ 0.025	≤ 0.03
Cupper [%]	≤ 0.30	≤ 0.11
Hardness Rockness C [%] HRC	60-66	27-39
Hardness Vickers [%] HV	700-860	280-380

The ball for both set-ups is made of 100Cr6 and has a diameter of 12.7 mm, due to a chrome content of less than 10.5 %, the ball is not considered stainless steel. (Rähse, 2014) The essential difference between the ball-on-three-pins and ball-on-three-plates set-up is the chemical composition leading to a different hardness of the pins and plates. The 6x25x3 mm plates are made of 1.4301 steel, which consist of more than 10.5 % chrome and are thereby considered stainless steel. (Rähse, 2014) Stainless steels are characterized by forming a thin, superficial protective layer when reacting with air. This protective layer regenerates itself after minor damage under the influence of air and moisture. (Rähse, 2014) Alternatively to the stainless-steel plates, the pins are made out of 100Cr6, like the ball.

Both the ball-on-three-plates set-up and the ball-on-three-pins set-up were tested on the rheometer MCR 302 by Anton Paar (see Figure 16).

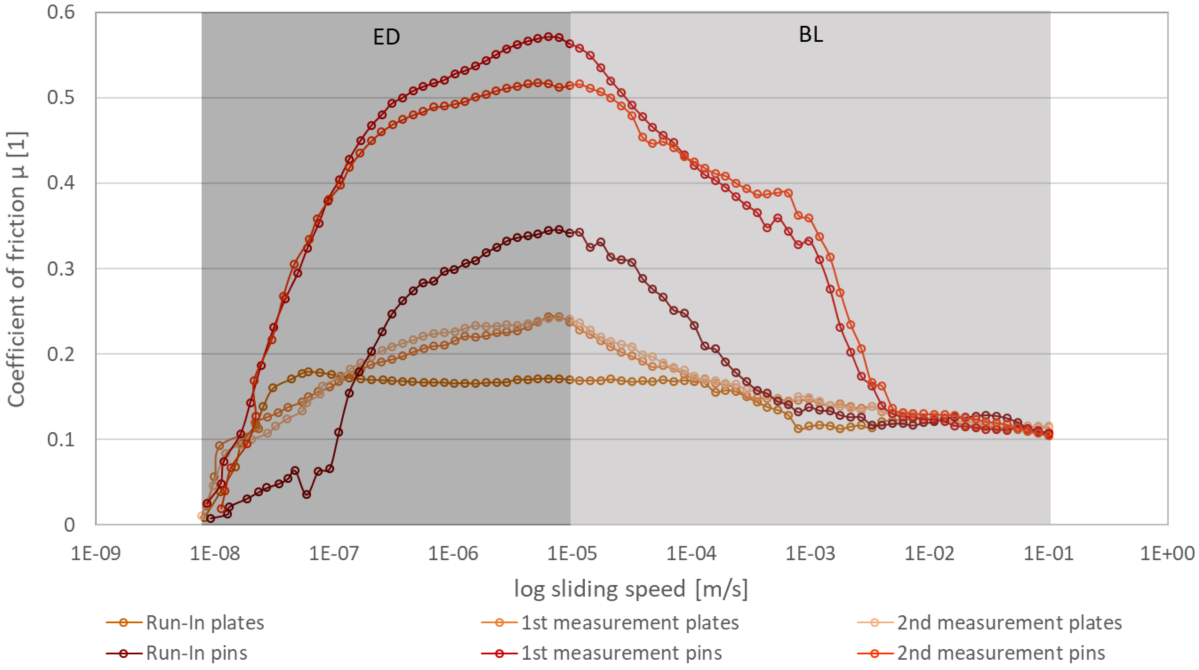

Figure 16: Measurements ball-on-three-pins versus ball-on-three-plates PAO8 80 °C with a maximum coefficient of friction of 0.6 µ and the calculated regime of lubrication (5 N)

Figure 16 illustrates why the run-in was not used for data evaluation; only the mean values of measurement 1 and 2 were evaluated. Moreover, the results show an increased coefficient of friction for the ball-on-three-pins set-up, however the same curve progression for pins versus plates set-up was observed. The increased coefficient of friction can be explained by the fact that both the ball and the pins are made of 100Cr6. Generally, 100Cr6 balls are the standard material for axle bearings. As mentioned above, 100Cr6 has a higher HRC than stainless steel, which is the material used for the plates. For all further tribological tests, the ball-on-three-plates set-up was chosen. The reason for that was that the ball-on-three-plates set-up and the ball-on-three-pins set-up indicate the same trend, and both lead to reproducible data for further evaluation. On the other hand, stainless steel is mandatory needed in the chemical, pharmaceutical and food industry and therefor preferentially used in the tribotests. (Rähse, 2014) Providing additional information, the theoretically calculated lubrication regime for PAO8 is illustrated by the light grey chart above the curves (boundary lubrication BL), mixed and elastohydrodynamic lubrication were not reached according to the theoretical calculation. The dark grey chart illustrates the run-in, effectively the assimilation of the material i.e., elastic deformation (ED). This theoretical lubrication regime calculation is further explained in the next paragraphs.

4.2.1.2. Selection of parameters

By using the minimum film thicknesses (Hm), surface roughness tests and the calculated α-values, λ-values were calculated for different normal forces [N] being 0.01 N, 0.1 N, 0.5 N, 1 N, 5 N and 10 N (see Appendix 25) according to chapter 2.1.1.

From this table it can be stated that with increasing normal force, the λ-value decreases, however that the normal force itself does not significantly alter the λ-values. It must be noted that the rheometer MCR302 has a limitation in the appliable normal force and speed. The maximum normal force that can be applied is 50 N. However, the recommended maximum tribological normal force for Stribeck curves by the manufacturer is only 5 N (equaling 10.61 N total normal fore according to the calculation in chapter 3.3). The minimum sliding speed is 1E-09 m/s. When taking Appendix 25 into account it can be noted that the sliding speed has more impact on the lambda-values, than the normal force, which is also in correlation with literature presented in chapter 2.4.1. Therefore, the recommended normal force setting of 5 N and the absolute minimum sliding speed (1E-09 m/s) up to the maximum sliding speed (0.1 m/s), where no wear was observed, were chosen as test parameters.

The chosen sliding speeds apply to human applications, including among others the human knee during walking (0.05 m/s) (Burris, Ramsey, Graham, Price, & Moore , 2019) and eye movement (0.0001 m/s) (Sterner, et al., 2017). An example from the food industry is e.g., a twin-screw extruder, which can reach 8 to 60 turns per minute, whereas the rheometer MCR302 can perform up to 3000 turns per minute. (Vauck & Müller, 1999) Another machine comparable to an extruder used in food production is a two-roll press, operating with a roll circumferential speed of 0.2 to 1 m/s, which is also comparable to the rheometer MCR302, operating from 1E-8 to 1.4 m/s. A two roll press is among others used for the production of pellets. (Vauck & Müller, 1999)

Figure 17 illustrates the run-in, first measurement (repetition 1) and second measurement (repetition 2) of PAO8 at 80 °C when applying 5 N and 10 N respectively. The charts above the Stribeck curves indicate the theoretically calculated lubrication regime of PAO8 at 80 °C, when applying 5 N.

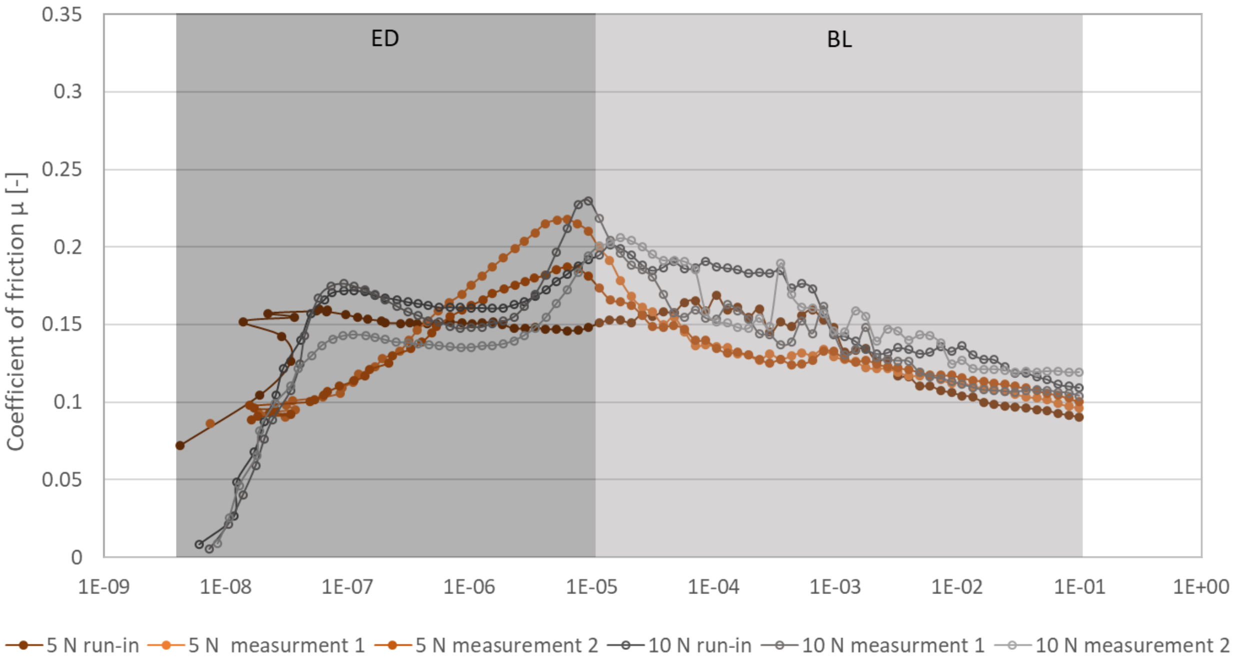

Figure 17:PAO8 80 °C different normal force settings (5 N and 10 N) with a maximum coefficient of friction of 0.35 µ

Similar to Figure 6 and Figure 7, Figure 17 depicts that the normal force does not significantly alter the resulting Stribeck curve, as expected, and discussed in chapter 2.4.1.

Figure 18 demonstrates the effect of changing the measurement duration when using the same sample (PAO8) and the same remaining settings (10 N and 80 °C).

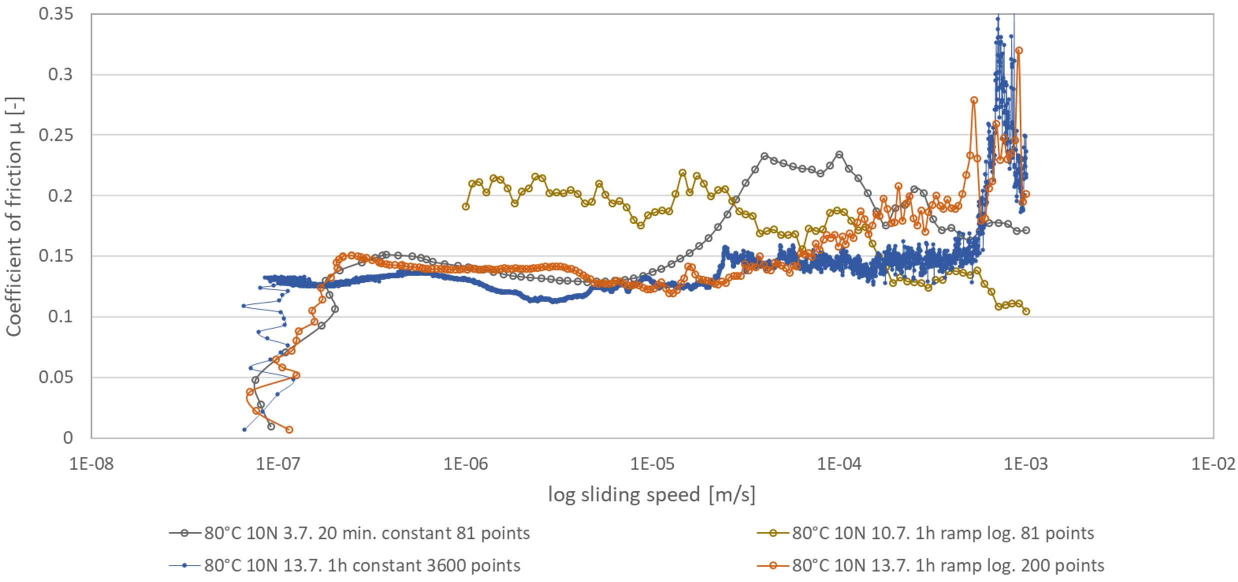

Figure 18:PAO8 80 °C 10 N changing the duration of tests with a maximum coefficient of friction of 0.35 µ

According to Figure 18 the measurement “80 °C 10N 10.7. 1 h ramp log. 81 points” depicts a measurement error. This measurement error might have been caused by poorly closed screws to fixate the plates in the plate holder.

When comparing the other three curves in Figure 18, the setting “constant” or “logarithmic ramp” seems to largely influence the resulting Stribeck curves, especially from the sliding speed 1E-05 onwards. In the main part of the Stribeck curves (1E-07 to 1E-05), the different settings (logarithmic ramp/constant and different number of points) do not influence the resulting Stribeck curves dramatically, as the curves stay within ± 0,5 µ (coefficient of friction). Notably, the total measuring time (20 min or 1 h) also does not significantly change the resulting Stribeck curves.

The effect of different measurement days (repeatability) and different operators (reproducibility) will be further discussed in chapter 4.3.3.

4.2.1.3. Base oil and additive selection and concentration

Following the viscosity and lambda-value calculations for all potential base oils in question, it was decided to use PAO8 as base oil for the blends with conventional friction modifiers (1wt %). For the bio-based friction modifiers a water-soluble basic solution as a potential environmentally friendly alternative to the conventional base oils, was suggested. According to Xie, et al. (2015) water lubricated bearing has great potential for energy conservation, sustainable development and environmental protection and has therefore already been used in water pumps and ships. Tribological tests were among others performed on a water lubricated bearing test rig. (Xie, Rao, Na, Liu, & Chen, 2015) Distilled ICP-grade water was chosen as reference when comparing with bio-based lubricants. In Brazil, the mineral diesel contains a very low sulfur concentration (10 ppm), causing a deficiency in lubricity, further affecting the performance, which ultimately leads to failures of engines. In some studies, the effect of glycerin as friction modifier and antiwear additive was tested in different concentrations (7.5 % and 15 %), resulting in improved lubricity (decreased friction) and wear reduction. (Uchoa, Neto, Santos, & Neto, 2017) Recently, nanoparticles arose as interesting new friction modifiers, including studies on silver nanoparticle-enhanced polyethylene glycol (PEG) lubricants. These lubricants exhibit next to great reductions in wear and friction, at already 1.5% wt PEG, also excellent stabilities due to coating agents, i.e., poly(vinyl pyrrolidone). Additionally, Stribeck curve analysis indicated that friction is not only reduced in boundary lubrication, but also in mixed lubrication. (Ghaednia, Hossain, & Jackson, 2016)

Consequently, glycerin and polyethylene glycol were selected as benchmarks for water-soluble basic solutions. As it can be seen in Figure 19, polyethylene glycol tribologically performed best under the given parameters for the tribological tests.

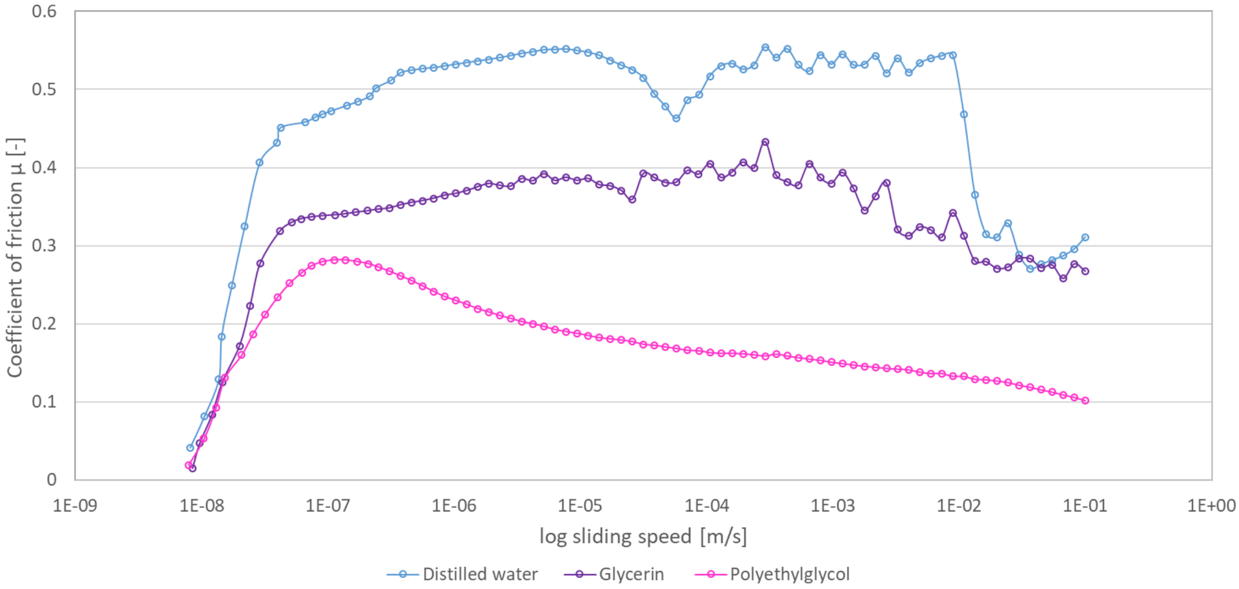

Figure 19: Mean bio-based references 30 °C with a maximum coefficient of friction of 0.6 µ

The goal for the bio-based basic solution being spiked with bio-based friction modifiers was thereby to obtain a Stribeck curve comparable to the best benchmark (polyethylene glycol). It must be noted that all benchmarks were used in pure and non-additive form. Generally, literature also suggests a combination of mineral oils and a low concentration of vegetable oil or fat may impart the oiliness and thereby make the spiked mineral oil as effective in reducing wear and friction, as the pure vegetable oil or fat. (Spikes H. , 2015) Consequently, this suggestion will also be considered in this thesis.

The test temperature for the conventional friction modifiers in PAO8 was 80 °C, since this is in the range of typical oil sump temperature. Additionally, friction modifiers ought to work at the beginning of mixed lubrication and at moderate temperatures, before for example anti-wear additives intervene. (Mang & Dresel, 2017) Due to the expected instability of bio-based friction modifiers at elevated temperatures, initial tests with distilled water as reference when comparing with bio-based lubricants were performed at 30 °C. Continuative tests for the bio-based friction modifiers were performed by adding 1wt % and 3wt % to distilled water at 30 °C. Further tests also included adding those amounts of bio-based friction modifier to PAO8 at 80 °C, to directly compare it to the PAO8 1wt % conventional friction modifier mixtures.

Lastly, the effect of the best performing bio-based friction modifiers was observed, by further measuring those additives without basic solutions, including both dipping of the material and pure solutions (approximately 0.7 mL per tribological test).

Further explaining the used concentration of friction modifiers, the recommended concentration in basic solution of 1wt % for the conventional (OFM) friction modifiers, was also used for the bio-based friction modifiers. (Tang & Li, 2014) According to the product information sheet of Sigma Aldrich, 1wt % Hydroxypropyl methylcellulose (HPMC) is soluble in water, being the basic solution for the tribological tests. (Sigma Aldrich, 2020) Therefore, next to a concentration of 1wt %, 3wt % were also tested, as Hiremath et al. (2019) state the recommended usage being 2 to 5wt % HPMC in water. (Hiremath, Nuguru, & Agrahari, 2019) The recommended manufacturing method for HPMC was used for all bio-based friction modifiers. (Aldrich, 2003) This procedure includes heating 1/3 of the required volume of water to 90 °C, adding the sample while stirring on the magnetic stirrer and further adding the rest (2/3) of the cold water. Afterwards 30 minutes stirring is recommended. The conventional friction modifiers were stirred for 1h at 60 °C and 600 rpm on the magnetic stirrer. Due to solubility problems, oleamide was additionally stirred 10 minutes at 120 °C at 600 rpm. As mentioned above, the bio-based friction modifier and distilled water mixtures were only measured at 30 °C, because of the possible temperature instability. Consequently, the bio-based mixtures were also stirred for 1 hour [h] at 600 rpm, but only at room temperature.

HPMC was chosen, as biopolymers have already been used as lubricant additives, offering a green and sustainable alternative. (Mu, Shi, Hua, Zhuang, & Zhu, 2017) The general knowledge of viscosity alteration due to the usage of agar, lead to the inclusion of agar as bio-based friction modifier. Microalgae were chosen, as they have a fast growth rate and can survive harsh conditions. Therefore, polysaccharides, including alginic acid (see chapter 2.3.1) being products of algae, were selected as potential friction modifiers. Moreover, microalgae could also be used for lipid production, as they mainly produce unsaturated fatty acids, like rapeseed oil. (Tang, et al., 2020) Additionally, edible bio-based natural products like salmon oil and rapeseed oil were taken under consideration for the tribological test, as they are both pure and easily accessible. Next to the pure versions, the interest arose to further inspect these oils as possible waste products, however in this case purification steps must be considered. (El-

Mashad, Zhang, & Avena-Bustillos, 2008) Generally, plant and vegetable oils, like rapeseed oil, have been used as alternative fuels for some years. When using oils directly, several disadvantages arise like high viscosities, further leading to poor fuel atomization during injection and ultimately incomplete combustion. These problems can be overcome by further converting the oils into biodiesel (i.e., fatty acid alkyl esters). Most research on biodiesel has been done on soybean oil and rapeseed oil in the United States and Europe, respectively. Much less research was performed on converting animal-based oils into biodiesel, even though an estimation of over a million tons of fish by-products are annually generated by fishing industries in solely Alaska. (Chiou, et al., 2008) Worldwide, 250 000 MT of fish processing waste from salmon farming could be converted into useful products, like for example biodiesel. (El-Mashad, Zhang, & Avena-Bustillos, 2008) With that knowledge, salmon oil was further inspected in this thesis, as additionally no substantial tribological tests were found (see chapter 2.4).

Lastly, lubricants, being fully formulated and edible for the use in skin contact, were taken under consideration for tribological tests. Among other reasons, they were tested as they are composed of among others both cellulose and glycerin.

The internal standard operating procedure (SOP) can be found in Appendix 3.

4.2.2. Conventional versus bio-based friction modifiers

The following sub-chapter visualizes the results of the tribological tests of the conventional versus bio-based friction modifiers (FM).

Figure 20 compares the conventional reference (PAO8) with the 1wt % conventional friction modifiers at 80 °C.

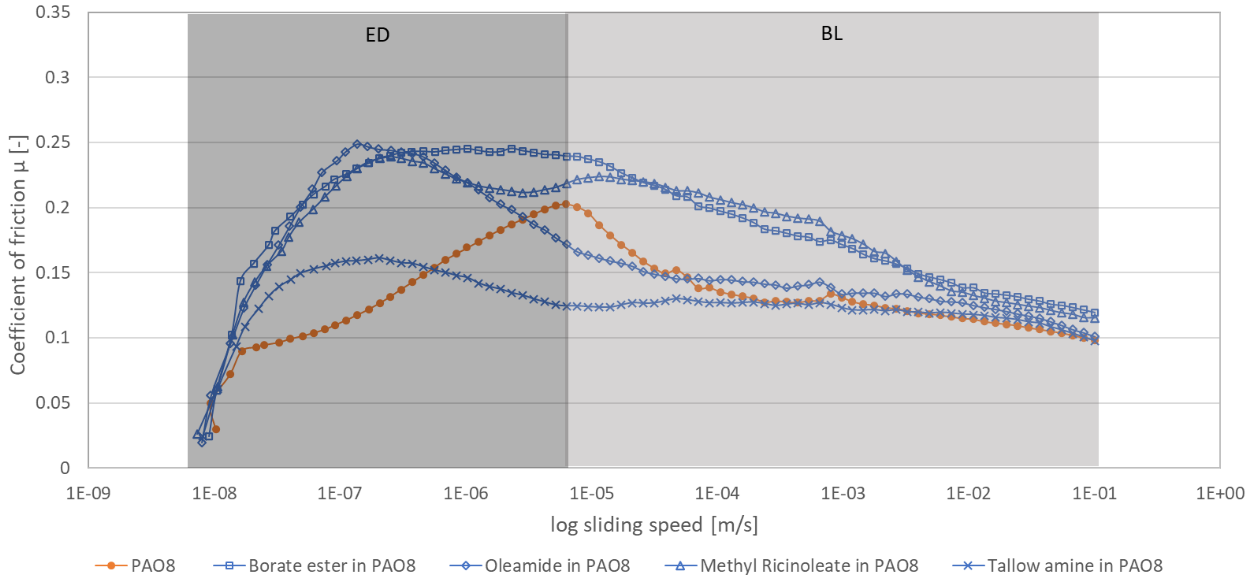

Figure 20: Mean curve of conventional reference versus 1wt % conventional FM in PAO8 at 80 °C with a maximum coefficient of friction of 0.35 µ

Regarding the mean PAO8 curve in correlation to the conventional friction modifiers, it seems as if PAO8 results in a longer run-in time. Comparing tallow amine in PAO8 to the other friction modifiers (borate ester in PAO8, oleamide in PAO8 and methyl ricinoleate in PAO8), tallow amine in PAO8 has a very low maximum coefficient of friction [µ]. Moreover, oleamide in PAO8 has the steepest slope, indicating stick-slip friction, as the sliding velocity increases, and the coefficient of friction decreases drastically. Generally, stick-slip friction occurs when the static coefficient of friction is higher than the dynamic coefficient of friction. This effect disappears as soon as the two friction partners are completely separated by the lubricant, indicating elastohydrodynamic lubrication. (Derler & Rotaru, 2013)

Figure 20 indicates that all samples slowly slide to the end of boundary lubrication, as indicated by the charts in the graph, which are the theoretically lambda regime calculations for PAO8. Summarizing the conventional friction modifiers (1wt %), in boundary lubrication tallow amine in POA8 can be significantly distinguished from the other conventional friction modifiers in PAO8. To achieve the desirable tribological behavior, at first a high coefficient of friction, then a steep slope (namely stick-slip friction) and towards mixed lubrication, where friction modifiers are supposed to work (Mang & Dresel, 2017), a very low friction, the combination of a mixture of friction modifiers should be considered. Probably by creating a mixture of two linear molecules oleamide and tallow amine in PAO8 (see 2.3.1), the tribological behavior could be driven towards the optimum.

Figure 21 compares the bio-based reference (distilled water) with the benchmarks (glycerin and polyethylene glycol) and the bio-based 1wt % friction modifiers mixtures in distilled water at 30 °C.

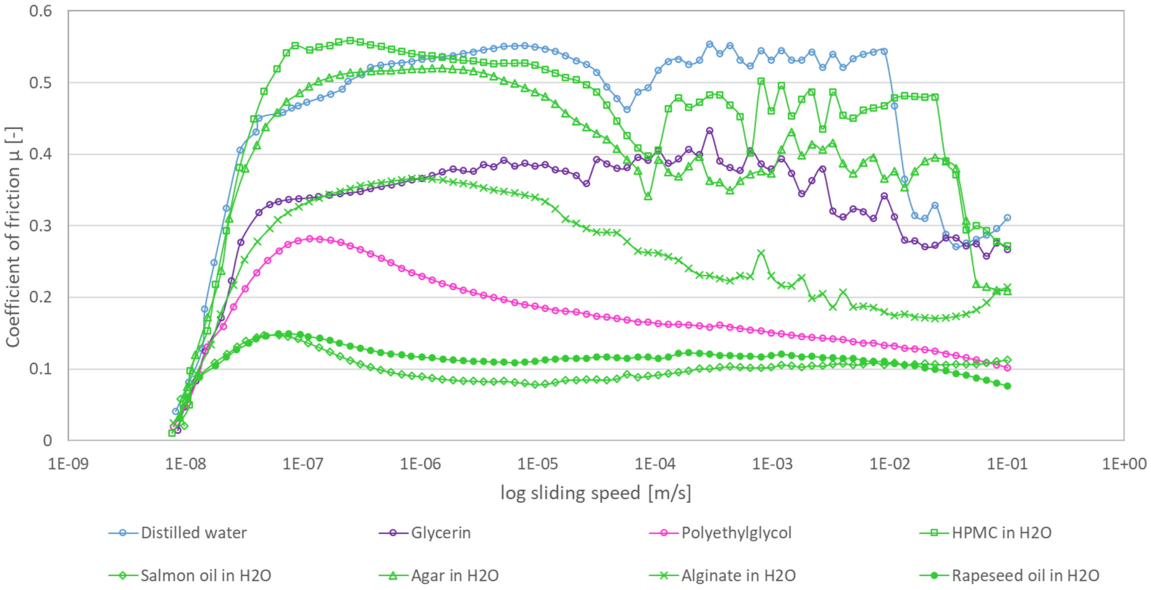

Figure 21: Mean curve of bio-based reference and benchmarks versus bio-based FM at 30 °C with a maximum coefficient of friction of 0.6 µ

Regarding the wear scars in Appendix 7 the reflected-light microscope images indicate similar wear scars for polyethylene glycol and glycerin, even though they seem to affect different layers of the surface. The high coefficient of friction for the distilled water measurement, can also be confirmed by the huge wear scar depicted in Appendix 27. Comparing the bio-based reference (distilled water) to the bio-based friction modifiers (1wt %) it can seen that alginic acid calcium salt from brown algae in distilled water, salmon oil in distilled water and rapeseed oil in distilled water behave different than the reference (distilled water). Hydroxypropyl methylcellulose in distilled water and agar in distilled water do not seem to have an influence, as their Stribeck curves cannot be significantly discriminated from the reference. Moreover, it must be noted that hydroxypropyl methylcellulose in distilled water produces the highest and salmon oil in distilled water and rapeseed oil in distilled water produce the lowest coefficient of friction [µ]. Like oleamide in PAO8 (see Figure 20), alginic acid calcium salt from brown algae in distilled water indicates the steepest slope, which might be caused by a stick-slip effect. Concerning hydroxypropyl methylcellulose in distilled water it must be noted that a yellowish color change before and after the tribological test was observed. This color change might be due to the mechanical impact of the tribological test or due to an oxidation reaction of the materials and solutions used.

For the agar mixtures in distilled water, it was seen that the agar sedimented after the tribological test. This sedimentation could be caused by the missing linkage between water and agar, as the temperature during the test (30 °C) was not high enough, even though the agar was dispersed in distilled water before the measurement.

Figure 22 compares the conventional friction modifiers at 80 °C and the bio-based friction modifiers at 30 °C, both at 1wt %.

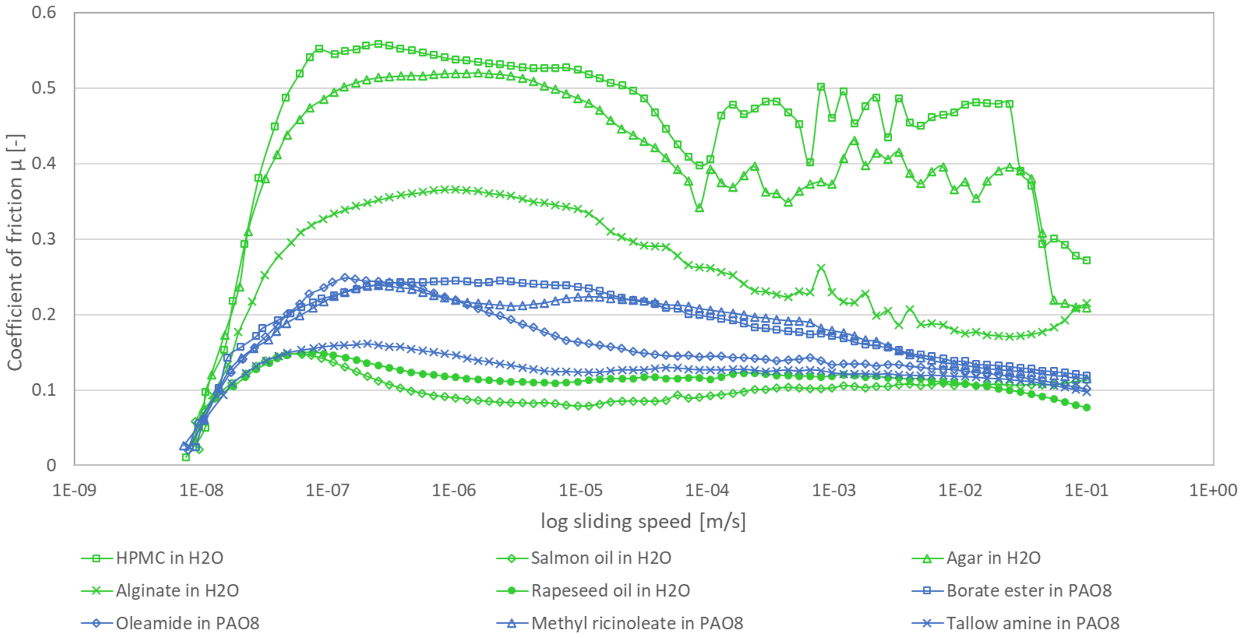

Figure 22: Mean curve of conventional FM at 80 °C versus bio-based FM at 30 °C with a maximum coefficient of friction of 0.6 µ

Comparing the conventional to the bio-based friction modifiers, notably at different temperatures due to their optima, however at the same (1wt %) concentration, both salmon oil in distilled water and rapeseed oil in distilled water perform better than the best conventional friction modifier, tallow amine in PAO8. Moreover, it can be noted that all conventional friction modifiers perform similar (0.1 to 0.25 µ), whereas huge difference in coefficient of friction can be seen for the bio-based friction modifiers. Figure 22 indicates that bio-based friction modifiers can be at least as good as conventional friction modifiers at their respective optima.

This raises the question, whether bio-based friction modifiers also perform at least as good as conventional friction modifiers under the same (PAO8 at 80 °C) conditions.

Before discussing results concerning this question, the concentration effect (1wt % and 3wt %) of bio-based friction-modifiers had to be clarified (see Figure 23).

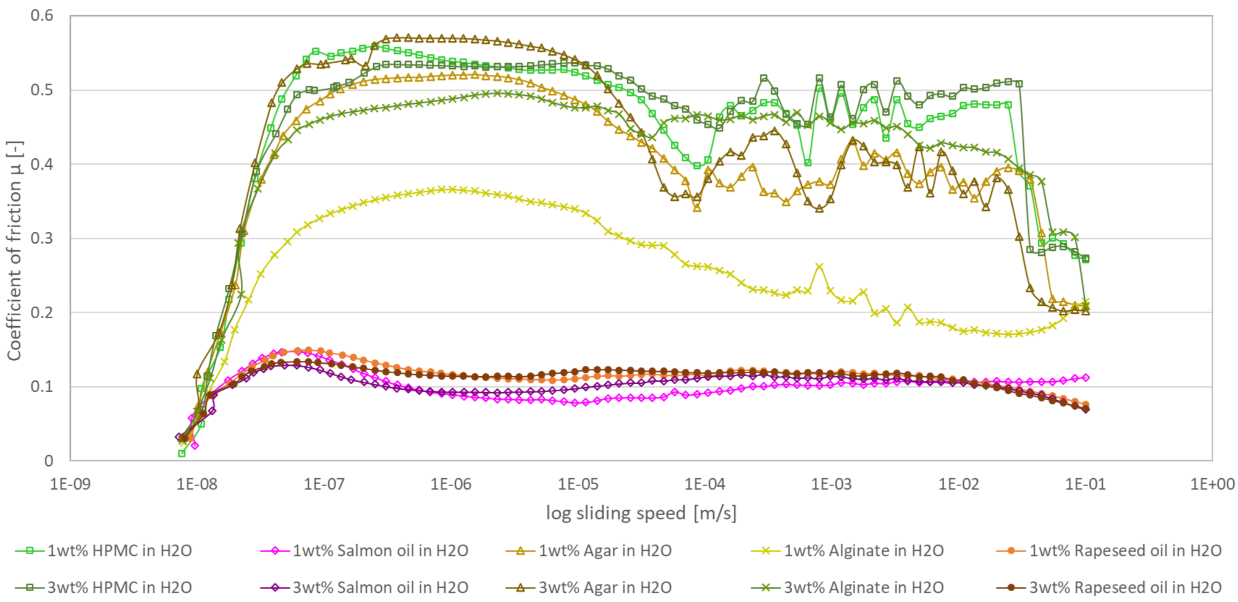

Figure 23: Mean curve of 1wt % bio-based FM at 30 °C versus mean curve of 3wt % bio-based FM at 30 °C with a maximum coefficient of friction of 0.6 µ

In the figure above it can be clearly observed that only for alginic acid calcium salt from brown algae in distilled water a concentration effect can be seen. For alginic acid calcium salt from brown algae in distilled water the critical concentration is 1wt %, as the maximum coefficient of friction [µ] increases from 0.38 µ to 0.5 µ. For all the other bio-based friction modifiers no concentration effect concerning the lubrication properties can be identified. Comparing this to the wear scar images by the reflected-light microscope, it must be stated that for salmon oil the 3wt % dilutions seem to have a slightly bigger wear scar in relation to the pure and 1wt % dilution, indicating that a higher concentration than 1wt % of salmon oil in water does not significantly improve the lubrication of the materials. For rapeseed oil the pure and both dilutions (1wt % and 3wt %) images all depict comparable wear scars. (see Appendix 7)

Figure 24 compares the conventional friction modifiers and the bio-based friction modifiers under the same conditions (80 °C in PAO8) including the reference (PAO8).

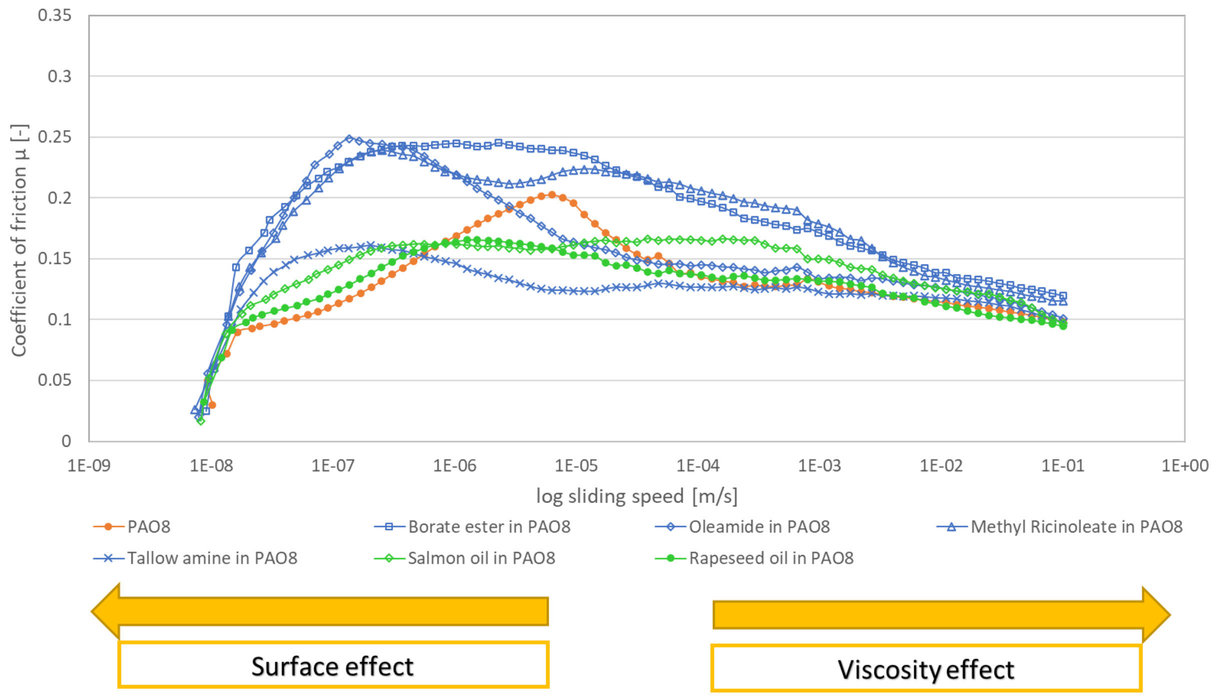

Figure 24: Mean curve of conventional FM versus mean curve of bio-based FM under the same conditions including the reference (PAO8) with a maximum coefficient of friction of 0.6 µ

According to the figure above it can be stated that salmon oil in PAO8 and rapeseed oil in PAO8 can perform as good as tallow amine in PAO8 under the same conditions. However, rapeseed oil in PAO8, salmon oil in PAO8 and tallow amine in PAO8 all perform significantly different than oleamide in PAO8, borate ester in PAO8 and methyl ricinoleate in PAO8. The yellow errors below the figure indicate that during the tribological test at low sliding speed the surface of the materials mainly influences the coefficient of friction, due to a pronounced liquid film leading to less solid-solid interactions. The higher the sliding speed gets, the less influential the speed is and the more impact the viscosity of the used lubricant has. In chapter 2.1.1 the importance of the viscosity for the Stribeck curve is stated. Following these statements, the figure indicates that for rapeseed oil in PAO8 and salmon oil in PAO8 the viscosity probably plays a bigger role than for tallow amine in PAO8, as the maximum coefficient of friction [µ] is prolonged for the bio-based samples.

Moreover, when comparing the curves to the reference curve (PAO8), Figure 24 visualizes that certain friction modifiers neutralize the effect of PAO8 more than others. Borate ester for example neutralizes the effect of PAO8 completely by dissolving the “valley” of the curve. Lastly, it can also be speculated for salmon oil and rapeseed oil in PAO8 at 80 °C that a state between boundary and mixed lubrication is reached at 0.1 m/s, which is in line with the theoretically expected working range of friction modifiers. (Mang & Dresel, 2017)

Table 7: Viscosity-temperature values [mm²/s] for liquid references (PAO8 and H_2O) and samples determined by Stabinger viscosimeter SVM 3000

Temperature [°C]	**Sample**	**Viscosity-temperature [mm^2/s]**	**Temperature [°C]**	**Sample**	**Viscosity-temperature [mm^2/s]**
30	PAO8	69.39	80	PAO8	12.48
30	Distilled water	0.878	80	Borate ester	5.14
30	Borate ester	60.89	80	Methyl ricinoleate	5.07
30	Methyl ricinoleate	25.01	80	Tallow amine	15.95
30	Tallow amine	126.19	80	Salmon oil	10.35
30	Salmon oil	38.95	80	Rapeseed oil	12.05
30	Rapeseed oil	51.37	80	-	-

Comparing tallow amine to the other measured samples in Table 7, tallow amine has by-far the highest viscosity temperature value at both 30 °C and 80 °C, indicating that it is the thickest sample. In comparison the 30 °C measurement for distilled water has by far the lowest viscosity value, indicating the temperature dependence of the viscosity. The Stribeck curves seen in Figure 24 underlines the statement that the higher the viscosity, the lower the viscosity of friction at constant normal force (5 N) and constant sliding speed (e.g., 1E-07 m/s), especially in boundary lubrication. Moreover, it can be stated that with increasing sliding speed, the coefficient of friction also decreases for all samples.

Figure 25 compares the bio-based friction modifiers at 30 °C and at 80 °C including both water and PAO8 as references.

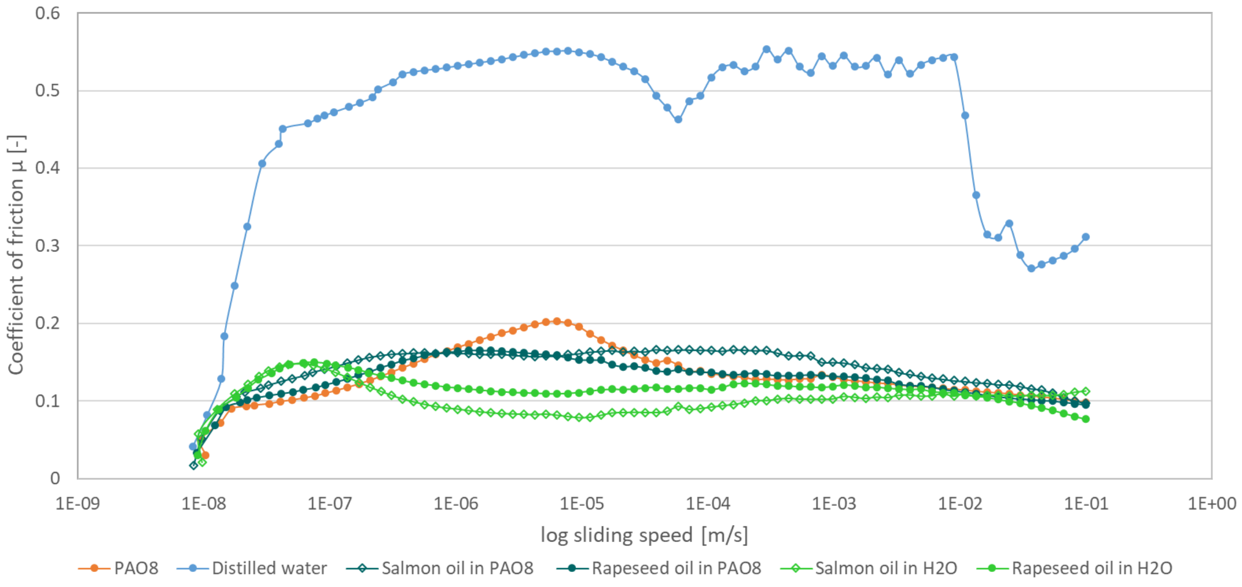

Figure 25: Mean curve of bio-based FM in PAO8 at 80 °C versus mean curve of bio-based FM in H2O at 30 °C including both water and PAO8 as references with a maximum coefficient of friction of 0.6 µ

The figure above clearly indicates the above speculation that due to a different (higher) viscosity the PAO8 mixtures have a shifted static friction comparing them to the water mixtures. From Figure 25 it can be speculated that the beginning of mixed lubrication is reached earlier for the water mixtures compared to the PAO8 mixtures.

A last test was performed to underline the statement that bio-based friction modifiers can be at least as good as conventional friction modifiers. This included the identification of the effect of water on the bio-based samples.

Figure 26 compares the bio-based friction modifiers at 30 °C pure, coated and mixed with water (1wt %).

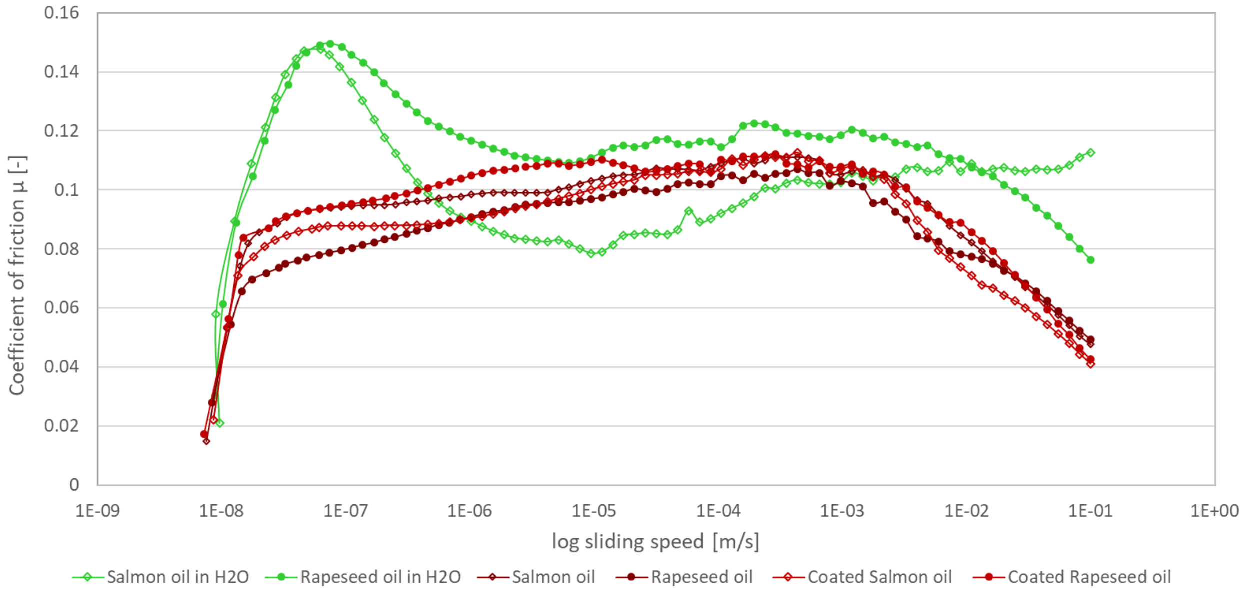

Figure 26: Mean curve of bio-based FM at 30 °C versus mean curve of coated and pure bio-based FM at 30 °C with a maximum coefficient of friction of 0.16 µ

For the pure samples, simply approximately 1 mL of rapeseed oil and salmon oil was analyzed, for the coated samples the plates and ball used for the tribological test were dipped in rapeseed oil and salmon oil. From the figure above it can be seen that pure and coated salmon oil and rapeseed oil cannot significantly be distinguished. From a sustainable point of view, the coated alternative is more promising than using 1 mL pure sample. Comparing the coated and pure samples to the mixtures in water, it can be stated that the pure and coated samples result in the most stable coefficient of friction [µ]. Yet, the images of the reflected-light microscope and the Stribeck curves indicate that the addition of 1wt % salmon or rapeseed oil already significantly improves both the friction and anti-wear properties comparing it to pure water. However, the usage of 1wt % of salmon oil or rapeseed oil in water might be a good alternative, as using mainly water is cheaper and leads to a lower biological footprint. Summarizing, water would also be a good cooling medium and less sample in total would be needed and therefore a 1wt % of either rapeseed oil or salmon oil is recommended, when an inconsistent friction is not necessary (see course of the curves in

Figure 26).

4.3. Quality management

4.3.1. Cause-and-Effect diagram

After analysis and evaluation of the method, performed measurements and the sample matrix possible causes for the variability of Stribeck curves measured on the rheometer MCR 302, a cause-and-effect diagram was created (see Figure 27).

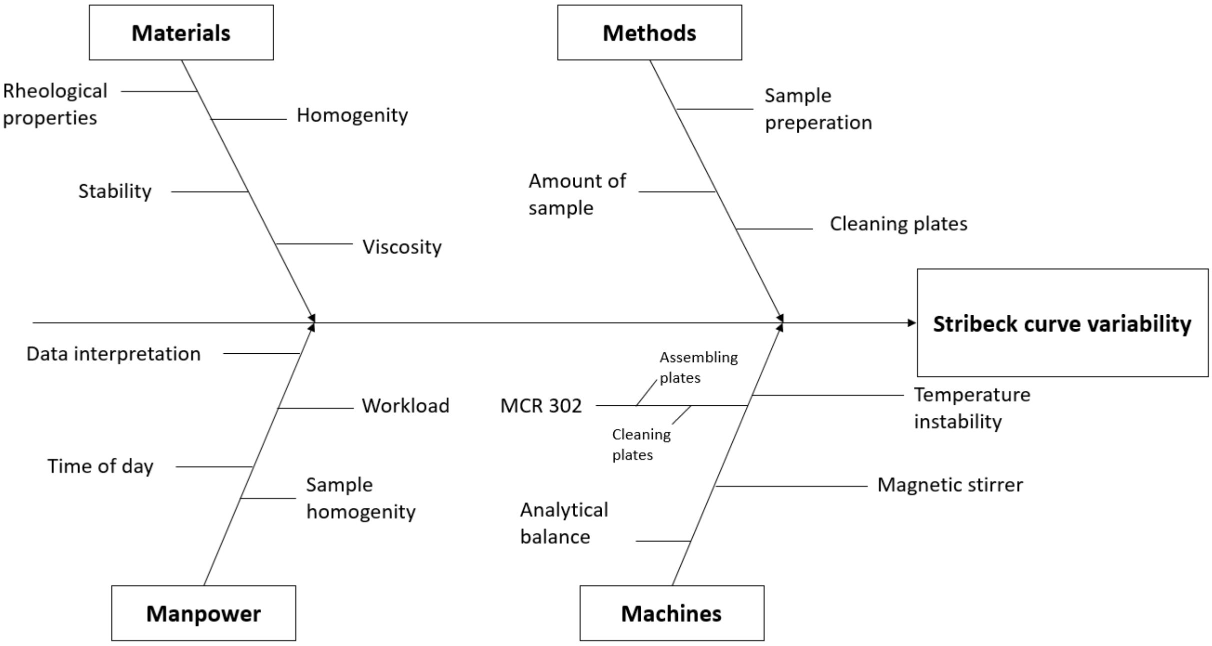

Figure 27: Cause and effect diagram for Stribeck curve variability on rheometer MCR302

As it can be seen in Figure 27, the causes for measurement variability of Stribeck curves were categorized in the four Ms (materials, methods, manpower and machines). Using this cause-and-effect diagram, a fault tree analysis (FTA) was conducted.

4.3.2. Fault Tree Analysis (FTA)

The resulting failures from materials, methods, manpower and machines depicted in the cause-and-effect diagram, were used as initial information for the following fault tree analysis.

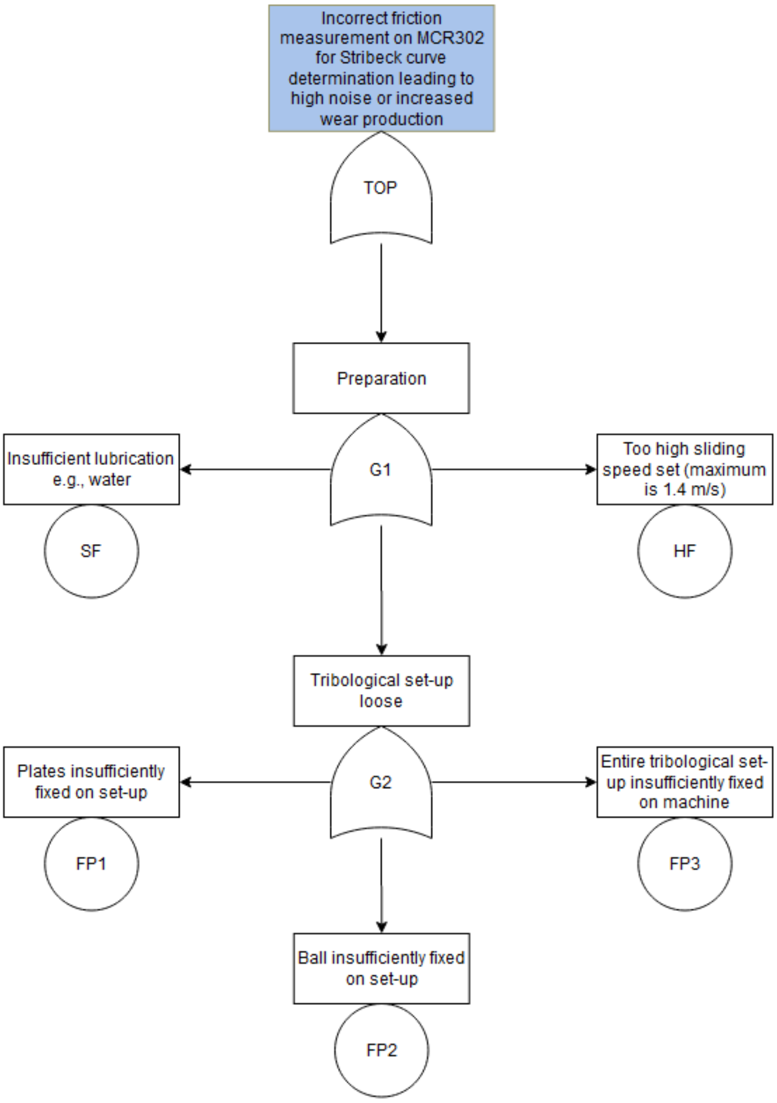

Figure 28: Fault tree analysis for Stribeck curve variability on rheometer MCR302

Figure 28 illustrates the FTA, which is a top-down deductive failure analysis, as explained in chapter 2.6.2. Thereby, the top event, marked in blue, indicates the consequence of faults and as a first step this top event was determined by answering the questions “What?- **Incorrect friction measurement**”, “Where?-**on MCR302**” and “When?-**for Stribeck curve determination**”. After that, the events causing the fault (top event) were listed. In this case only “or” gates were used, resulting from “preparation” and causing the top event. The abbreviations used in Figure 28, indicate “SF- **sample failure**”, “HF- **handling failure**” and “FPx- **failure of…**”.

4.3.3. Accuracy test Rheometer MCR302

As explained in 2.6.3, to determine the accuracy for the tribological set-up of the rheometer MCR302, trueness and precision tests are required. Generally, a confidence interval being marked in red, was calculated using the average standard deviation for the sliding speed 1E-5 m/s, in which the measurements may vary. Consequently, for this thesis the confidence interval was defined for the maximum coefficient of friction, being 1E-5 m/s sliding speed.

4.3.3.1. Trueness test

Figure 29 illustrates the means of the first and second measurement, as explained in Figure 14. The mean measurement by the manufacturer is estimated to be the “true value”.

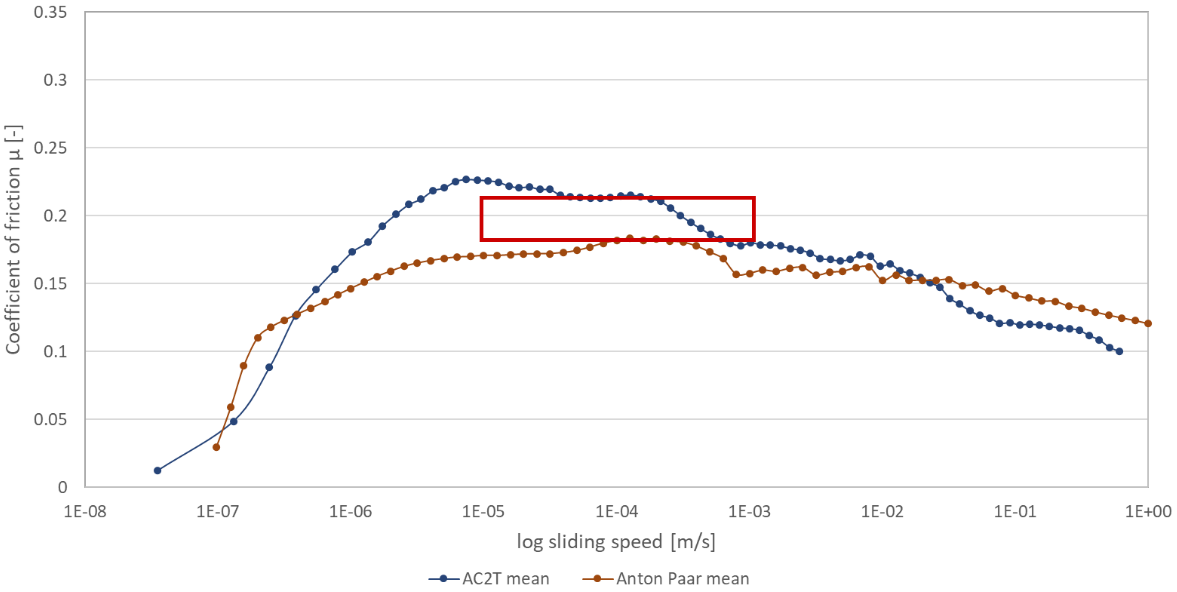

Figure 29: PAO8 80 °C trueness with a maximum coefficient of friction of 0.35 µ

According to Figure 29, it can be seen that the maximum coefficients of friction fluctuate less than the confidence interval. Thereby it can be assumed that the performed tests included in this thesis, are true. Nevertheless, it would be recommended to participate in ring tests to determine the accuracy regularly.

4.3.3.2. Precision test

To determine the precision, both repeatability and reproducibility tests are needed, as further explained in chapter 2.6.3. Figure 30 and Figure 31 illustrate the repeatability and reproducibility tests on the rheometer MCR302 using the tribological set-up.

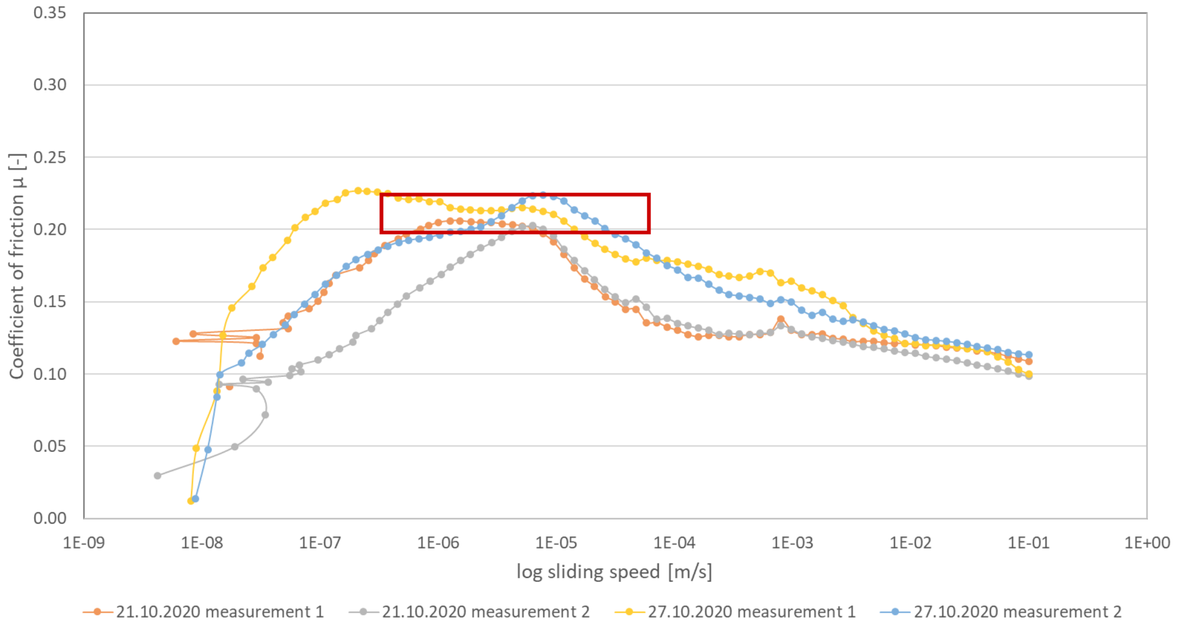

Figure 30: PAO8 80 °C repeatability with a maximum coefficient of friction of 0.35 µ

On the one hand, looking at the marked area in Figure 30 it can be seen that even though the curves do not look identical, their maximum coefficients of friction only fluctuate less than the confidence interval.

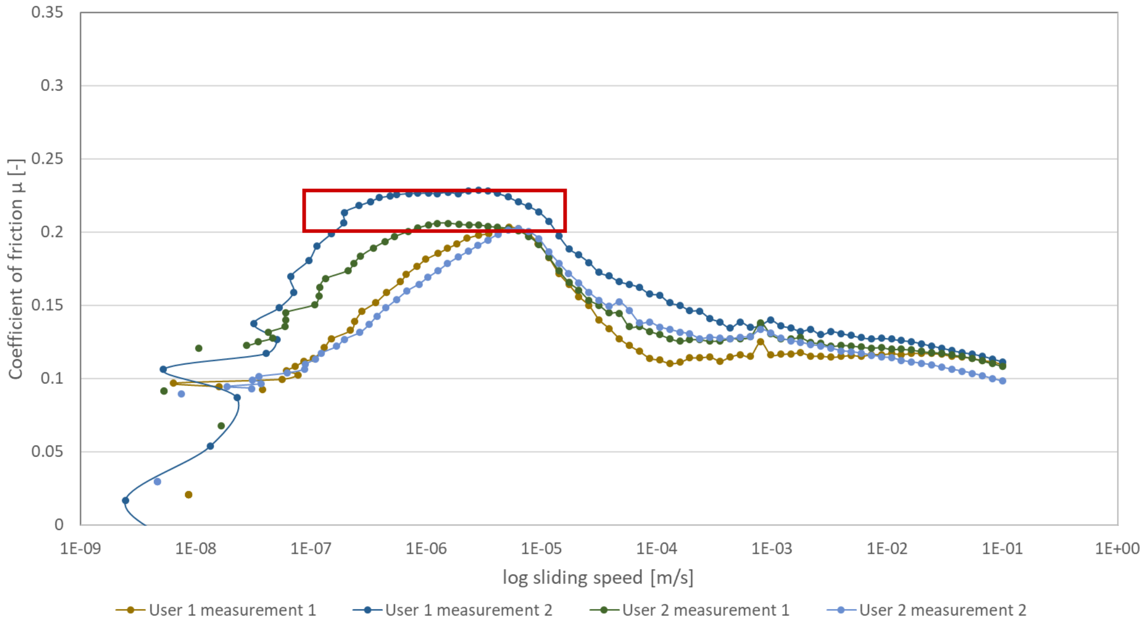

Figure 31: PAO8 80 °C reproducibility with a maximum coefficient of friction of 0.35 µ

On the other hand, the same effect can also be observed for the reproducibility depicted in Figure 31. As for the repeatability, the reproducibility of the coefficient of friction as well fluctuates less than the confidence interval between the different users.

Since the measurements are within the confidence interval, a good repeatability, as well as a good reproducibility of the tribological set-up for the rheometer MCR302 by Anton Paar is indicated. The result varies over the height of the coefficient of friction and over the sliding speed. The available resources are not sufficient to make a mathematically statistically significant statement.

Concluding, it can be stated that the measurements on the rheometer MCR302 performed in this thesis are accurate. For both the trueness and precision tests the maximum coefficient of friction is within the confidence value, implying that the effect of random and systematic error is not significant. By determining the accuracy, essential steps towards method validation are taken.

4.3.4. SWOT Analysis

The conduction of a cause-and-effect diagram, a fault tree analysis and the determination of accurate results using the tribological set-up on the rheometer MCR302, leads to the last step concerning quality management. A SWOT (Strengths, Weaknesses, Opportunities and Threats) analysis thematizing the method development and the experiments was performed in this thesis. (see Figure 32) AP stands for Anton Paar, the manufacturer of the rheometer MCR302.

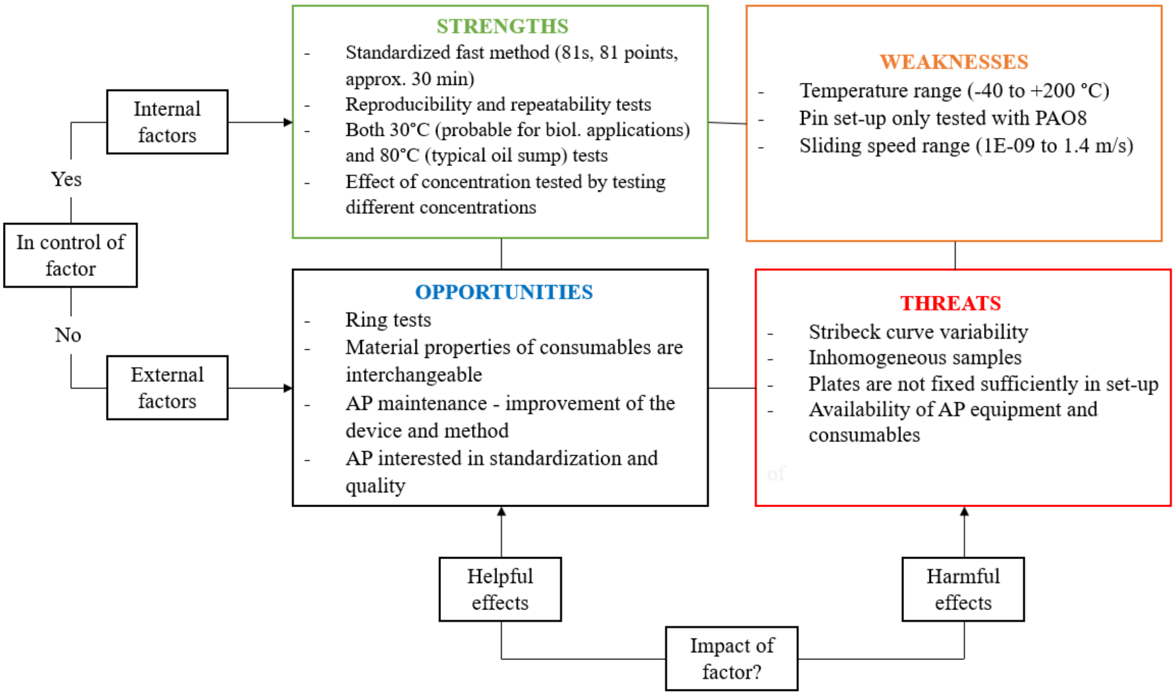

Figure 32: SWOT analysis for method development and experiments performed in this thesis

Regarding the SWOT analysis, at first the external factors were brainstormed, being “Threats” and “Opportunities”, and further external factors were both matched to the internal factors and converted, which changes a harmful to a helpful factor. Especially, the external factor “Opportunities” is useful, as it can be used as input for future related experiments and project.

5. Conclusion and future aspects

Concluding from the depicted results, a successful Stribeck curve method development for the rheometer MCR302 using a ball (100Cr6) on three plates (1.4301 steel) set-up was performed by obtaining accurate results for the selected friction modifier mixtures both in PAO8 and in distilled water. Generally, it was observed for both the conventional and bio-based friction modifier mixtures the chosen set-up led to a Stribeck curve at a state between boundary and mixed lubrication at 0,1 m/s, which is in line with the theoretically expected working range of friction modifiers at the beginning of mixed lubrication before for example wear additives intervene. (Mang & Dresel, 2017)

Comparing the conventional friction modifiers in PAO8 to the bio-based friction modifiers in PAO8 at 80 °C and in distilled water at 30 °C, it can be stated that bio-based friction modifiers, namely rapeseed oil and salmon oil, can perform at least as good as the best performing conventional friction modifier, namely tallow amine. From the wear scar images observed by the reflected-light microscope it can be concluded that as little as 1wt % of both rapeseed and salmon oil is enough to produce a comparable wear scar as the pure samples. This further indicates the possibility of changing from oil-based to an environmentally friendly water-based lubrication with the addition of as little as 1 wt% bio-based friction modifier, making it a cheaper system, as the water and oil mixtures perform equivalent within the confidence interval of 0.05 µ Lastly, additional chemical analysis of the samples, including infrared spectroscopy (ATR) and elemental analysis (ICP-OES) complete this thesis. Summarizing the results of the elemental analysis, are not surprising, since most of the analyzed samples in question consist of carbon, hydrogen, and oxygen, except for borate ester and alginic acid calcium salt.

Prospectively, the method used in this thesis could be prolonged at the minimum and maximum coefficient of friction could be tested. With the prolonged method, the stability of the samples, especially of the bio-based friction modifiers in water mixtures, could be tested. Rancidity and foam formation should also be taken under consideration, regarding the stability of the bio-based friction modifiers in water. Moreover, the maximum temperature at which both the conventional and bio-based friction modifiers are effective could be of interest, as no precise maximum temperature is defined for friction modifiers in literature, even though they apparently work best at moderate temperatures (see chapter 4.2.1). In case of issues with high temperatures for the bio-based friction modifier mixtures in water, workarounds like cooling systems or a nitrogen atmosphere should be considered. Additionally, the minimum concentration of the individual friction modifiers, at which a positive effect is still observed, could be investigated. After tribological tests on the rheometer MCR302, mass spectroscopy could be used to determine the aging effects of the friction modifier and other lubricant components on a molecular level. This may result in knowledge about the interaction of the components, but also of the weak parts in the molecule when it comes to stability, depending on the applied method and device. Moreover, wear tests could be conducted on the used materials. An essential question for bio-based lubricants in water is how a homogenous mixture can be achieved in machines. Building up on this thesis the usage of waste oil, such as salmon oil (El-Mashad, Zhang, & Avena-Bustillos, 2008) or waste cooking oils (WCO) (Hisham, et al., 2017) e.g., rapeseed oils for tribological testing should be considered.

This thesis could be an essential step towards the development of a more sustainable food-grade or even class 1 food-based lubricant, indicating that bio-based friction modifiers can be as good in terms of friction modification as conventional friction modifiers. However, it must be noted that, as mentioned above, the stability of the products was not tested entirely. Moreover, the expenses of the bio-based friction modifiers must be considered, favoring rapeseed oil. Yet, the question emerges, if salmon oil can it be as cheap as conventional friction modifiers, if it is extracted from waste products.

6. References

Abdollahzadeh, G., & Rastgoo, S. (2015). Risk Assessment in Bridge Construction Projects Using Fault Tree and Event Tree Analysis Methods Based on Fuzzy Logic. *ASCE-ASME J. Risk and Uncert. in Engrg. Sys., Part B: Mech. Engrg.,1(3)*.

Adekola, K. (2016). Engineering Review Food Extrusion Technology and Its Applications.

Anton Paar. (2020). Ball-on-three-Plates/Pins (BTP) Calculation.

Antonsson, E., & Grote, K. (2009). Springer handbook of mechanical engineering. *New York Springer*.

Besser, C. (2015, März). Impact of bio-ethanol as oxygenated fuel component in gasoline on the engine oil performance. Österreich.

Besser, C., Agocs, A., Ronai, B., Ristic, A., Repka, M., Jankes, E., . . . Dörr, N. (2019). *Generation of engine oils with defined degree of degradation by means of a large scale artificial alteration method.* Tribology International.

Biochem. (2020, 12 14). Retrieved from http://biochem.ch/Bipweb_all/bipweb/lexikon/metaboliten/agar/agar.html

Burris, D., Ramsey, L., Graham, B., Price, C., & Moore , A. (2019). How Sliding and Hydrodynamics Contribute to Articular Cartilage Fluid and Lubrication Recovery. Springer.

Campen, S., Green, J., Lamb, G., Atkinson, D., & Spikes, H. (2012). *On the Increase in Boundary Friction with Sliding Speed* . Springer.

Chiou, B.-S., El-Mashad, H., Avena-Bustillos, R., Dunn, R., Bechtel, P., McHugh, T., . . . Zhang, R. (2008). *Biodiesel from waste salmon oil.* American Society of Agricultural and Biological Engineers ISSN 0001-2351.

Coates, J. (2000). *Interpretation of Infrared Spectra, A Practical Approach.* John Wiley & Sons Ltd .

Czichos, H., & Mang, T. (2014). *Enzyclopedia of Lubricants and Lubrication.* Springer Berlin Heidelberg.

Derler, S., & Rotaru, G.-M. (2013). Stick-slip phenoma in the frictionof human skin. *Wear*.

Detmold, L. (2021, 3 15). Retrieved from https://www.leax-detmold.de/de/getriebe/kunststoffindustrie.html

Dörr, N. (2019). CONDITION MONITORING – DER SCHMIERSTOFF ALS INFORMATIONSTRÄGER. *VORLESUNG 164.346*.

Dörr, N., Agocs, A., Besser, C., Ristic , A., & Frauscher, M. (2019). *Engine Oils in the Field: A Comprehensive Chemical Assessment of Engine Oil Degration in a Passenger Car.* Tribology Letters.

ECHA. (2020, 12 13). Retrieved from https://echa.europa.eu/substance-information/-/substanceinfo/100.005.550

ECHA. (2020, 12 13). Retrieved from https://echa.europa.eu/substance-information/-/substanceinfo/100.004.063

ECHA. (2020, 12 14). Retrieved from https://echa.europa.eu/substance-information/-/substanceinfo/100.057.369

Elementar Analysensysteme GmbH. (2017). Variants Operating Instructions vario MACRO cube Analyzer.

El-Mashad, H., Zhang, R., & Avena-Bustillos, R. (2008). *A two-step process for biodiesel production from salmon oil* . Biosystems Engineering.

European Commission. (2018). *Revision of the European Ecolabel Criteria for Lubricants - JRC Technical Reports.*

European Lubricating Grease Institution. (2016). *General Information.* Netherlands.

European Union. (2021, 03 29). *European Commission - Energy, Climate change, Environment.* Retrieved from https://ec.europa.eu/

Gallego, R., Arteaga, J., Valencia, C., Díaz, M., & Franco, J. (2015). *Gel-like dispersions of HMDI-crosslinked lignocellulosic materials in castor oil: towards completely renewable lubricating grease formulations.* ACS Sustainable Chemistry & Engineering .

Ghaednia, H., Hossain, M., & Jackson, R. (2016). *Tribological Performance of Silver Nanoparticle-Enhanced Polyethylene Glycol Lubricants.* Tribology Transactions.

Grote, K.-H., & Antonsson, E. (2009). *Springer Handbook of Mechanical Engineering, Chapter 5 Tribology.*

Grote, K.-H., Bender, B., & Göhlich, D. (2018). *Dubbel - Taschebuch für den Maschinenbau.*

Guegan, J., Southby, M., & Spikes, H. (2019). *Friction Modifier Additives, Synergies and Antagonisms.* Springer.

Günzler, H., & Böck, H. (1975). *IR-Spektroskopie Eine Einführung* . Weinheim: Verlag Chemie GmbH.

Hamrock, B., & Dowson, D. (1977). Isothermal Elastohydrodynamic Lubrication of Point Contacts. *ASME*.

Hekmatpanah, M. (2011). The application of cause and effect diagram in the oil industry in Iran: The case of four liter oil canning process of Sepahan Oil Company. *African Journal of Business Management Vol. 5(26),* pp. pp. 10900-10907.

Henschel. (2021, 3 15). Retrieved from https://www.henschel.eu/produkte/extrudergetriebe/doppelschnecken-extrudergetriebe/parallele-doppelschnecken-gegenlauf/

Hiremath, P., Nuguru, K., & Agrahari, V. (2019). *Chapter 8 - Material Attributes and Their Impact on Wet Granulation Process Performance.* Academic Press.

Hisham, S., Kadirgama, K., Ramasamy, D., Noor, M., Amirruddin, A., Najafi, G., & Rahman, M. (2017). Waste cooking oil blended with the engine oil for reduction of friction and wear on piston skirt. *Fuel*.

Höfler, A. (2020, 08 04). *Tec-Science*. Retrieved from https://www.tec-science.com/de/mechanik/gase-und-fluessigkeiten/viskositat-von-flussigkeiten-und-gasen/

HSM Hochleistungswerkstoffe Stahl & Metall. (2020). Werkstoffdatenblatt 1.4301/X5CrNi18-10.

Hyun, K.-C., Min, S., Choi, H., Park, J., & Lee, I. (2015). Risk analysis using fault-tree analysis (FTA) and analytic hierarchyprocess (AHP) applicable to shield TBM tunnels. *Tunnelling and Underground Space Technology*.

Ingram , M., Noles, J., Watts, R., Harris , S., & Spikes, H. (2011). *Frictional properties of automatic transmission fluids: part 1: measurement of friction-sliding speed behaviour.*

Khalkar, S., Bhowmick, D., & Pratap, A. (2013). *Synthesis and Effect of Fatty Acid Amides as Friction Modifiers in Petroleum Base Stock.* Jounral of Oleo Science.

Khonsari, M., & Booser, E. (2008). Applied Tribology 2e: Bearing Design and Lubrication. *John Wiley & Sons, Ltd*.

Kozdrach, R. (2020). *The tribological properties of lubricating greases produced on vegetable base and modified of polytetrafluoroethylene.* TRIBOLOGIA - Finnish Journal of Tribology 1-2 vol 37.

Kozdrach, R. (2020). *The tribological properties of lubricating greases produced on vegetable base and modified polytretrafluoroethylene.* Tribologia.

Lewinska, A., Zebrowski, J., Duda, M., Gorka, A., & Wnuk, M. (2015). *Fatty Acids Profile and Biological Activities of Linseed and Rapeseed Oils.* Molecules.

Mang, T., & Dresel, W. (2017). Lubricants and Lubrication, Third Version, Volume 1.

Masri, M., Jurkowski, W., Shaigani, P., Haack, M., Mehlmer, N., & Brück, T. (2018). *A waste-free, microbial oil centered cyclic bio-refinery approach based on flexible macroalgae biomass.* Germany : Elsevier Ltd. .

Matthies, H.-J., & Renius, K. T. (2008). *Einführung in die Ölhydraulik, Physikalische Grundlagen ölhydraulischer Systeme.* Wiesbaden: Vieweg+Teubner Verlag & GWV Fachverlage GmbH.

Meyer, D., Bayarri, S., Tarrega, A., & Costell, E. (2011). *Inulin as texture modifier in dairy products.* Food Hydrocolloids.

Meyer, V. (2007). Measurement uncertainty. *Journal of Chromatography* , 15-24.

Misra, K. (2008). Applications of Performability Engineering Concepts. *Handbook of Performability Engineering*, 985-996.

Mu, L., Shi, Y., Hua, J., Zhuang, W., & Zhu, J. (2017). *Engineering Hydrogen Bonding Interaction and Charge Separation.* American Chemical Society .

Nadkarni, R. (1991). The Quest for Quality in the Laboratory. *Analytical Chemistry* , ,.

Oldehof, M., Leeuwen , J., Nauta, M., Kaste, D., Odekerken-Rombouts, Y., Vredenbregt, M., . . . Barends, D. (2011). Consistency of FMEA used in the validation of analytical procedures. *Journal of Pharmaceutical and Biomedical Analysis*, 592-595.

Oppermann, A. K., Verkaaik, L. C., Stieger, M., & Scholten, E. (2017). *Influence of double (w1/o/w2) emulsion composition on lubrication properties.* The Royal Society of Chemistry .

PubChem. (2020, 12 14). Retrieved from https://pubchem.ncbi.nlm.nih.gov/compound/5354133#section=Non-Human-Toxicity-Excerpts

Rähse, W. (2014). Praktische Hinweise zur Wahl des Werkstoffs von Maschinen und Apparaten. *Chem. Ing. Tech.*, pp. 1163-1179.

Rausand, M., & Hoyland, A. (2004). *System Reliability TheoryModels, Statistical Methods,and Applications.* Wiley.

Richard, S., Moslemi, S., Sipahutar, H., Benachour , N., & Seralini, G.-E. (2005). Differential Effects of Glyphosate and Roundup on Human Placental Cellsand Aromatase.

Rizvi, S. (2009). *A Comprehensive Review of Lubricant Chemistry, Technology, Selection and Design.* ASTM International.

Rudnick, L. (2009). *Lubricant Additives: Chemistry and Applications.* USA: CRC Press.

Saarstahl. (2020, 09 13). *Saarstahl*. Retrieved from https://www.google.com/url?sa=t&rct=j&q=&esrc=s&source=web&cd=&ved=2ahUKEwiZrc6Xn-brAhWQh1wKHR13CsYQFjAAegQIBRAB&url=https%3A%2F%2Fwww.saarstahl.com%2Fsag%2Fdownloads%2Fdownload%2F9183&usg=AOvVaw1PjG7dmvUCyMzVYHZdBenf

Sarsby, A. (2016). *SWOT Analysis - A guide to SWOT for business studies students.* Leadership Library.

Schaeffler Technologies. (2002). Schmierung von Wälzlagern Grundlagen Schmierverfahren Schmierstoffauswahl und -prüfung Aufbewahrung und Handhabung.

Schreiner, M. (2019). Food Chemistry lecture BOKU .

Sigma Aldrich. (2020, 12 14). Retrieved from https://www.sigmaaldrich.com/catalog/substance/hydroxypropylmethylcellulose12345900465311?lang=de&region=AT

Sigma Aldrich. (2020, 12 14). Retrieved from https://www.sigmaaldrich.com/catalog/product/sigma/21054?lang=de&region=AT

Sigma Aldrich. (2020, 11 03). Product Information Sheet (Hydroxypropyl)methyl cellulose. USA.

Smith, T., & Ahuja, S. (2003). *US Patent No. EP1310532NWB1.*

Sommer, K., Heinz, R., & Schöfer, J. (2010). *Verschleiß metallischer Werkstoffe.* Wiesbaden: Vieweg + Teubner.

Spikes, H. (2006). Sixty years of EHL. *LUBRICATION SCIENCE*.

Spikes, H. (2015). Friction Modifier Additives. *Tribology Group, Imperial College London, UK*.

Stachowiak, G., & Batchelor, A. (2000). Engineering Tribology 2nd edition.

Stempfel, E., & Baumann, M. (2012). *Einführung in das Gebiet der lebensmittelverträglichen Schmierstoffe.*

Sterner, O., Karageorgaki, C., Zürcher , M., Zürcher , S., Scales, C., Fadli, Z., . . . Tosatti , S. (2017). Reducing Friction in the Eye: A Comparative Study of Lubrication by Surface-Anchored Synthetic and Natural Ocular Mucin Analogues. ACS Publications.

T+S Tribologie und Schmierungstechnik. (2016). Lebensmittelverträgliche Schmierstoffe.

Tang, D., Khoo, K., Chew, K., Tao, Y., Ho, S.-H., & Show, P. (2020). *Potential utilization of bioproducts from microalgae for the quality enhancement of natural products.* Elsevier Ltd.

Tang, Z., & Li, S. (2014). A review of recent developments of friction modifiers for liquidlubricants (2007–present). *Current Opinion in Solid State and Materials Science 18,* pp. 119-139.

Techpilot. (2021, 3 14). *Techpilot.* Retrieved from https://www.techpilot.de/lexikon/extrusion/

Thermo Scientific . (2015). Spektrometerserie iCAP 7000 .

Tsokolar-Tsikopoulos, K., Katsavou, I., & Krokida, M. (2015). *The effect of inulin addition on structural and textural properties of extruded products under several extrusion conditions.* Journal of Food Science and Technology.

Uchoa, I., Neto, A., Santos, E., & Neto, E. (2017). *Evaluation of Lubricating Properties of Diesel Based Fuels Micro Emulsified With Glycerin.* Materials Research.

Umweltbundesamt. (2020, 12 13). Retrieved from https://www.umweltbundesamt.de/themen/chemikalien/chemikalien-reach/einstufung-kennzeichnung

Vauck, W., & Müller, H. (1999). *Grundoperationen chemischer Verfahrenstechnik.* Wiley-Ych.

Wang, L., Zhou, J., Duszczyk, J., & Katgerman, L. (n.d.). *Friction in aluminium extrusion—Part 1: A review of friction testing techniques for aluminium extrusion.* 2012: Tribology International.

Watter, H. (2017). *Hydraulik und Pneumatik 2. Fluide und Fluideigenschaften* . Springer Verlag.

Wellmitz, J., & Glutschke, M. (2005). Leitlinie zur Methodenvalidierung. *Qualitätssicherung im Bund/Läner-Messprogramm Nord- und Ostsee (BLMP).*

Widder, L. (2014). *A novel approach to characterization of industrial lubricant additives in boundary surface tribofilms by atmospheric pressure matrix assisted laser desorption/ionization.*

Xie, Z., Rao, Z.-S., Na, T., Liu, L., & Chen, R. (2015). *Theoretical and experimental research on the friction coefficient of a water lubricated bearing with consideration of wall slip effects.* China: EDP Sciences.

List of figures

List of tables

Index of abbreviations

DHA	Docosahexaenoic acid
EHA	Eicosapentaenoic acid
EC	European Council
EEC	Council of the European Communities
EU	European Union
FA	Fatty acid
FM	Friction modifier
FMEA	Failure mode and effect analysis
FTA	Fault tree analysis
FTIR-ATR	Fourier-Transform-Infrared spectrometer - Attenuated total reflection
HPMC	Hydroxypropyl methylcellulose
HRC	Hardness Rockness C
HV	Hardness Vickers
ICP-OES	Inductively coupled plasma - optical emission spectrometry
SWOT	Strength, weaknesses, opportunities, and threats analysis
M	Molar mass
MCR	Modular Compact Rheometer
PAO	Polyalphaolefin
ZDDP	Zinc dithiophosphate

7. Appendix

Appendix 1: Structural formula dominant fatty acids in rapeseed oil

“Lipids consist of a broad group of compounds that are generally soluble in organic solvents but only sparingly soluble in water” (Fennema, 1996)

“Lipids are fatty acids and their derivatives, and substances related biosynthetically or functionally to these compounds” (Christie, 1993)

Generally, the double bonds in the FA control their melting point: more double bonds, leading to a less tight packing of the FA molecule, further leading to a low melting point and a fluid cell membrane.

With the help of desaturases, linoleic and linolenic acids can be converted into arachidonic and docosahexaenoic acids, respectively.

Excursion triglycerides (TGA): “TGA account for the major portion of most food lipids. In most fatty food, the lipid fraction is composed of usually > 98% TGA, which normally contain more than 90 % FA, egg lipids are an exception below 70 % of FA leading to a very lean meat.”

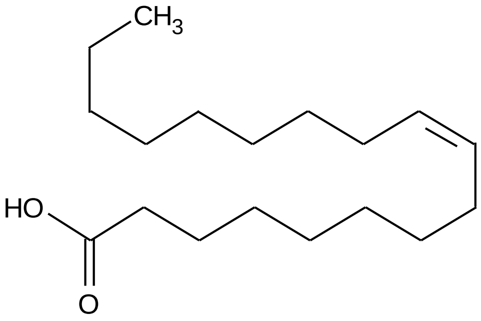

Appendix 1: Oleic acid (C18:1, (9Z)-Octadec-9-enoic acid) 62.5 % in rapeseed oil

Oleic acid is an unsaturated FA. Including one cis-double bonds, preventing a tight packing of the FA molecules, and leading to a low melting point (13.4 °C) and keeping the cell membranes fluid.

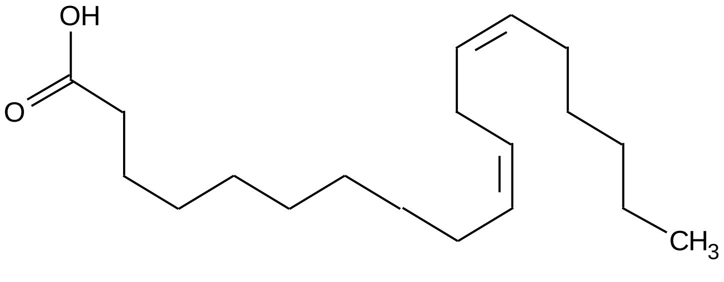

Appendix 2: Linoleic acid (C18:2, (9Z,12Z)-octadeca-9,12-dienoic acid) 19.6 % in rapeseed oil

Linoleic acid is a polyunsaturated omega-6 fatty acid (FA), being important precursors for eicosanoids (e.g., arachidonic acid found in eggs), which are further important components of complex lipids (e.g., DHA). The inclusion of one two cis-double bonds, prevents a tight packing of the FA molecules, and leads to a low melting point (-5 °C) and ultimately keeps the cell membranes fluid.

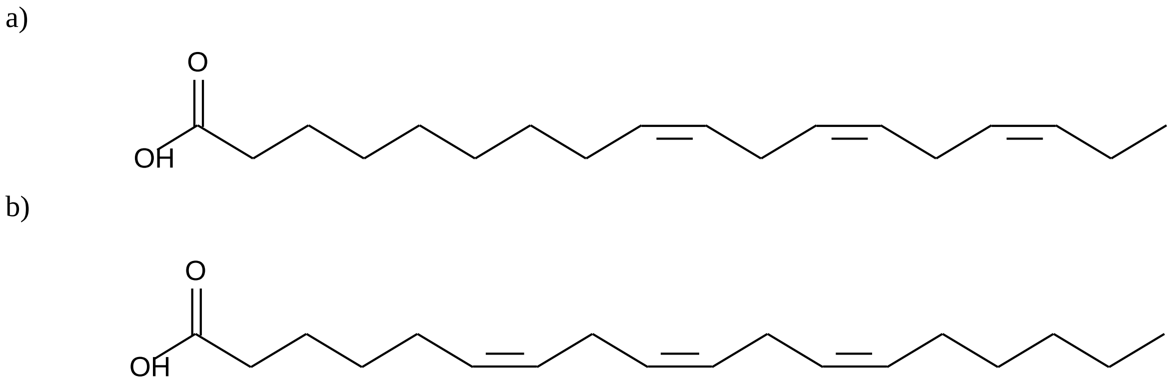

Appendix 3: Linolenic acid (C18:9) 10.0 % in rapeseed oil, a) α-linolenic acid omega-3 FA (n-3, (9Z,12Z,15Z)-octadeca-9,12,15-trienoic acid), b) γ-linolenic acid omega-6 FA (n-6, all-cis-6,9,12-octadecatrienoic acid)

α-linolenic acid is a polyunsaturated omega-3 FA and γ-linolenic acid is a polyunsaturated omega-6 FA, being important precursors for eicosanoids (e.g., arachidonic acid), which are further important components of complex lipids (e.g., DHA). The inclusion of one two cis-double bonds, prevents a tight packing of the FA molecules, and leads to a low melting point (-11 °C) and ultimately keeps the cell membranes fluid.

Appendix 2: Structural formula dominant fatty acids in salmon oil

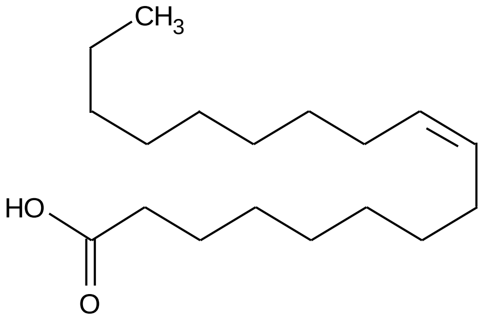

Appendix 4: Oleic acid (C18:1, (9Z)-Octadec-9-enoic acid) 18.22 g/100 g in salmon oil

Oleic acid is an unsaturated FA. Including one cis-double bonds, preventing a tight packing of the FA molecules, and leading to a low melting point (13.4 °C) and keeping the cell membranes fluid.

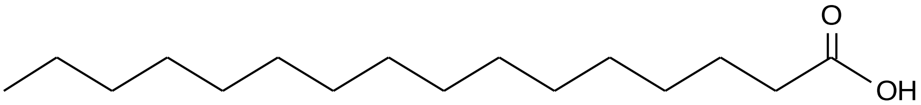

Appendix 5: Palmitic acid (C16:0, Hexadecanoic acid) 14.83 g/100 g in salmon oil

Palmitic acid is a saturated FA (no double bonds), leading to a tight packing of the FA molecules and this additionally to the long chain length leads to a high melting point.

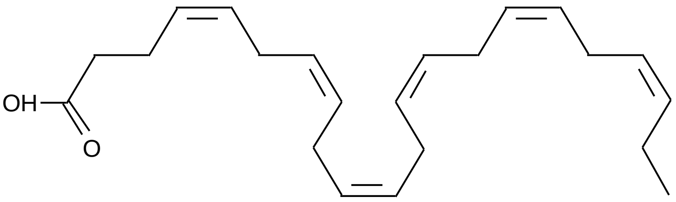

Appendix 6: Docosahexaenoic acid DHA (C22:6, (4Z,7Z,10Z,13Z,16Z,19Z)docosa-4,7,10,13,16,19-hexaenoic acid) 13.63 g/100 g in salmon oil

DHA is essential for the brain and central nervous tissue and therefore essential in pregnancy for the nourishment of the embryo (also for small children). Polyunsaturated FA, like DHA, arachidonic acid and EPA are essential in cell membranes, making α-linolenic acids and linoleic acids **essential FA**.

Omega-3 Eskimo paradoxon: eat a lot of fish, leading to few heart attacks, but nose bleeding (works hand in hand with Aspirin/cyclooxygenase inhibitor).

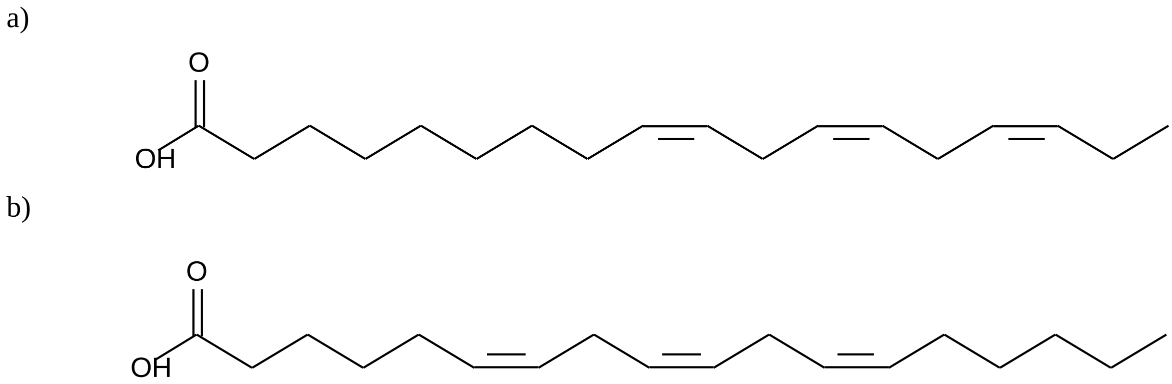

Appendix 7: Linolenic acid (C18:9) 11.67 g/100 g in salmon oil, a) α-linolenic acid omega-3 FA (n-3, (9Z,12Z,15Z)-octadeca-9,12,15-trienoic acid), b) γ-linolenic acid omega-6 FA (n-6, all-cis-6,9,12-octadecatrienoic acid)

α-linolenic acid is a polyunsaturated omega-3 FA and γ-linolenic acid is a polyunsaturated omega-6 FA, being important precursors for eicosanoids (e.g., arachidonic acid), which are further important components of complex lipids (e.g., DHA). The inclusion of one two cis-double bonds, prevents a tight packing of the FA molecules, and leads to a low melting point and ultimately keeps the cell membranes fluid.

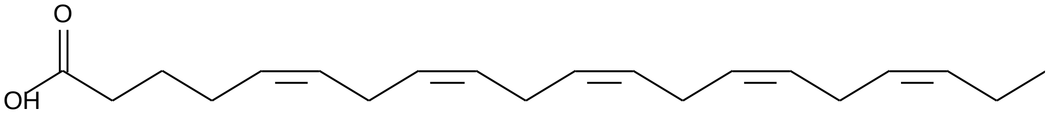

Appendix 8: Eicosapentaenoic acid EPA (C20:5, (5Z,8Z,11Z,14Z,17Z)-icosa-5,8,11,14,17-pentaenoic acid) 11.13 g/100 g in salmon oil

EPA are built up of omega-3 and omega-6 FA (e.g., linolenic acid and linoleic acid) being and Eicosanoids, like EPA, are essential components of complex lipids (e.g., DHA).

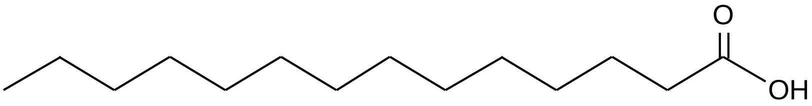

Appendix 9: Myristic acid (C14:0, Tetradecanoic acid) 6.85 g/100 g in salmon oil

Myristic acid is a saturated FA (no double bonds), leading to a tight packing of the FA molecules and this additionally to the long chain length leads to a high melting point.

Appendix 3: Rheometer MCR 302 SOP

STANDARD ARBEITSANWEISUNG

„RHEOMETER“

GERÄT: MCR_302, GERÄTE NR. 5189 (K) & 7189 (NON-K)

KOSTENSTELLE: 97189

1. Inhaltsverzeichnis

2. Gender Hinweis

- Aus Gründen der besseren Lesbarkeit wird auf die gleichzeitige Verwendung der männlichen und weiblichen Sprachform verzichtet. Sämtliche Personenbezeichnungen gelten gleichermaßen für beiderlei Geschlecht. Die Formulierung in einer Geschlechtsform ist jedenfalls nicht wertend.

3. Abkürzungsverzeichnis

ACA	Advanced chemical analyses
LUB	Lubricants (Schmiermittel)
MCR	Modular Compact Rheometer

Gegenstand und Geltungsbereich

- Diese Arbeitsanweisung regelt organisatorisch den Zugriff und die Analytik mit der Theta Probe™ (Thermo Fisher Scientific, Ser. Nr. A1318). Das Gerät befindet sich im Regelbetrieb in permanentem Bereitschaftszustand (24/7 Betrieb). Nur zu Reparatur- und Wartungsarbeiten wird die Anlage heruntergefahren bzw. das Vakuum der Analysekammer gebrochen.

- Gerätenummern: 7189 und 5189, Kostenstelle 97189

- Gerätezuordnung: Pool LUB

- Geräteaufstellung: LUB Labor BT B EG (RI 1, Z.00.001)

- Geräteverantwortlich: Rosa Maria Eder Stellvertretung: Anto Puljic
- allgemeine Kontaktdaten Gerätehersteller und Service:
    - **Anton Paar Austria GmbH**
        - Ankerstrasse 6
        - 8054 Graz Austria
        - T: +43 - 316 - 269571 – 805
        - M: +43 - 664 – 88616230
        - F: +43 - 316 - 269571 – 00
    - Dr. Stefan Holler
        - Area Sales Manager

4. Methodenbeschreibung, Rheometer Messprinzip

Abbildung 1: Rheometer MCR_302 AC²T mit tribologischem Aufsatz

- Grundsätzlich geht es in der Rheologie (auch Fließkunde) darum das Verformungs- und Fließverhalten aller Arten von Materialien zu beschreiben. Dafür wird P-PTD 200/56 (Peltier-Temperaturregelung für Parallelplatten- und Kegelplattensysteme) verwendet. Mit Hilfe des tribologischen Systems können Reibung und Verschleiß zwischen Materialien, die aneinander reiben, bestimmt werden. Als tribologisches System wird T-PTD 200 verwendet. Technische Daten zu T-PTD 200 befinden sich in Anhang 4. Mit Hilfe des PTDs können Proben von **-4°C bis 200°C** gemessen werden.

- Die Beziehung zwischen dem Reibungskoeffizienten und der Gleitgeschwindigkeit wird in der "Stribeck-Kurve" (siehe Abbildung 2) dargestellt:
  - Reibung an den Grenzen (Boundary Friction): hier ist die Geschwindigkeit niedrig. 2 Oberflächen interagieren und bestimmen die Reibung (µ = FF : FN).
  - Mischreibung (Mixed Friction): Das Schmiermittel wird in den Raum zwischen den Oberflächen transportiert und die Aufwärtskräfte des Schmiermittels drücken die Oberflächen auseinander. Dabei wird ein hydrodynamischer Druck aufgebaut und der direkte Kontakt wird reduziert. Je weiter die Flächen auseinander geschoben werden, desto geringere ist die Reibung.
  - Elasto-hydrodynamische Reibung: Wenn sich Oberflächen nicht mehr berühren, besteht minimale Reibung.
  - Hydrodynamische Reibung: Filme verhindern/verringern Verschleiß und mit zunehmender Geschwindigkeit wird der Film dicker.
- Wenn die Viskosität zunimmt, nimmt die Fließgeschwindigkeit ab und die Oberflächen werden auseinander gedrückt. Die Steigung der Kurve nimmt mit zunehmender Viskosität zu.

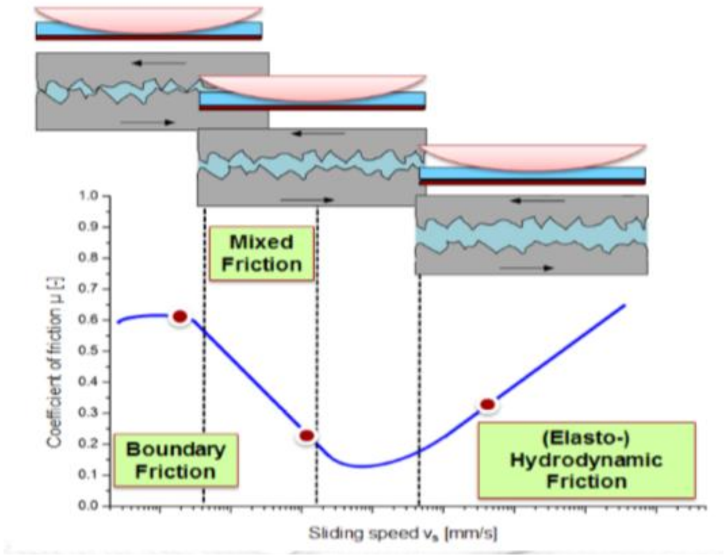

Abbildung 2: Stribeckkurve

Grundsätzliches zum Betrieb des Gerätes

- Das Gerät darf nur von speziell geschulten Mitarbeitern unter Beachtung allgemeiner Sicherheitsrichtlinien betrieben werden (in Anhang 3 befinden sich besondere Sicherheitshinweise). Schulungsberechtigt sind der Poolleiter ACA, der Geräteverantwortliche bzw. von diesen Personen direkt Beauftragte. Gerätebücher, Manuals und allgemeine Dateien sind unter folgendem Link abgelegt: \\fileserver\ac2tdata\2-Pools\23-LUB\200-Infrastructure\Geraete-Bestand\Rheometer-MCR302
- Weiterführende Wartungs- und Reparaturarbeiten sind nur in Abstimmung mit der Poolleitung bzw. dem Geräteverantwortlichen durchzuführen
- Es sind vom Benutzer die allgemeinen Laborsicherheitsrichtlinien sowie weiterführende übergeordnete Richtlinien von AC²T zu beachten. Die Analysen erfordern speziell gereinigte

Arbeitsmaterialien, es ist daher spezifisch darauf zu achten, dass Arbeitsmaterialien in der Probenvorbereitung nach Gebrauch ordnungsgemäß verwahrt, Arbeitsmaterialien nicht vom spezifizierten Probenvorbereitungsplatz entfernt werden, spitze und scharfe Gegenstände keinesfalls offen liegen gelassen werden.

5. Ordentlicher analytischer Betrieb, Routinebetrieb

1.3.1. Auftrag, Vorbereitung, Probenannahme

- Mit dem Auftraggeber (intern oder extern) sind, optimalerweise vor der Probenübernahme, die Eignung der Proben für die analytische Methode abzuklären. Spezifische Parameter zu Anforderungen an Vakuumtauglichkeit, Probengeometrie und thematischer Fragestellung sind festzuhalten. Da die Rheometer Analyse eine komplexe Analytik darstellt, und nicht unbedingt zu erwarten ist, dass der jeweilige Kunde die Eigenheiten der Methode kennt, so ist der Kunde über die Möglichkeiten und Einsatzgrenzen zu informieren.

- Abzuklären sind demnach zumindest:

- Hinweis auf Handhabung der Probe: bei allen Proben und damit in Kontakt kommenden (Hilfs-)Instrumenten ist auf äußerste Sauberkeit zu achten. Proben dürfen nur mit geeigneten Schutzhandschuhen angegriffen werden (Schutz der Probenoberfläche vor jeglicher Verunreinigung).
- spezifische Fragestellung und Projektzuordnung (Projektnummer, Kostenstelle)
- Anlage der Probe im LIMS (bereitgestellt vom Pool LUB) durchzuführen.
- Probenhandhabe, ggf. Organisation und Hilfestellung zu vorbereitenden physikalischen, chemischen und/oder mechanischen notwendigen Maßnahmen
- Art und Reinigung der Proben: in der Regel sind nur speziell für die Analytik vorgesehene hochreine Lösemittel zugelassen
- Zeithorizont der Analytik und Abschätzung des Aufwandes
- Art und Form von Datenbereitstellung und Analysebericht

1.3.2. Durchführen der Analytik, Arbeit am Gerät

- Gerätebücher, die die Gerätenutzung und die analytischen Möglichkeiten dokumentieren, sind unter \\fileserver\ac2tdata\2-Pools\23-LUB\200-Infrastructure\Geraete-Bestand\Rheometer-MCR302 zu finden.
- **Überprüfen**
- Allgemeinzustand des Geräts: Versorgung Druckluft, Computer, sonstige Hinweise auf Fehler (LED-Lichter, Sicherungen)
- Laborbuch: die Analysen sind in einem Laborbuch beim Gerät zu dokumentieren, besonders sind Auffälligkeiten während oder durch die Analytik zu dokumentieren.
- Arbeitsmaterialien: Vollständigkeit für Probenreinigung und Probenmontage
- **Probenvorbereitung**
- Die Vorbereitung der Proben erfolgt gemäß Kundenanforderung und Aufgabenstellung.
- Neue Materialien, welche in Kontakt mit der Probe kommen werden, werden kurz in Isopropanol eingelegt, um Oberflächenverunreinigungen zu entfernen.
- **Probenreinigung und Probenaufbringung**
- Eine Reinigung ist immer in Absprache mit dem Kunden vorzunehmen – ggf. sind geeignete Vorschläge zu unterbreiten.
- Zulässige Hilfsmittel zur Montage sind am Arbeitsplatz Rheometer MCR 302 und in den zugehörigen Laden verfügbar. Keinesfalls dürfen ohne Rücksprache mit dem Geräteverantwortlichen andere oder weitere Hilfsmittel verwendet werden.
- Bezüglich der Probenaufbringung ist die Füllmenge bzw. Füllhöhe (tribologisches System) speziell zu beachten (siehe o). Weiters ist beim tribologischen System darauf zu achten, nicht auf das Trimmen der Probe zu vergessen.
- Für das Platte-Platte/Kegel-Platte System werden die Materialien mit Isopropanol, Toluol und Petrolether gereinigt.
- Für das Tribosystem verwendete Material werden in einem Becherglas mit Isopropanol im Ultraschallbad gereinigt.
- **Rheometer Analyse der Probe(n)**
- Anhang 1 beinhaltet Bildschirmaufnahmen für die schrittweise Durchführung.

Inbetriebnahme und Initialisierung für Platte/Platte-Systeme und Kegel/Platte System:

- **ACHTUNG:** Stellen Sie sicher, dass bei Luftlagergeräten die Druckluftversorgung und das Filtersystem angeschlossen sind und der richtige Druck eingestellt ist.

- **ACHTUNG:** Vermeiden Sie Verkratzen oder sonstige Beschädigungen des Messsystems und/oder des Zubehörs.

- Schalten Sie das Gerät ein, um es zu starten. Warten Sie, bis das Gerät startet. Dieser Vorgang dauert etwa eine Minute. Das Gerät ist bereit, wenn auf dem Display in der ersten Zeile „Status: O.K.“ angezeigt wird.

- Starten Sie den Computer, das Betriebssystem und anschließend die Rheometer-Software.

- Schließen Sie das Zubehör an, z.B. einen externen Temperaturregler oder ein Wasserbad (falls zutreffend).

- <u>Bei Verwendung einer Temperiereinheit ist die Verwendung eines Kühlers zwingend notwendig.</u>

- Initialisieren Sie das Gerät mit Hilfe der Software, um die Kommunikation zu ermöglichen. Während der Initialisierung bewegt sich der Messkopf an die höchste Position, um den Spaltsensor zu überprüfen. Der Rotor führt mehrere Umdrehungen bei hoher Geschwindigkeit durch, um den Positionssensor zu überprüfen.

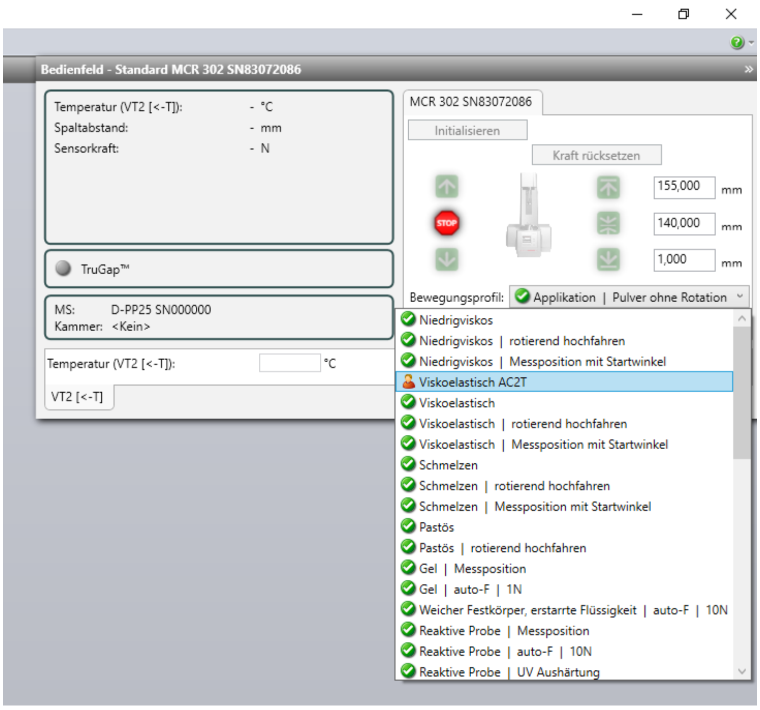

Bedienfeld - Standard MCR 302 SN83072086

Temperatur (VT2 [<-T]): - °C
Spaltabstand: - mm
Sensorkraft: - N

MS: D-PP25 SN000000
Kammer: <Kein>

Temperatur (VT2 [<-T]): °C

155,000 mm
140,000 mm
1,000 mm

Bewegungsprofil: Applikation | Pulver ohne Rotation

Abbildung 3: Bewegungsprofil Viskoelastisch für Platte/Platte und Kegel/Platte

- Wenn es sich nicht um die erste Inbetriebnahme handelt, können Sie mit der Messung fortfahren.

- Senden Sie die erforderliche Temperatur an das Zubehör und montieren Sie das Messsystem.

- Gehen Sie bei Zylinder-Messsystemen zur Messposition, und warten Sie, bis ein thermisches Gleichgewicht erreicht ist. Starten Sie bei Messsystemen, die einen Nullspalt erfordern, das

Nullspaltverfahren, und gehen Sie nach dessen Abschluss zur Messposition. Warten Sie, bis ein thermisches Gleichgewicht erreicht ist, und wiederholen Sie die Nullspalt-Einstellung.

- Legen Sie die Messparameter wie in der Software- Anleitung beschrieben fest.
- Bewegen Sie den Kopf des Geräts nach oben, und bringen Sie die Probe auf.
- Gehen Sie zur Trimmposition (Kegel/Platte- und Platte/Platte-Messsysteme), trimmen Sie die Probe, und gehen Sie anschließend zur Messposition. Bei Zylinder-Messsystemen können Sie direkt zur Messposition gehen.
- Achten Sie darauf, dass die Dichtung der Temperiereinheit geschlossen aufliegt (ohne Spalt):

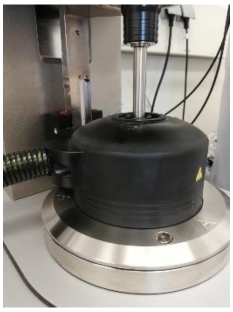

Abbildung 4: Temperiereinheit muss geschlossen aufliegen

- Warten Sie, bis ein thermisches Gleichgewicht erreicht ist, und beginnen Sie mit der Messung.
- Nehmen Sie nach der Messung das Messsystem ab und bewegen Sie den Kopf des Geräts nach oben.
- Entfernen Sie die Probe und reinigen Sie sowohl das obere als auch das untere Messsystem.
- Montieren Sie das Messsystem für die nächste Messung erneut.

Inbetriebnahme und Initialisierung für Einweg Platte/Platte-Systeme und Kegel/Platte System:

- Einstellungen umstellen: Bei Hardwarekonfiguration “Messsystem“ auf „D“ für disposable ändern:

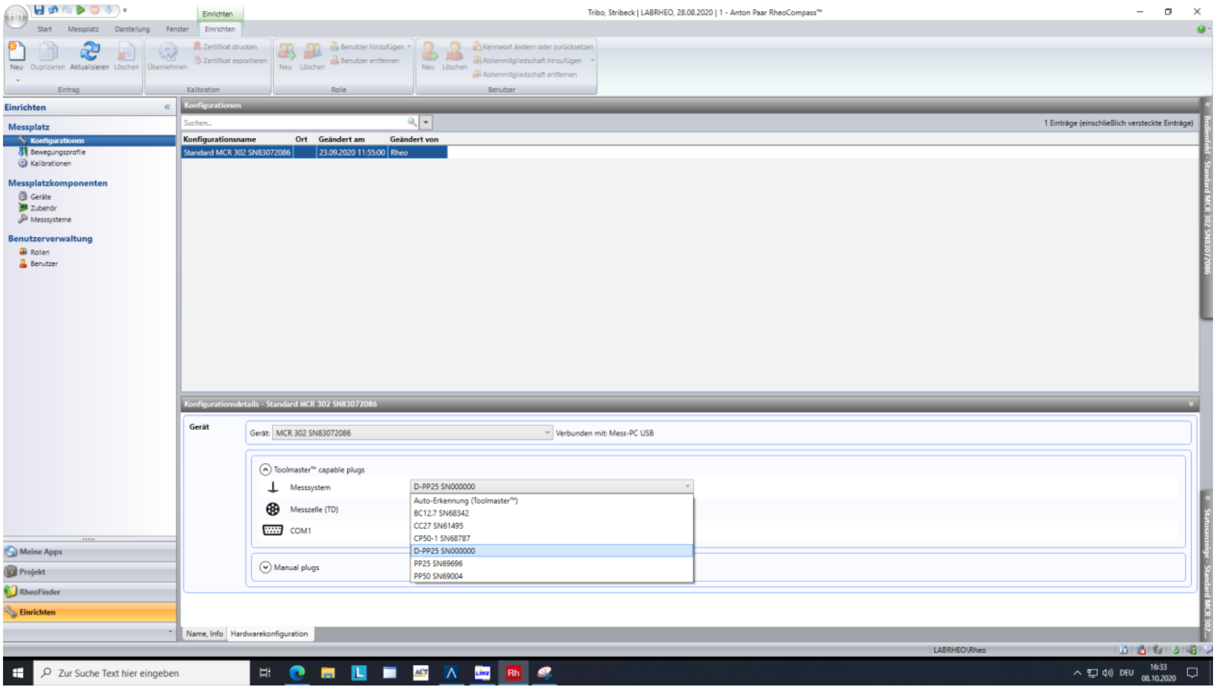

Gerät: MCR 302 SN83072086 Verbunden mit: Mess-PC USB

Messsystem: D-PP25 SN000000

Abbildung 5: Änderung in Hardware für Einwegmaterial (Messsystem)

- Einstellung des Bewegungsprofils
- Montieren des Messsystems und der Messzelle (auf die Mehrwegplatte)
- **Achtung beim Montieren des Messsystems: es darf keine Hebelkraft nach oben ausgeübt werden, da diese das Luftlager zerstören könnte.**

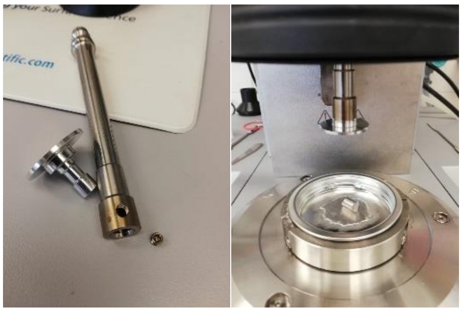

Abbildung 6: Einwegmaterial: Platte 25 mm und Aluminiumplatte

- Weiteres Vorgehen wie bei mehrweg Platte/Platte System und Kegel/Platte System.

Inbetriebnahme und Initialisierung für Tribologie System:

- Messverfahren wählen (Vorlagen in RheoCompass)
    - Neue Arbeitsmappe erstellen

  - Wählen Sie aus "Standardvorlagen" - "Alle".
  - Messparameter anpassen: Standardeinstellungen verwenden

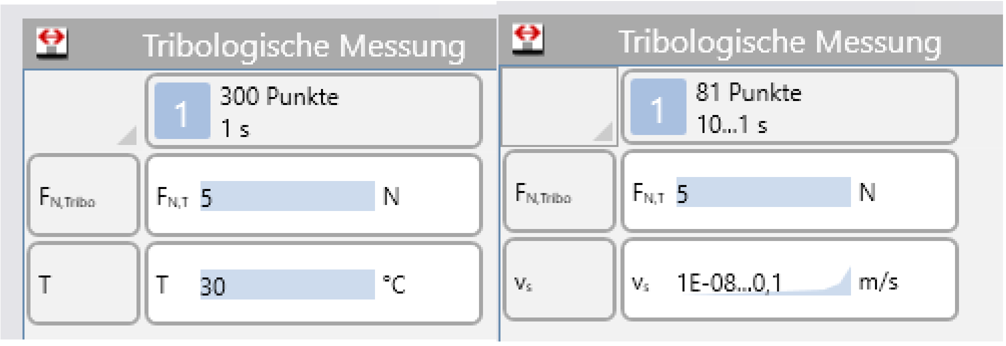

300 Punkte
1 s
F$_{N,T}$ 5 N
T 30 °C

81 Punkte
10...1 s
F$_{N,T}$ 5 N
v$_s$ 1E-08...0,1 m/s

Abbildung 7: Einstellungen für Stribeckkurven Standardmessungen

- Montage der Probekugel auf der Messkugel
- Welle auf MCR montieren
  - Welle in die Kupplung einführen (durch H-PTD 200, falls installiert),
  - Enge Kopplung (Messsystem wird erkannt von Toolmaster)
- Montage des Probenhalters
  - Probenplatten in den Probenhalter legen
  - Probenplatten mit Senkkopfschrauben und Fixierung befestigen (2 mm Inbusschraube)
  - Probenhalter auf T-PTD 200 montieren (2,5 mm Inbusschraube)
- Bei Verwendung einer Temperiereinheit ist die Verwendung eines Kühlers zwingend notwendig.
- Vorläufige Einstellungen in der Systemsteuerung (im Register Systemsteuerung)
  - "Reset Normal Force" mit montierter Messwelle (inkl. Messkugel).
  - Verwenden Sie "Tribologie" als Spalteinstellung.

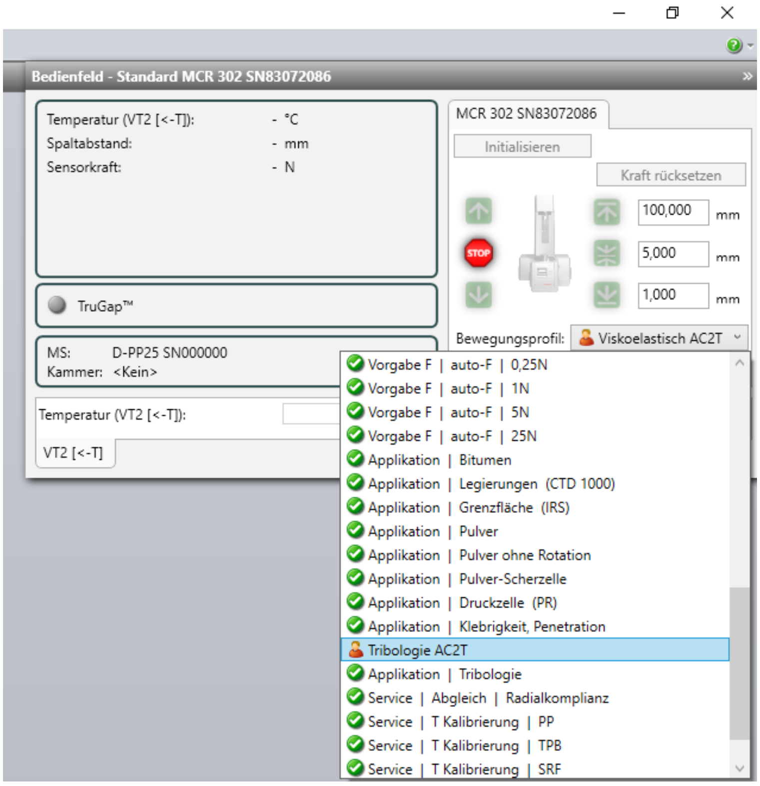

Bedienfeld - Standard MCR 302 SN83072086

Temperatur (VT2 [<-T]): - °C
Spaltabstand: - mm
Sensorkraft: - N

MS: D-PP25 SN000000
Kammer: <Kein>

MCR 302 SN83072086
100,000 mm
5,000 mm
1,000 mm
Bewegungsprofil: Viskoelastisch AC2T

Abbildung 8: Bewegungsprofil Tribologisch für zB Stribeckkurven und Haftreibkurven

  - Temperatur einstellen (stellen Sie sicher, dass die Gegenkühlung eingeschaltet ist)
- Regler im Bedienfeld einstellen (im Register Regler)
  - Stellen Sie den CSR-Controller auf "Manuell" und 80 % ein
  - Dynamics NF-Regler auf "Manuell" einstellen und 50 %
- Zur Messposition fahren:
  - Drücken Sie die Taste "Messposition" in der "Systemsteuerung",
  - Die Position wird automatisch eingestellt, wobei die Normalkraft überwacht wird.
- Massenträgheit und Motorausrichtung
  - Im Register "Systemsteuerung" unter "Systemsteuerung":
  - Fahren Sie auf eine Position 1 mm oberhalb der Messposition (kein fester Wert, da die Position durch die Normalkraft FN gesteuert wird), stellen Sie sicher, dass die Normalkraft FN = 0 N ergibt und der Messkegel frei läuft
- Im Register "Service" in der "Systemsteuerung":
  - Bestimmen Sie die Trägheit durch Auswahl der Messsystem-Schaltfläche im Abschnitt "Trägheit".
    - Anhang E: T-PTD 200 - Kurzanleitung B74IB006DE-K 23

    - Führen Sie die Motoreinstellung durch, indem Sie den Motoreinstellknopf wählen.
- Einfüllen des Probenschmiermittels
    - Schmiermittel in den Probenhalter einfüllen
    - Messposition anfahren

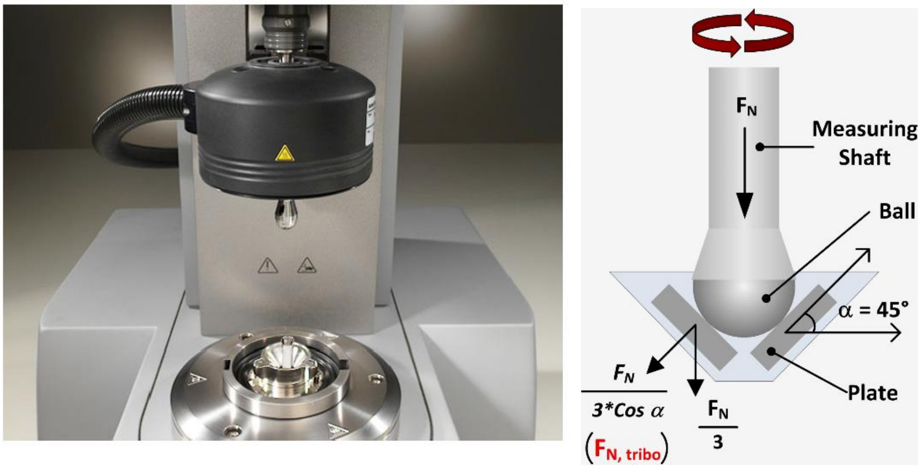

Abbildung 9: Messsystem Tribologisch ball on 3 plates

- Drücken Sie Start im "Messfenster".
- Probenname einfügen (Register "Informationstexte und Start") und optionale Wartezeiten (Registerkarte Temperatur Einstellungen, wenn die Temperatur erreichen muss definierte Werte oder Registerkarte "Warten vor dem Start Test" in jedem anderen Fall) - weitere Einzelheiten siehe RheoCompass Handbuch

Empfehlung von Anton Paar bei Stribeckkurven

    - Vor Beginn der Messung eine Leerlauf Messung zum Warmlaufen durchführen.
    - Messung von 3 Stribeckkurven hintereinander: Die erste ist der Einlauf (Run-In) und von der zweiten und dritten kann der Mittelwert berechnet werden

Start

Information
zur Vorlage

Baustein
Prepare | MCR | Tri...

Messung
Normalkrafteinstellung

Ansicht
Diagramm: Stribeckku...

Messung
Stribeckkurve

Messung
Stribeckkurve

Messung
Stribeckkurve

Ende

Abbildung 10: Standardeinstellungen bei Normalkrafteinstellung und Stribeckkurve

- Drücken Sie "Test jetzt starten".
- Folgende Messsysteme sind derzeit bei AC2T vorhanden:

Platte/Platte-System:

- Die Probe sollte sich genau außen am Rand des Messsystems befinden (siehe Abbildung 10). Idealerweise wird jeglicher Probenüberschuss (Trimmposition) genau über der Messposition
- entfernt; anschließend wird das System an die Messposition bewegt. Sowohl zu große als auch zu
- kleine Probenmengen führen zu schwerwiegenden Fehlern in den Messdaten.

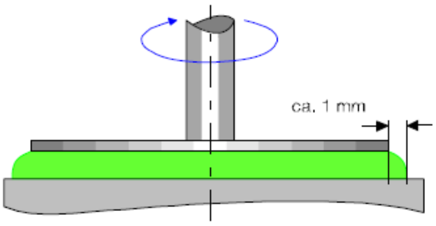

Abbildung 11: Probenverteilung Platte/Platte System

Vorteile des Platte/Platte-Systems:

- Für Proben mit hoher Viskosität geeignet
- Hoher Scherratenbereich
- Kleines Probenvolumen
- Leicht zu befüllen und zu reinigen

Nachteile des Platte/Platte-Systems:

- Spaltverlust der Substanzen bei zu hohen
- Scherraten
- Verschiedene Scherraten im Spalt
- Trocknen der Proben

- Schneller Temperaturangleich
- Anpassbarer Messspalt
- Proben mit kleinen Partikeln können gemessen werden

Kegel/Platte System:

○ Siehe Platte/Platte System und Abbildung 12.

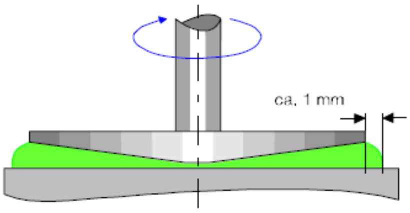

Abbildung 12: Probenverteilung Kegel/Platte System

Vorteile des Kegel/Platte-Systems:

- Konstante Scherrate im gesamten Spalt dank Kegelform
- Kleines Probenvolumen
- Leicht zu befüllen und zu reinigen
- Schneller Temperaturangleich

Nachteile des Platte/Platte-Systems:

- Spaltverlust der Substanzen bei zu hohen

Scherraten

- - Verschiedene Scherraten im Spalt
- - Trocknen der Proben

Tribologie System

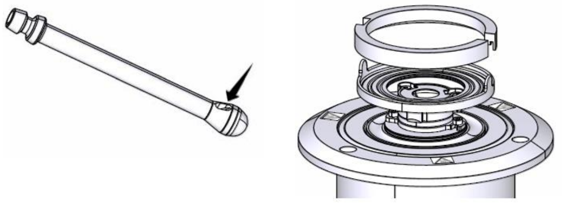

Abbildung 13: T-PTD 200

○ Siehe Kapitel Inbetriebnahme und Initialisierung für Tribologie System.

○ Speichern und Export

○ Abbildung 14 zeigt wie das Projekt/die Messung (nach dem Drücken auf den grünen Start Knopf beispielsweise benannt werden kann).

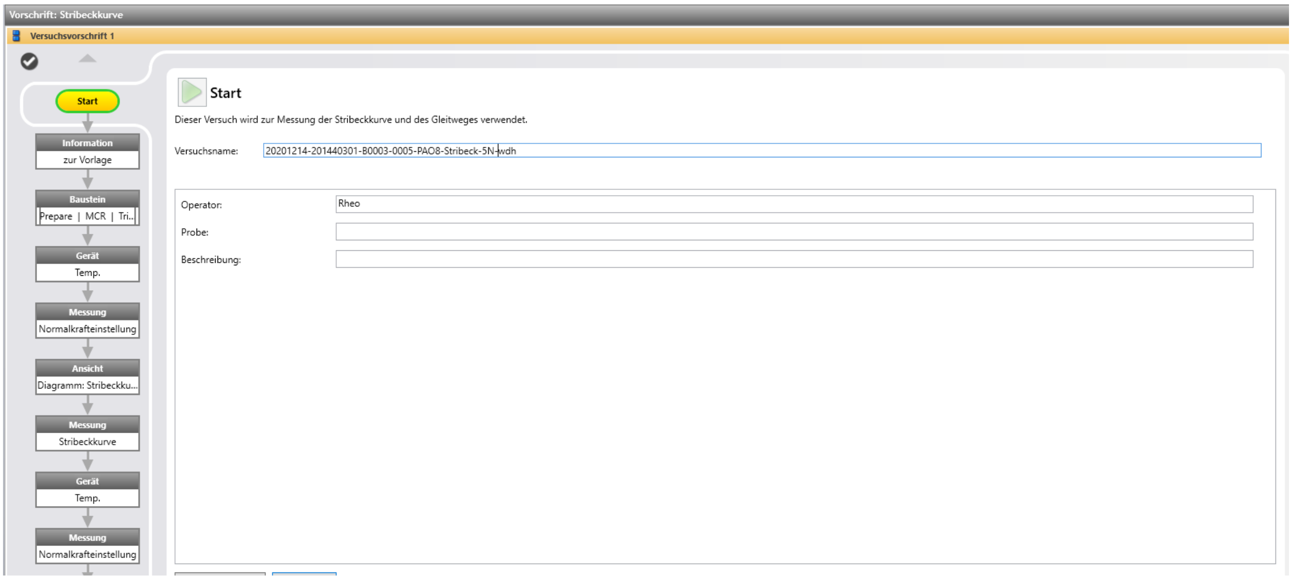

Start

Dieser Versuch wird zur Messung der Stribeckkurve und des Gleitweges verwendet.

Versuchsname: 20201214-201440301-B0003-0005-PAO8-Stribeck-5N-wdh

Operator: Rheo

Probe:

Beschreibung:

Abbildung 14: Benennung des Projektes

- In Abbildung 15 wird dargestellt, wie man das Projekt/die Messung speichern kann.

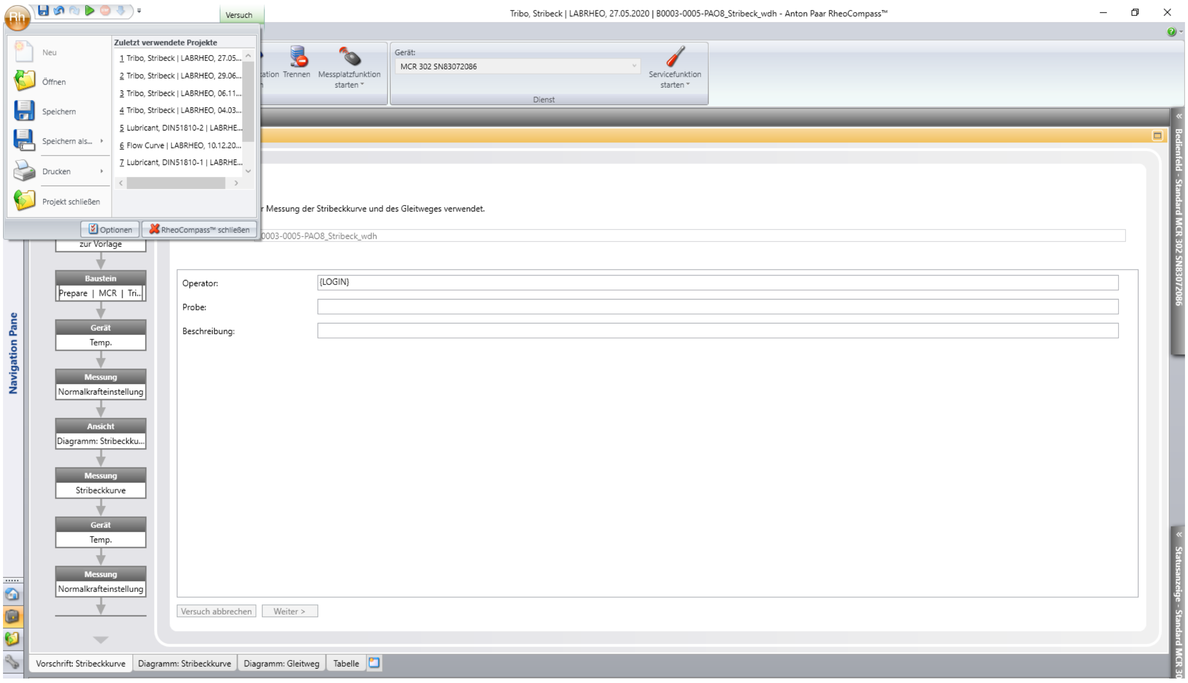

Operator: {LOGIN}

Probe:

Beschreibung:

Abbildung 15: Speichern des Projektes

- Abbildung 16 zeigt die Datenbank des RheoCompass.

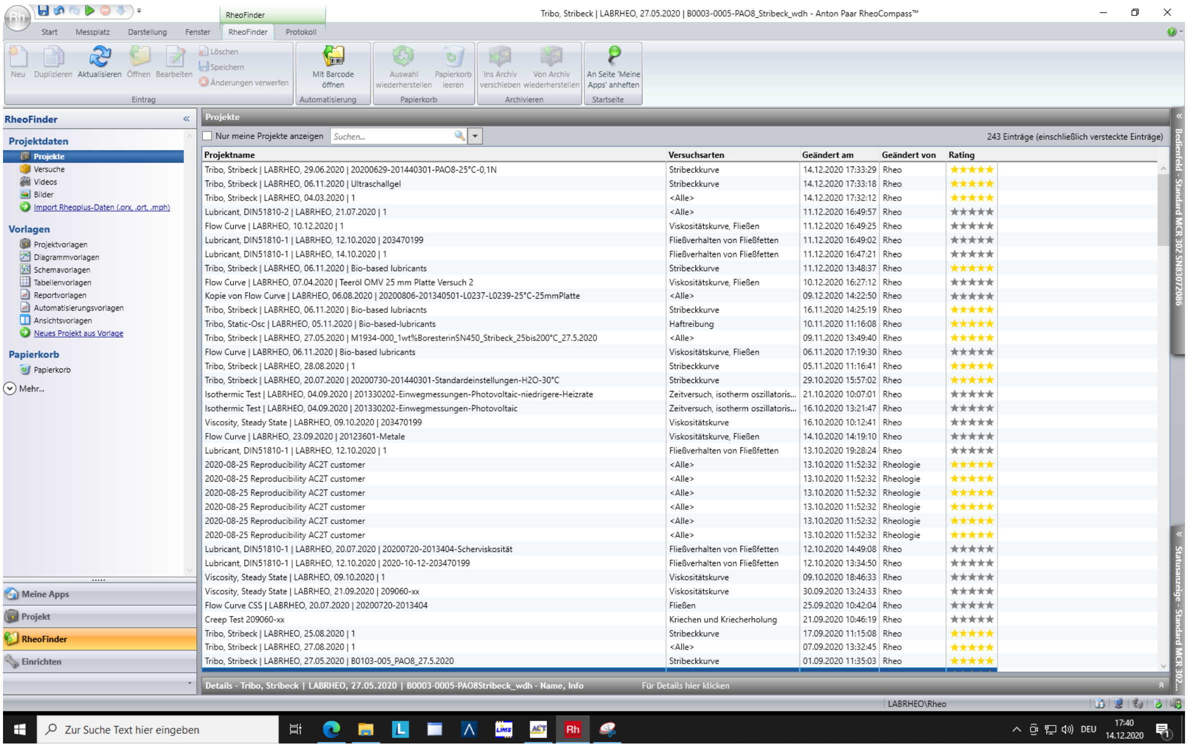

Tribo, Stribeck | LABRHEO, 27.05.2020 | B0003-0005-PAO8_Stribeck_wdh - Anton Paar RheoCompass™

Projekte

☐ Nur meine Projekte anzeigen Suchen... 243 Einträge (einschließlich versteckte Einträge)

Projektname	Versuchsarten	Geändert am	Geändert von	Rating
Tribo, Stribeck | LABRHEO, 29.06.2020 | 20200629-201440301-PAO8-25°C-0,1N	Stribeckkurve	14.12.2020 17:33:29	Rheo	★★★★★
Tribo, Stribeck | LABRHEO, 06.11.2020 | Ultraschallgel	Stribeckkurve	14.12.2020 17:33:18	Rheo	★★★★★
Tribo, Stribeck | LABRHEO, 04.03.2020 | 1	<Alle>	14.12.2020 17:32:12	Rheo	★★★★★
Lubricant, DIN51810-2 | LABRHEO, 21.07.2020 | 1	<Alle>	11.12.2020 16:49:57	Rheo	☆☆☆☆☆
Flow Curve | LABRHEO, 10.12.2020 | 1	Viskositätskurve, Fließen	11.12.2020 16:49:25	Rheo	☆☆☆☆☆
Lubricant, DIN51810-1 | LABRHEO, 12.10.2020 | 203470199	Fließverhalten von Fließfetten	11.12.2020 16:49:02	Rheo	☆☆☆☆☆
Lubricant, DIN51810-1 | LABRHEO, 14.10.2020 | 1	Fließverhalten von Fließfetten	11.12.2020 16:47:21	Rheo	☆☆☆☆☆
Tribo, Stribeck | LABRHEO, 06.11.2020 | Bio-based lubricants	Stribeckkurve	11.12.2020 13:48:37	Rheo	★★★★★
Flow Curve | LABRHEO, 07.04.2020 | Teeröl OMV 25 mm Platte Versuch 2	Viskositätskurve, Fließen	10.12.2020 16:27:12	Rheo	☆☆☆☆☆
Kopie von Flow Curve | LABRHEO, 06.08.2020 | 20200806-201340501-L0237-L0239-25°C-25mmPlatte	<Alle>	09.12.2020 14:22:50	Rheo	☆☆☆☆☆
Tribo, Stribeck | LABRHEO, 06.11.2020 | Bio-based lubriacnts	Stribeckkurve	16.11.2020 14:25:19	Rheo	★★★★★
Tribo, Static-Osc | LABRHEO, 05.11.2020 | Bio-based-lubricants	Haftreibung	10.11.2020 11:16:08	Rheo	★★★★★
Tribo, Stribeck | LABRHEO, 27.05.2020 | M1934-000_1wt%BoresterinSN450_Stribeck_25bis200°C_27.5.2020	<Alle>	09.11.2020 13:49:40	Rheo	★★★★★
Flow Curve | LABRHEO, 06.11.2020 | Bio-based lubricants	Viskositätskurve, Fließen	06.11.2020 17:19:30	Rheo	☆☆☆☆☆
Tribo, Stribeck | LABRHEO, 28.08.2020 | 1	Stribeckkurve	05.11.2020 11:16:41	Rheo	★★★★★
Tribo, Stribeck | LABRHEO, 20.07.2020 | 20200730-201440301-Standardeinstellungen-H2O-30°C	Stribeckkurve	29.10.2020 15:57:02	Rheo	★★★★★
Isothermic Test | LABRHEO, 04.09.2020 | 201330202-Einwegmessungen-Photovoltaic-niedrigere-Heizrate	Zeitversuch, isotherm oszillatoris...	21.10.2020 10:07:01	Rheo	☆☆☆☆☆
Isothermic Test | LABRHEO, 04.09.2020 | 201330202-Einwegmessungen-Photovoltaic	Zeitversuch, isotherm oszillatoris...	16.10.2020 13:21:47	Rheo	☆☆☆☆☆
Viscosity, Steady State | LABRHEO, 09.10.2020 | 203470199	Viskositätskurve	16.10.2020 10:12:41	Rheo	☆☆☆☆☆
Flow Curve | LABRHEO, 23.09.2020 | 20123601-Metale	Viskositätskurve, Fließen	14.10.2020 14:19:10	Rheo	☆☆☆☆☆
Lubricant, DIN51810-1 | LABRHEO, 12.10.2020 | 1	Fließverhalten von Fließfetten	13.10.2020 19:28:24	Rheo	☆☆☆☆☆
2020-08-25 Reproducibility AC2T customer	<Alle>	13.10.2020 11:52:32	Rheologie	★★★★★
2020-08-25 Reproducibility AC2T customer	<Alle>	13.10.2020 11:52:32	Rheologie	★★★★★
2020-08-25 Reproducibility AC2T customer	<Alle>	13.10.2020 11:52:32	Rheologie	★★★★★
2020-08-25 Reproducibility AC2T customer	<Alle>	13.10.2020 11:52:32	Rheologie	★★★★★
2020-08-25 Reproducibility AC2T customer	<Alle>	13.10.2020 11:52:32	Rheologie	★★★★★
2020-08-25 Reproducibility AC2T customer	<Alle>	13.10.2020 11:52:32	Rheologie	★★★★★
Lubricant, DIN51810-1 | LABRHEO, 20.07.2020 | 20200720-2013404-Scherviskosität	Fließverhalten von Fließfetten	12.10.2020 14:49:08	Rheo	☆☆☆☆☆
Lubricant, DIN51810-1 | LABRHEO, 12.10.2020 | 2020-10-12-203470199	Fließverhalten von Fließfetten	12.10.2020 13:34:50	Rheo	☆☆☆☆☆
Viscosity, Steady State | LABRHEO, 09.10.2020 | 1	Viskositätskurve	09.10.2020 18:46:33	Rheo	☆☆☆☆☆
Viscosity, Steady State | LABRHEO, 21.09.2020 | 209060-xx	Viskositätskurve	30.09.2020 13:24:33	Rheo	☆☆☆☆☆
Flow Curve CSS | LABRHEO, 20.07.2020 | 20200720-2013404	Fließen	25.09.2020 10:42:04	Rheo	☆☆☆☆☆
Creep Test 209060-xx	Kriechen und Kriecherholung	21.09.2020 10:46:19	Rheo	☆☆☆☆☆
Tribo, Stribeck | LABRHEO, 25.08.2020 | 1	Stribeckkurve	17.09.2020 11:15:08	Rheo	★★★★★
Tribo, Stribeck | LABRHEO, 27.08.2020 | 1	<Alle>	07.09.2020 13:32:45	Rheo	★★★★★
Tribo, Stribeck | LABRHEO, 27.05.2020 | B0103-005_PAO8_27.5.2020	Stribeckkurve	01.09.2020 11:35:03	Rheo	★★★★★

Details - Tribo, Stribeck | LABRHEO, 27.05.2020 | B0003-0005-PAO8Stribeck_wdh - Name, Info   Für Details hier klicken

LABRHEO\Rheo

Abbildung 16: Datenbank des RheoCompass

- Zu guter Letzt zeigt Abbildung 17 den Export.

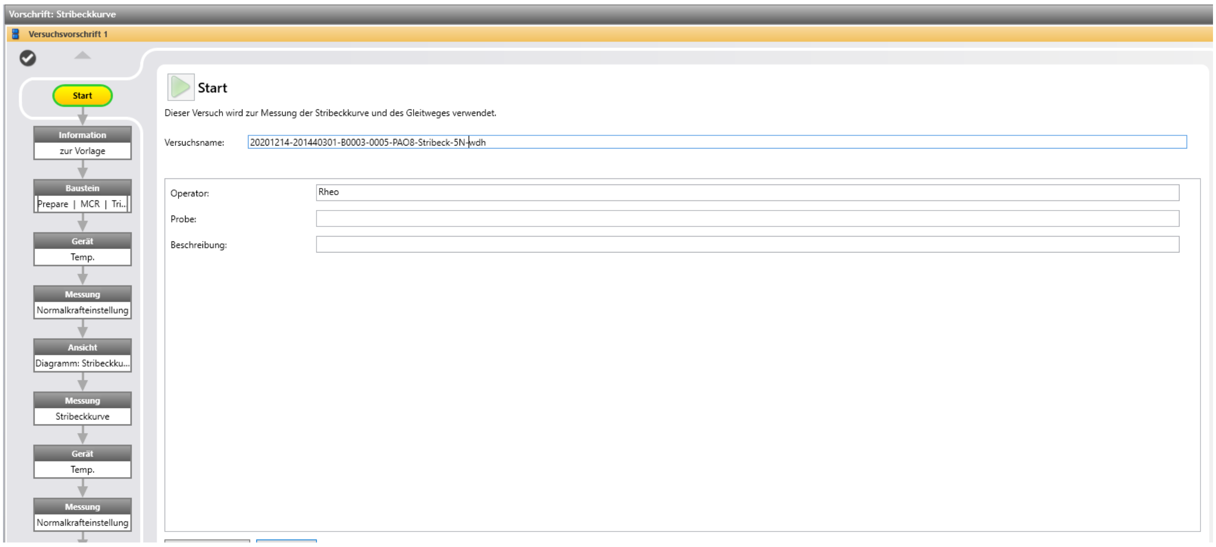

Start

Dieser Versuch wird zur Messung der Stribeckkurve und des Gleitweges verwendet.

Versuchsname: 20201214-201440301-B0003-0005-PAO8-Stribeck-5N-wdh

Operator: Rheo

Probe:

Beschreibung:

Abbildung 17: Exportieren der Daten

- ## Abdrehen des Geräts

- Nach Entfernen des Equipments (Platte, Kegel, Tribologisches) müssen der Hauptschalter (siehe Abbildung 18) und die zwei Schalter der Kühlung (siehe Abbildung 19) abgedreht werden.

Abbildung 18: Hauptschalter MCR302

Abbildung 19: Kühlung

- ## Dokumentation Geräteverwendung

- Unter der Gerätenummer 5189 (geförderter Bereich) bzw. 7189 (nicht geförderter Bereich ist die Geräteverwendung (Analysezeit) im BMD System zu dokumentieren. Als kleinste Dokumentationseinheit ist eine ganze Stunde festgelegt. Eine begonnene Analysestunde ist immer aufzurunden.

6. Außerordentlicher Betrieb

Kalibration

- Die Kalibration ist vom Geräteverantwortlichen bzw. von einem geschulten Mitarbeiter in dessen direkten Auftrag vierteljährig zu überprüfen. Bei Bedarf werden entsprechende Kalibrationsmaßnahmen gemäß Gerätebuch vorgenommen (siehe Anhang 2). Zur Kalibration müssen die Proben von Anton Paar angefordert werden.
- Service, Wartung und Reparaturen
- Alle 90 Tage muss ein Motorabgleich ohne Probe durchgeführt werden:

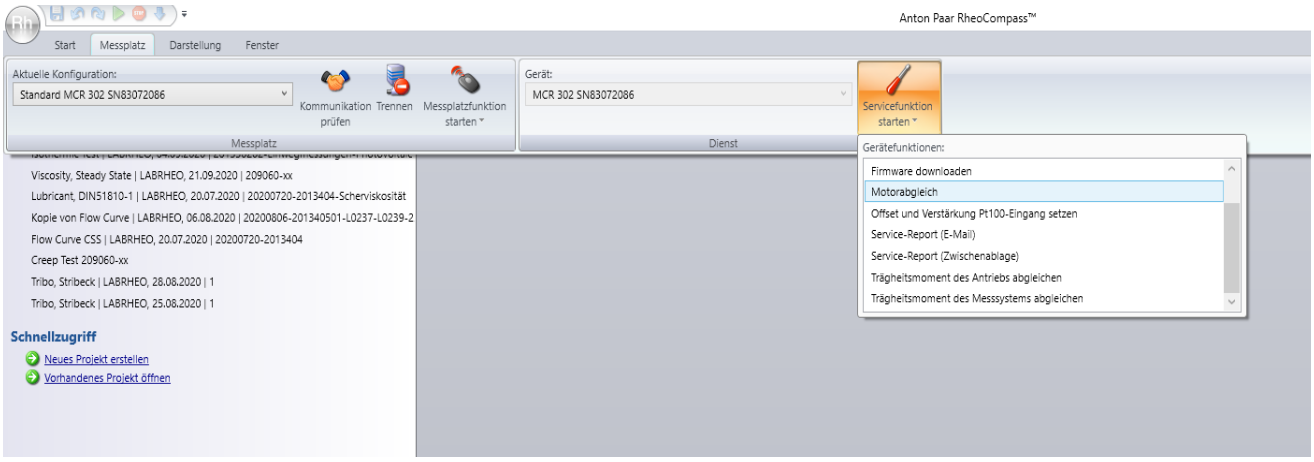

Aktuelle Konfiguration: Standard MCR 302 SN83072086

Gerät: MCR 302 SN83072086

Viscosity, Steady State | LABRHEO, 21.09.2020 | 209060-xx
Lubricant, DIN51810-1 | LABRHEO, 20.07.2020 | 20200720-2013404-Scherviskosität
Kopie von Flow Curve | LABRHEO, 06.08.2020 | 20200806-201340501-L0237-L0239-2
Flow Curve CSS | LABRHEO, 20.07.2020 | 20200720-2013404
Creep Test 209060-xx
Tribo, Stribeck | LABRHEO, 28.08.2020 | 1
Tribo, Stribeck | LABRHEO, 25.08.2020 | 1

Abbildung 20: Motorabgleich alle 90 Tage durchführen

- Weiterführende Servicearbeiten und Reparaturen sind jedenfalls mit dem Poolleiter und dem Geräteverantwortlichen abzusprechen (unter Einhaltung des Augen Prinzip) und im Laborbuch zu dokumentieren. Gegebenenfalls ist zur Hilfestellung bei Unsicherheiten oder weiterführenden technischen Problemen der spezifische Support von Anton Paar zu kontaktieren. Die Wartung für das MCR_302 ist **einmal** pro Jahr von einem autorisierten Anton-Paar-Servicetechniker durchzuführen.
- Verlauf, falls das Gerät für einen längeren Zeitraum außer Betrieb genommen wird:
- **Der Messkopf und das Luftlager sind besonders zu schützen!**
- Entfernen Sie das Messsystem und (falls zutreffend) die Temperiereinheit vom Rheometer. Falls zutreffend entfernen Sie auch das Schutzrohr vom Messkopf, andernfalls könnte das Luftlager beschädigt werden.
- Legen Sie den Transportschutz mit dem grauen Schaumgummi nach oben in die Mitte des Flanschs der Temperiereinheit.
- Wenn sich das MCR im Online-Betrieb befindet, drücken Sie die Taste ONLINE, um in den Offline- Betrieb zu wechseln (grüne LED leuchtet nicht).

- Verwenden Sie die Nach-unten-Pfeiltaste, um den Messkopf zu seiner niedrigsten Position zu bewegen.
- Wenn der Messkopf die niedrigste Position erreicht, wird die programmierte Folientaste "Park" (Parken) aktiviert.
- Drücken Sie die Taste "Park" (Parken). Der Messkopf bewegt sich noch weiter nach unten. Wenn auf dem Display der Positionswert "---.--- mm" angezeigt wird, ist die Parkstellung erreicht.
- Sie können das Gerät nun abschalten und von der Druckluftversorgung trennen.

In der nachfolgenden Abbildung werden die empfohlenen Wartungsarbeiten, welche regelmäßig durchgeführt werden sollen, aufgelistet:

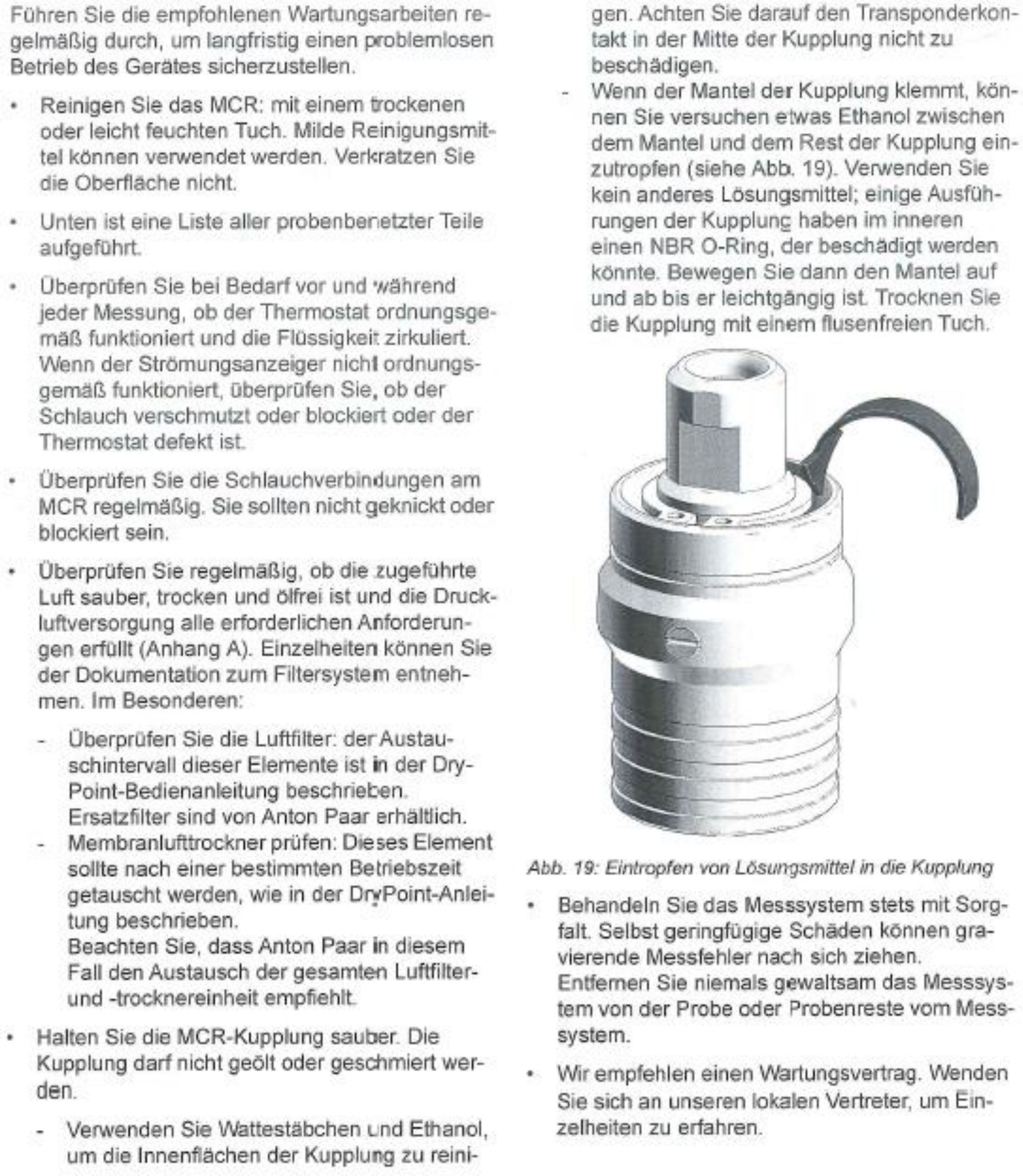

Führen Sie die empfohlenen Wartungsarbeiten regelmäßig durch, um langfristig einen problemlosen Betrieb des Gerätes sicherzustellen.

- Reinigen Sie das MCR: mit einem trockenen oder leicht feuchten Tuch. Milde Reinigungsmittel können verwendet werden. Verkratzen Sie die Oberfläche nicht.
- Unten ist eine Liste aller probenbenetzter Teile aufgeführt.
- Überprüfen Sie bei Bedarf vor und während jeder Messung, ob der Thermostat ordnungsgemäß funktioniert und die Flüssigkeit zirkuliert. Wenn der Strömungsanzeiger nicht ordnungsgemäß funktioniert, überprüfen Sie, ob der Schlauch verschmutzt oder blockiert oder der Thermostat defekt ist.
- Überprüfen Sie die Schlauchverbindungen am MCR regelmäßig. Sie sollten nicht geknickt oder blockiert sein.
- Überprüfen Sie regelmäßig, ob die zugeführte Luft sauber, trocken und ölfrei ist und die Druckluftversorgung alle erforderlichen Anforderungen erfüllt (Anhang A). Einzelheiten können Sie der Dokumentation zum Filtersystem entnehmen. Im Besonderen:
    - Überprüfen Sie die Luftfilter: der Austauschintervall dieser Elemente ist in der DryPoint-Bedienanleitung beschrieben. Ersatzfilter sind von Anton Paar erhältlich.
    - Membranlufttrockner prüfen: Dieses Element sollte nach einer bestimmten Betriebszeit getauscht werden, wie in der DryPoint-Anleitung beschrieben. Beachten Sie, dass Anton Paar in diesem Fall den Austausch der gesamten Luftfilter- und -trocknereinheit empfiehlt.
- Halten Sie die MCR-Kupplung sauber. Die Kupplung darf nicht geölt oder geschmiert werden.
    - Verwenden Sie Wattestäbchen und Ethanol, um die Innenflächen der Kupplung zu reinigen. Achten Sie darauf den Transponderkontakt in der Mitte der Kupplung nicht zu beschädigen.
    - Wenn der Mantel der Kupplung klemmt, können Sie versuchen etwas Ethanol zwischen dem Mantel und dem Rest der Kupplung einzutropfen (siehe Abb. 19). Verwenden Sie kein anderes Lösungsmittel; einige Ausführungen der Kupplung haben im inneren einen NBR O-Ring, der beschädigt werden könnte. Bewegen Sie dann den Mantel auf und ab bis er leichtgängig ist. Trocknen Sie die Kupplung mit einem flusenfreien Tuch.

Abb. 19: Eintropfen von Lösungsmittel in die Kupplung

- Behandeln Sie das Messsystem stets mit Sorgfalt. Selbst geringfügige Schäden können gravierende Messfehler nach sich ziehen. Entfernen Sie niemals gewaltsam das Messsystem von der Probe oder Probenreste vom Messsystem.
- Wir empfehlen einen Wartungsvertrag. Wenden Sie sich an unseren lokalen Vertreter, um Einzelheiten zu erfahren.

Abbildung 21: Regelmäßige Wartungsarbeiten

Appendix 4: ATR Spectra

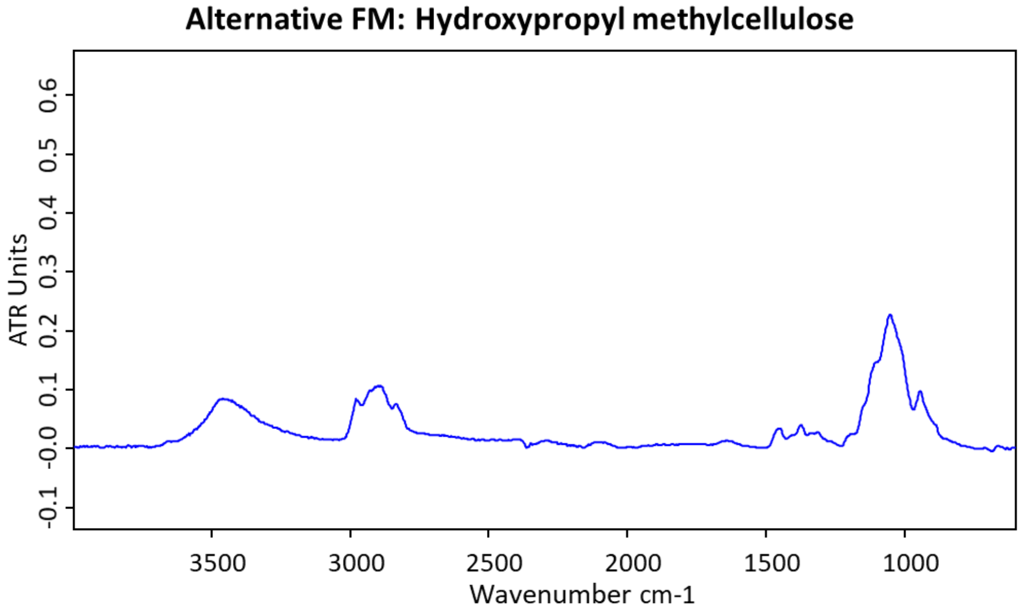

Appendix 10: ATR Spectrum HPMC

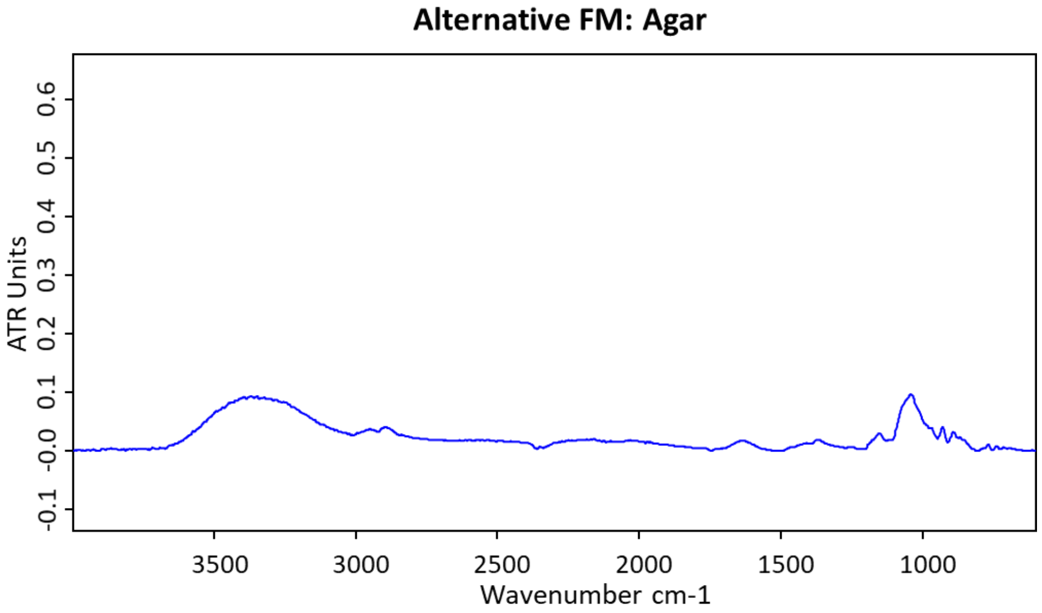

Appendix 11: ATR Spectrum Agar

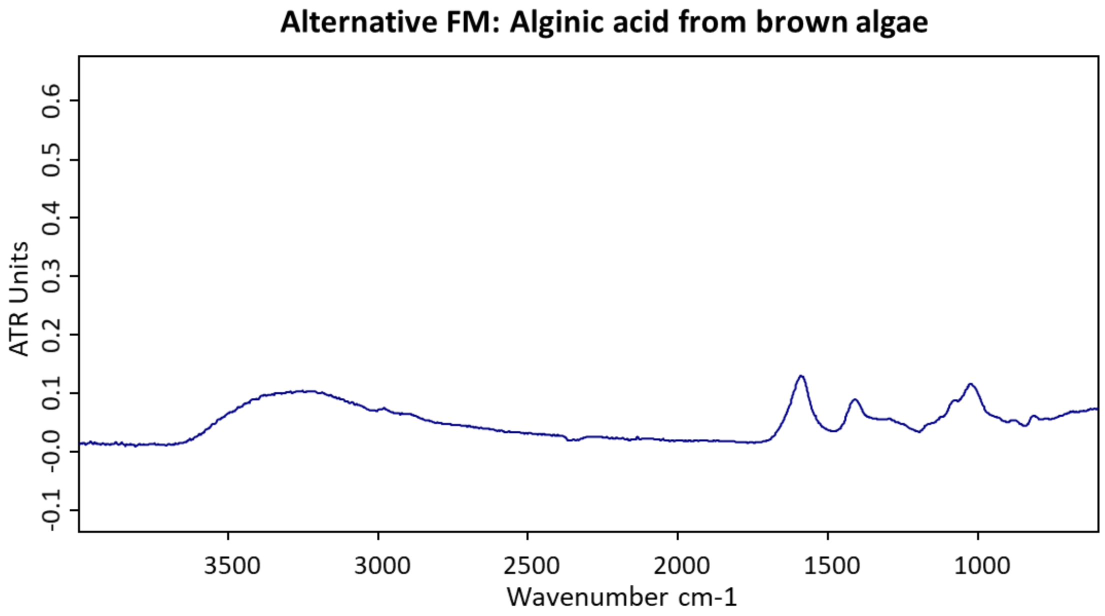

Appendix 12: ATR Spectrum Alginic acid calcium salt from brown algae

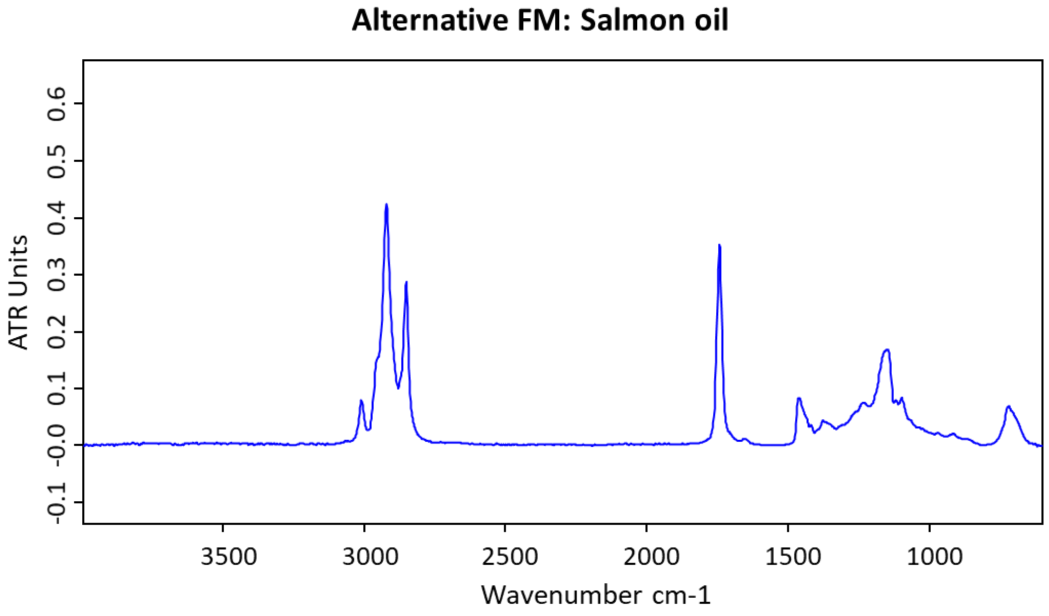

Appendix 13: ATR Spectrum Salmon oil

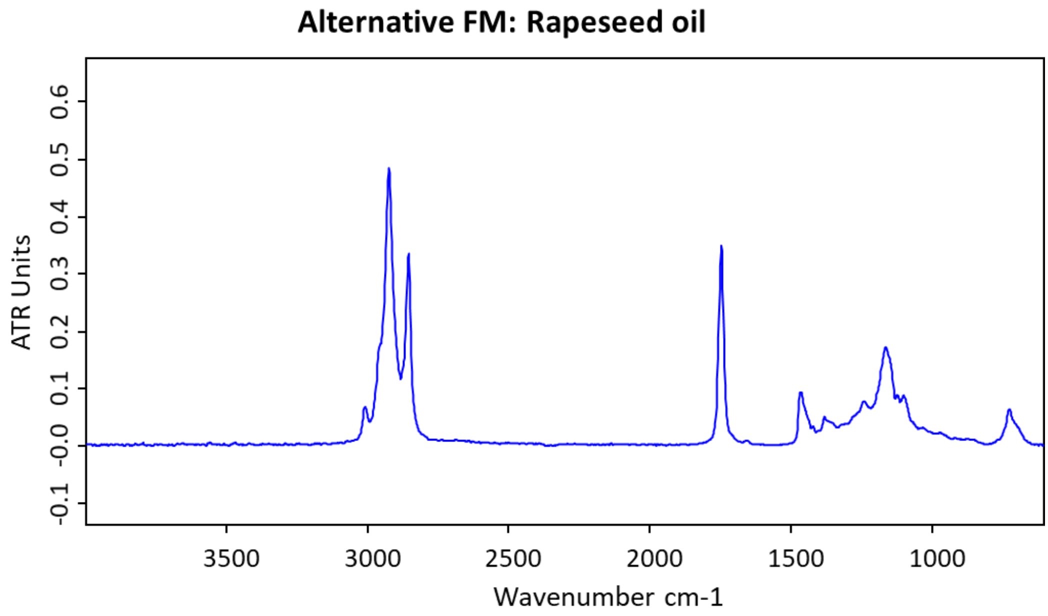

Appendix 14: ATR Spectrum Rapeseed oil

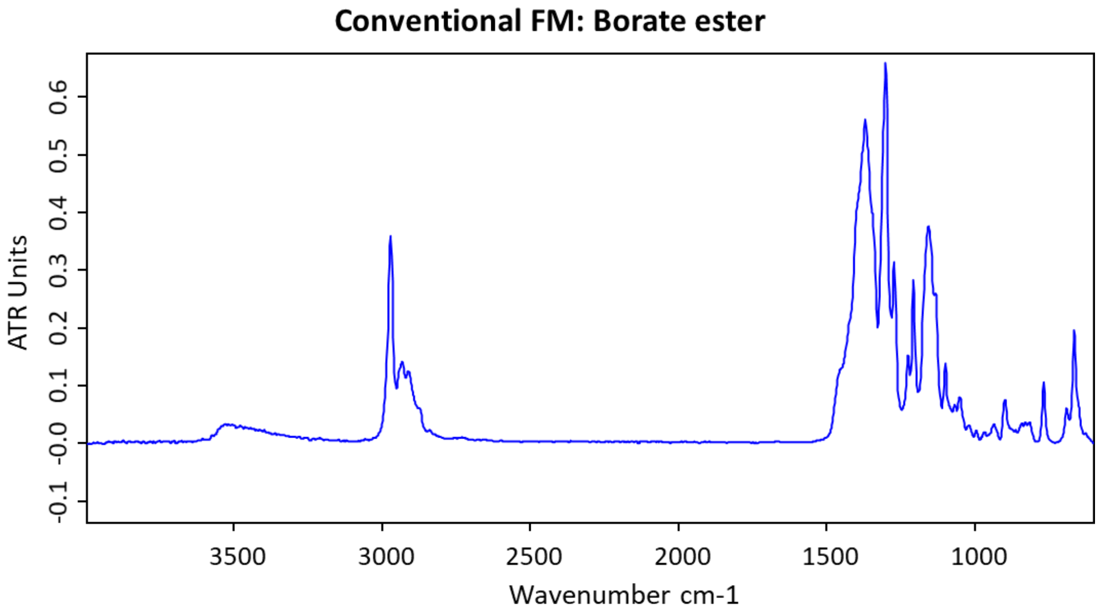

Appendix 15: ATR Spectrum Borate ester

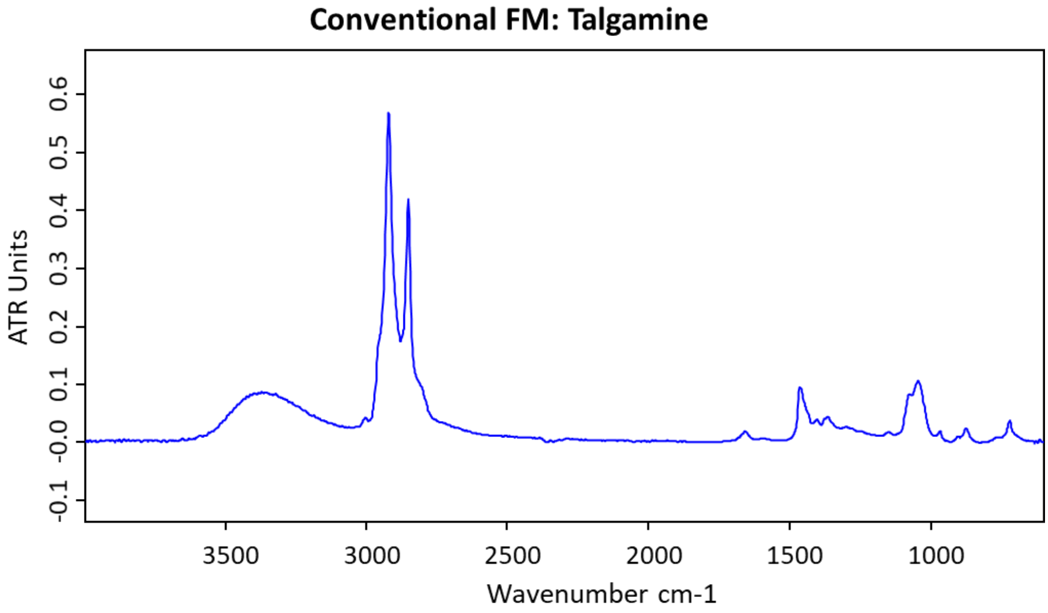

Appendix 16: ATR Spectrum Tallow amine

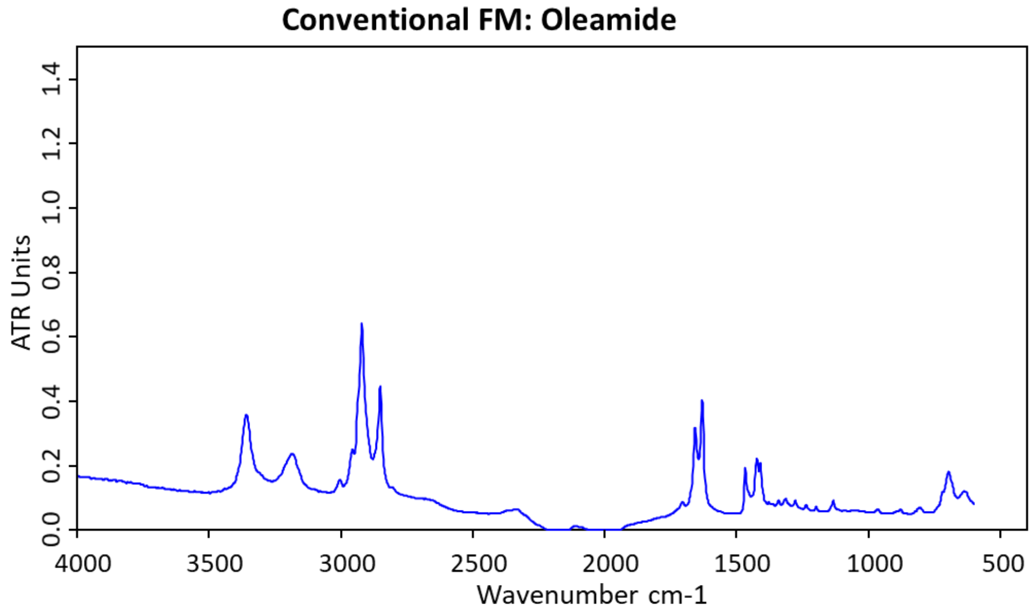

Appendix 17: ATR Spectrum Oleamide

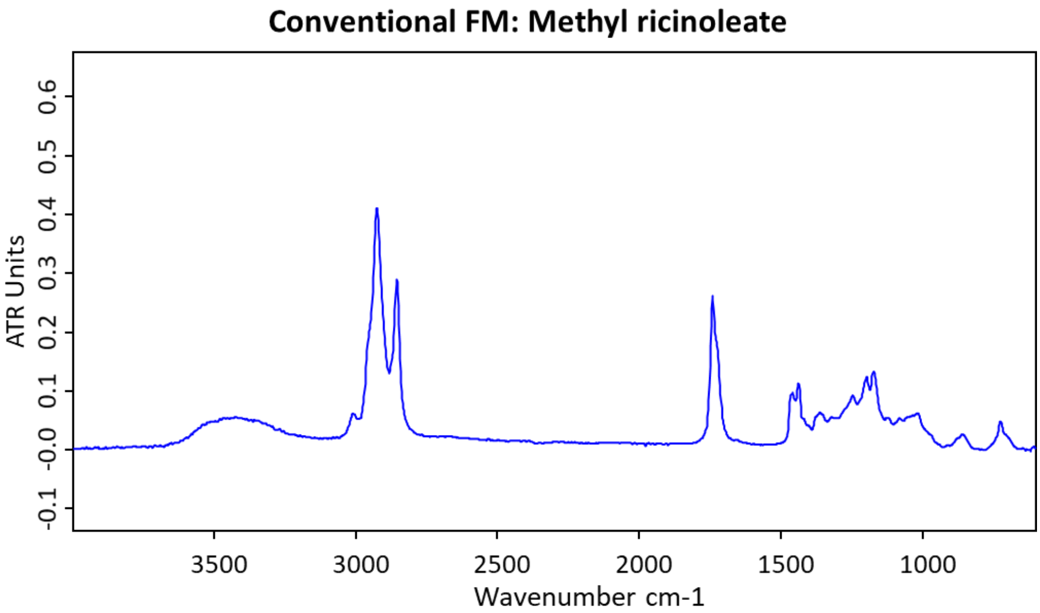

Appendix 18: ATR Spectrum Methyl ricinoleate

Appendix 5: ICP-OES results

Code	Al	B	Ba	Ca	Co	Cr	Cu
Hydroxypropyl methylcelullose	5	< 5	< 1	11	< 1	1	< 1
Agar	11	144	1	3100	< 1	< 1	< 1
Alginic acid calcium salt from brown algae	154	< 5	30	>14500	< 1	3	< 1
Salmon oil	< 5	< 5	< 1	< 5	< 1	< 1	< 1
Rapeseed oil	< 5	< 5	< 1	5	< 1	< 1	< 1
Borate ester	26	>12600	< 1	16	< 1	< 1	< 1
Tallow amine	< 5	<10	< 1	10	< 1	< 1	< 1
Oleamide	< 5	< 5	< 1	30	< 1	< 1	< 1
Methyl ricinoleate	< 5	< 5	< 1	< 5	< 1	< 1	< 1

Appendix 19: ICP-OES results (Al, B, Ba, Ca, Co, Cr, Cu) conventional and bio-based FMs

Code	Fe	K	Li	Mg	Mn	Mo	Na
Hydroxypropyl methylcelullose	14	< 10	< 10	2	< 1	< 1	3330
Agar	22	286	< 10	992	3	< 1	5000
Alginic acid calcium salt from brown algae	147	250	< 10	827	5	< 1	2040
Salmon oil	< 1	< 10	< 10	< 1	< 1	< 1	< 10
Rapeseed oil	< 1	< 10	< 10	< 1	< 1	< 1	< 10
Borate ester	< 1	< 10	< 10	2	< 1	< 1	65
Tallow amine	< 1	< 10	< 10	< 1	< 1	< 1	< 10
Oleamide	< 1	< 10	< 10	1	< 1	< 1	< 10
Methyl ricinoleate	< 1	< 10	< 10	< 1	< 1	< 1	< 10

Appendix 20: ICP-OES results (Fe, K, Li, Mg, Mn, Mo, Na) conventional and bio-based FMs

Code	Ni	P	Pb	S	Sb	Si	Sn
Hydroxypropyl methylcelullose	< 1	< 10	< 10	16	< 5	10	< 10
Agar	< 1	49	< 10	5290	< 5	33	< 10
Alginic acid calcium salt from brown algae	< 1	75	< 10	316	< 5	140	< 10
Salmon oil	< 1	< 10	< 10	< 10	< 5	< 10	< 10
Rapeseed oil	< 1	< 10	< 10	< 10	< 5	< 10	< 10
Borate ester	< 1	< 10	< 10	< 10	< 5	< 10	< 10
Tallow amine	2	< 10	< 10	< 10	< 5	< 10	< 10
Oleamide	< 1	< 10	< 10	<25	< 5	< 10	< 10
Methyl ricinoleate	< 1	< 10	< 10	50	< 5	< 10	< 10

Appendix 21: ICP-OES results (Ni, P, Pb, S, Sb, Si, Sn) conventional and bio-based FMs

Code	Ti	V	W	Zn
Hydroxypropyl methylcelullose	< 5	< 1	< 10	<10
Agar	< 5	< 1	< 10	<10
Alginic acid calcium salt from brown algae	7	< 1	< 10	<10
Salmon oil	< 5	< 1	< 10	<10
Rapeseed oil	< 5	< 1	< 10	<10
Borate ester	< 5	< 1	< 10	<10
Tallow amine	< 5	< 1	< 10	<10
Oleamide	< 5	< 1	< 10	<10
Methyl ricinoleate	< 5	< 1	< 10	<10

Appendix 22: ICP-OES results (Ti, V, W, Zn) conventional and bio-based FMs

Appendix 6: λ- values for theoretical lubrication regime calculation

PAO8	**$\mu_0$value [$\frac{mm^2}{s}$]**	**α value [$\frac{1}{Pa}$]**
25°C	87.636	1.58E-08
80°C	12.477	1.16E-08
100°C	7.8734	1,05E-08

Appendix 23: μ_0- and α- values of PAO8 at different temperatures (25 °C, 80 °C, 100 °C)

80°C	**$\mu_0$value [$\frac{mm^2}{s}$]**	**α value [$\frac{1}{Pa}$]**
PAO8	12.477	1.16E-08
PAO4	4.6403	9.86E-09
SN450	18.109	1.51E-08
SN150W	6.8622	1.43E-08

Appendix 24: μ_0- and α- values of different base oils at 80 °C

λ – values for theoretical lubrication regime calculation														
Normal force [N]														
Sliding speed [m/s]	**PAO8 80°C**	0.01	0.1	0.5	1	5	10	**PAO4 80°C**	0.01	0.1	0.5	1	5	10
	1E-7	3.76E-6	3.18E-6	2.88E-6	2.69E-6	2.39E-6	2.27E-6	1E-7	3.55E-7	3.00E-7	2.66E-7	2.53E-7	2.25E-7	2.14E-7
	1E-4	4.55E-4	3.85E-4	3.42E-4	3.25E-4	2.89E-4	2.75E-4	1E-4	2.08E-6	1.76E-6	1.56E-6	1.48E-6	1.32E-6	1.26E-6
	1E-1	4.65E-2	3.93E-2	3.49E-2	3.32E-2	2.95E-2	2.81E-2	1E-1	2.51E-4	2.13E-4	1.89E-4	1.80E-4	1.60E-4	1.52E-4
	SN450 80°C	0.01	0.1	0.5	1	5	10	**SN150W 80°C**	0.01	0.1	0.5	1	5	10
	1E-7	4.39E-6	3.71E-6	3.30E-6	3.14E-6	2.79E-4	2.65E-6	1E-6	2.16E-7	1.79E-7	1.59E-1	1.51E-7	1.35E-7	1.28E-7
	1E-4	4.25E-4	3.59E-4	3.20E-4	3.04E-4	2.70E-4	2.57E-4	1E-4	3.65E-6	3.09E-6	2.74E-6	2.61E-6	2.32E-6	2.20E-6
	1E-1	4.31E-2	3.64E-2	3.24E-2	3.08E-2	2.73E-2	2.60E-2	1E-1	3.54E-4	2.99E-4	2.53E-4	2.53E-4	2.25E-4	2.14E-4

Appendix 25: λ – valuesof different base oils at different normal forces [N] and sliding speeds [m/s] for theoretical lubrication regime calculation

Appendix 7: Wear scars on stainless steel plates observed with a reflected-light microscope

This chapter includes the wear scars of an empty run, of the four references (water, glycerin, polyethylene glycol and PAO8) and of the best performing conventional FM (tallow amine) and of the best performing bio-based FM (rapeseed and salmon oil including pure and dilutions).

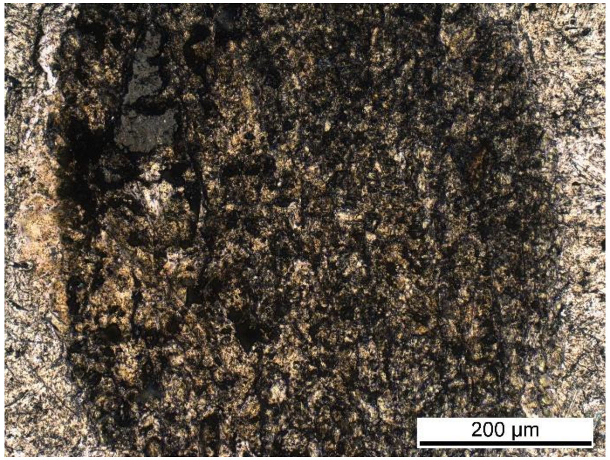

Appendix 26: Empty run 30°C wear on stainless steel plates

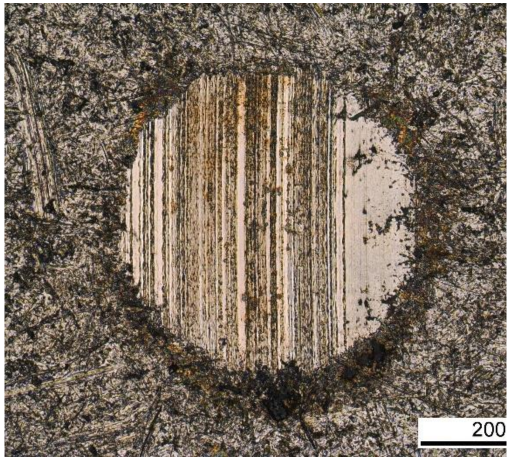

Appendix 27: Water 30°C wear on stainless steel plates

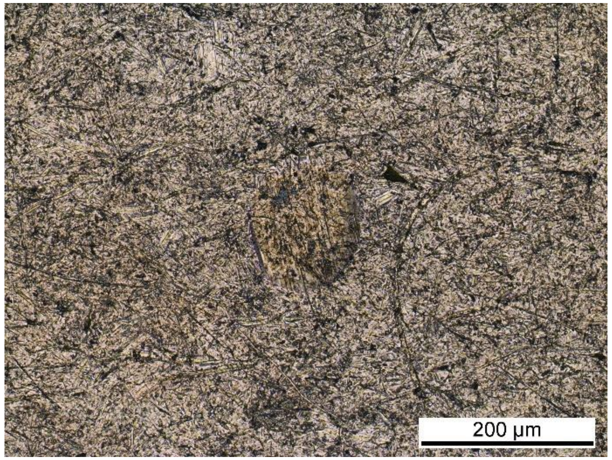

Appendix 28: Glycerin 30°C wear on stainless steel plates

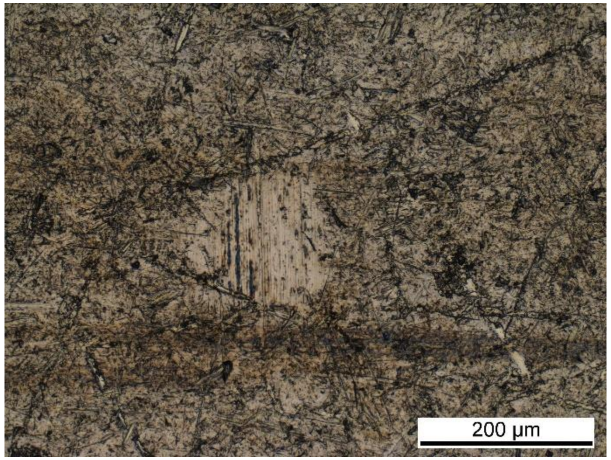

Appendix 29: Polyethylene glycol 30°C wear on stainless steel plates

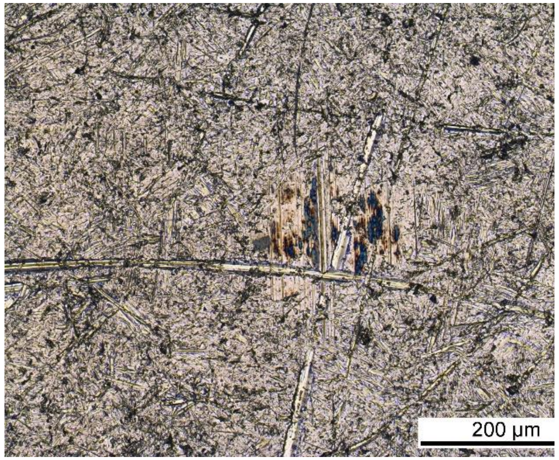

Appendix 30: PAO8 80°C wear on stainless steel plates

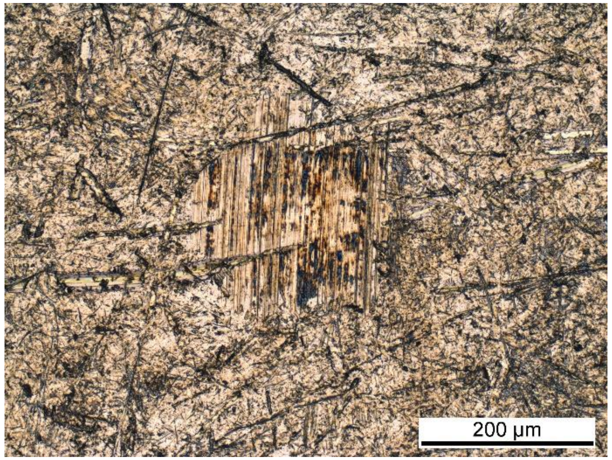

Appendix 31: 1wt % tallow amine in PAO8 80°C wear on stainless steel plates

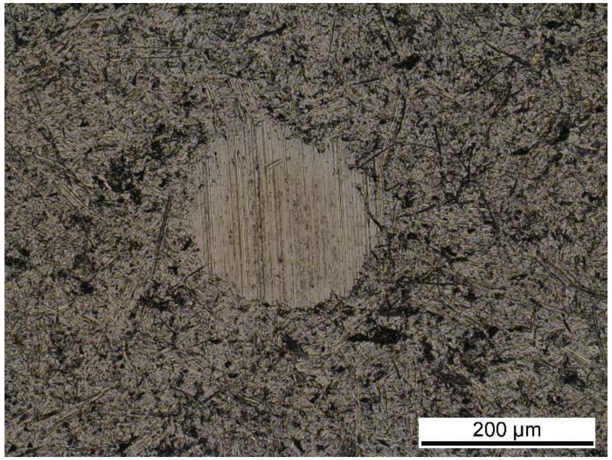

Appendix 32: Pure salmon oil 30°C wear on stainless steel plates

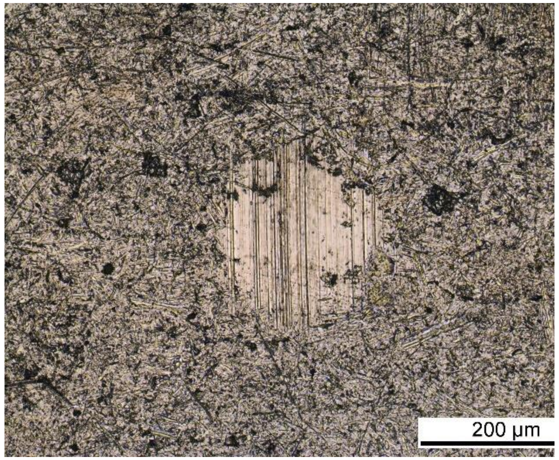

Appendix 33: 1wt % salmon oil 30°C wear on stainless steel plates

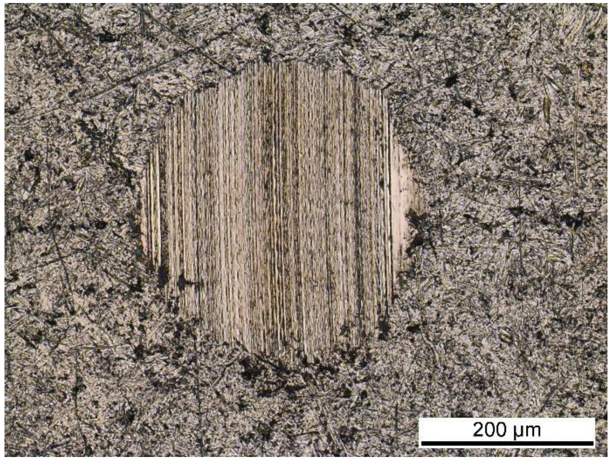

Appendix 34: 3wt % salmon oil 30°C wear on stainless steel plates

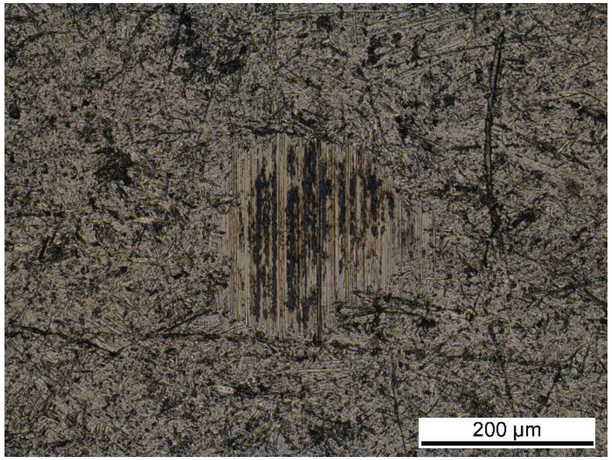

Appendix 35: Pure rapeseed oil 30°C wear on stainless steel plates

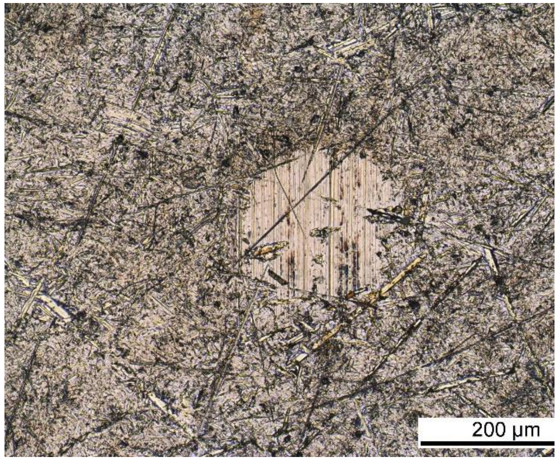

Appendix 36: 1wt % rapeseed oil 30°C wear on stainless steel plates

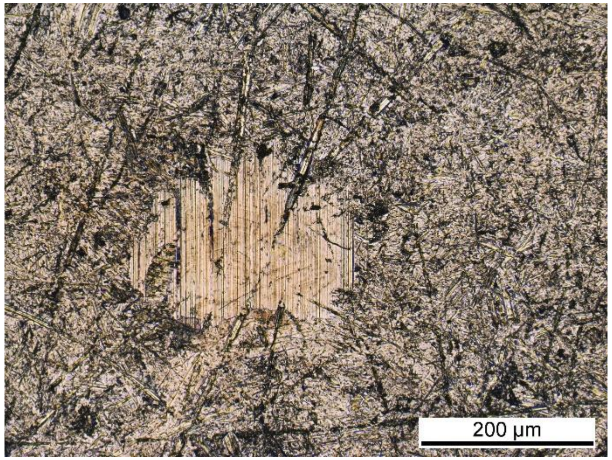

Appendix 37: 3wt % rapeseed oil 30°C wear on stainless steel plates

Further, the wear scars of initial tests were included (going up to the maximum 1.4 m/s):

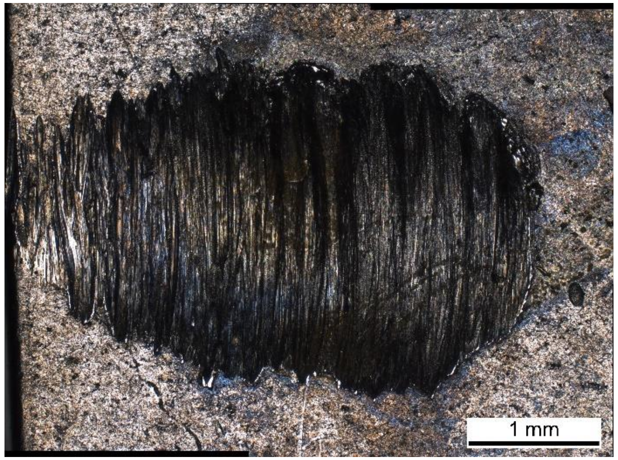

Appendix 38:1wt % tallow amine 80°C wear on stainless steel plates 1.4 m/s

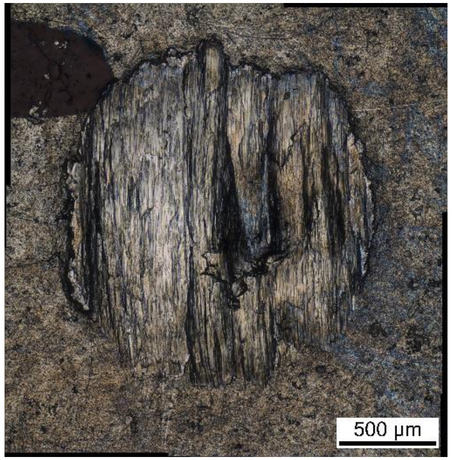

Appendix 39: PAO8 80°C wear on stainless steel plates 1.4 m/s